COMPUTER-BASED SLEEP APNEA DETECTION AND USE OF REBREATHE DEVICE ("SMART CO2") TO TREAT SLEEP APNEA

by

Mehdi Shokoueinejad

A dissertation submitted in partial fulfillment of

the requirements for the degree of

Doctor of Philosophy

(Biomedical Engineering)

at the

UNIVERSITY OF WISCONSIN – MADISON
2017

Date of final oral examination: 12/21/2016
Justin Williams, Professor, Biomedical Engineering
John Webster, Professor Emeritus, Biomedical Engineering
Jerome Dempsey, Professor Emeritus, Population Health Sciences
Christopher Brace, Associate Professor, Radiology and Biomedical Engineering
Jeremy Rogers, Assistant Professor, Biomedical Engineering
Alejandro Roldan-alzate, Assistant Professor, Mechanical and Biomedical Engineering

Abstract

While public awareness of sleep related disorders is growing, sleep apnea syndrome (SAS) remains a public health and economic challenge. Fueled by the obesity epidemic, in the US alone it is estimated that over 29.4 million adults suffer from sleep apnea, that 80–90% of those adults are living undiagnosed and untreated, and that the aggregate costs of undiagnosed adults with sleep apnea exceed $150 billion annually. Although various devices have been used to measure physiological signals, detect apneic events, and help treat sleep apnea, significant opportunities remain to improve the quality, efficiency, and affordability of sleep apnea care. As our understanding of respiratory and neurophysiological signals and sleep apnea physiological mechanisms continues to grow, and our ability to detect and process biomedical signals improves, novel diagnostic and treatment modalities emerge.

This dissertation presents a body of work that establishes the feasibility of using a computer based variable dead space rebreathe device ("Smart CO_2") to treat obstructive and central Sleep apnea. This device has the following characteristics: a) measure ventilation on a breath-by-breath basis to detect the occurrence of sleep apnea and/or hypopnea and b) automatically adjust the rebreathe dead space volume to deliver the minimum amount of CO_2 in a step-wise fashion to eliminate or significantly reduce the patient's apneas and hypopneas. We have tested the accuracy of this current "Smart CO_2" device in two ways. First, we used humans and mannequins to quantify, via mathematical modelling, the dynamics of CO_2 mixing of inflow gas and dead space air. This "Smart CO_2" variable dead space device elicited highly predictable (±3.5% error) alveolar PCO_2 levels with changing reservoir dead spaces, thereby ensuring that excessive CO_2 accumulation would not occur during rebreathing. Secondly, we developed algorithms that reliably switched the subject into and out of the device with

increasing/decreasing levels of rebreathe volume in response to simulated apneas and hypopneas. Based on the findings of this thesis, a "Smart CO_2" device that will reliably and accurately—and even comfortably—detect sleep-disordered breathing (SDB) in real time, provide step-wise increments in rebreathe volume and alveolar CO_2.

Acknowledgements

First and foremost I want to thank my senior advisors Prof. John G. Webster and Jerome Dempsey. It has been an honor to be one of your last Ph.D. students. I appreciate all your contributions of time, ideas, and funding to make my Ph.D. experience productive and stimulating. The joy and enthusiasm you have for my research was contagious and motivational for me, even during tough times in the Ph.D. pursuit. I would like to extend my best words of thanks to Prof. Justin Williams, Dr. Josh Medow, and Dr. Bermans J. Iskandar who have contributed immensely to my personal and professional time at the University of (Wisconsin-Madison).

I would also like to thank my committee members, Professor Christopher Brace, Professor Jeremy Rogers, Professor Alejandro Roldan for serving as my committee members.

The members of the Webster and Neural Interface Technology Research and Optimization (NITRO) lab have contributed immensely to my personal and professional time at the University of Wisconsin-Madison. The group has been a source of friendships as well as good advice and collaboration. I would like to acknowledge Mr. Fa Wang, Mrs. Xuan Zhang, Mr. Rayan Alkashgari and Dr. Icaro dos Santos . We worked together on the several projects, and I very much appreciated their enthusiasm, intensity, willingness to help me, and their amazing ability to do brain storming and help on concept development. Other past and present group members that I have had the pleasure to work with or alongside of are Dr. Amit Nimunkar, Dr. Nacera Meziane, Michele Chiang, Sam Lines, Ziyad Aloqalaa, Jake Levin, and Pete Klomberg; and the numerous summer and Co-Op students who have come through the lab.

Lastly, I would like to thank my family for all their love and encouragement. And most of all for my loving, supportive, encouraging friends, whose faithful support during the final stages of this Ph.D., is so appreciated. Thank you.

Dedication

This thesis is dedicated, in its entirety, to the One who has raised me even before I was in my mother's wombs. It is dedicated to the One who has taught me, inspired me and guided me throughout my life. I dedicated this humble endeavor to God, and I only pray that in spite of my weakness, it may be accepted, and to my family who has supported me throughout the journey.

Table of Contents

Abstract i
Acknowledgements iii
Dedication iv
Table of Contents v
List of Figures ix
List of Tables xii
Glossary xiii
1 Chapter 1 Introduction 1
1.1 Objectives 1
1.2 Chapters Summary 2
2 Chapter 2 Background and Significance of using CO_2 5
2.1 Treatment approaches to OSA. 5
2.2 Does utilizing CO_2 as a treatment for sleep apnea make sense? 5
2.3 Proof of principle: mild/moderate hypercapnia stabilizes breathing and reduces OSA! 6
2.4 Potential adverse effects of imposed hypercapnia. 8
3 Chapter 3 Sleep apnea diagnostic signal modalities 10
3.1 Introduction 10
3.2 Methods to diagnose and detect apneic events 11
3.3 Signal and sensors for detecting and diagnosing apneic events 13
3.3.1 Direct and indirect measurement of airflow 13
3.3.2 Measurement of the concentration or partial pressure of respiratory gases 20
3.3.3 Measurement of electropotentials 24
3.3.4 Patients' sleeping behavior and body movements in sleep 26
4 Chapter 4 Sleep Apnea Signal processing, algorithms, and techniques 29
4.1 Signal processing and data representations 31
4.1.1 Time-frequency based transforms 32
4.1.2 Multiresolution and wavelet based transforms 33
4.1.3 Nonlinear and other transforms 33
4.2 Algorithms and classification models 34
4.2.1 Amplitude and adaptive thresholding 34
4.2.2 Linear and kernel methods 35

4.2.3 Tree based models 36
4.2.4 Artificial neural networks 36
4.2.5 Fuzzy logic systems and networks 37
4.2.6 Deep learning 38
4.2.7 Low dimensionality Total variability based approaches 39
4.3 Discussion and Conclusion 41
Chapter 5 Current treatment modalities for SAS 44
4.4 Assistive devices 44
4.4.1 Types of PAP device 44
4.4.2 Current PAP technology 46
4.5 Therapeutic oral devices 50
4.5.1 Oral appliances 50
4.5.2 Types of oral devices 51
4.5.3 Comparison of oral appliances to CPAP 53
4.5.4 Comparisons between intra-oral devices 54
4.5.5 Compliance/Adherence issues of oral devices 55
4.5.6 Inspired CO_2 57
4.6 Discussion and conclusions 57
5 Chapter 6 A review of preventing central sleep apnea by inspired CO_2 62
5.1 Abstract 62
5.2 Introduction 62
5.3 Diagnosis 63
5.4 Sleep Apnea 64
5.5 Heart Failure 65
5.6 Current Treatments 66
5.7 Chemical Control of Breathing 68
5.8 Inspired CO_2 69
5.9 Conclusions 71
6 Chapter 7 A modeling study on inspired CO_2 rebreathing device for sleep apnea treatment by means of CFD analysis and experiment 73
6.1 Abstract 73
Nomenclature 74

6.2 Introduction 74
6.3 Device design 77
6.4 Analysis 79
6.4.1 Numerical Simulation 79
6.4.2 Experimental Study Model 84
6.4.3 Mathematical Modeling 84
6.5 Discussion 91
6.6 Conclusions 92
6.7 Supplementary Material 93
7 Chapter 8 Low Cost Sleep Apnea Therapy Device "Smart CO_2 Device" for Use in Home 94
7.1 Abstract 95
7.2 Introduction 95
7.3 Materials and Methods 97
7.4 Results 114
7.5 Conclusion 119
8 Chapter 9 Conclusion and Recommendations 120
8.1 Conclusions 120
8.2 Recommendation 121
9 Appendices 123
A. Review of Uroflowmetry Methods 123
A.1 Abstract 123
A.2 Introduction to Urodynamics 124
A.3 Cystometry and Fluoroscopy Techniques 126
A.4 Uroflowmetry 127
A.5 Conclusion 149
A.6 Acknowledgements 150
B. Video Voiding Device For Diagnosing Lower Urinary Tract Dysfunction in Men 151
B.1 Abstract 151
B.2 Introduction 152
B.3 Background 156
B.4 Materials and Methods 158
B.5 Results 161

B.6 Discussion 166
B.7 Conclusions 169
B.8 Acknowledgements 170
B.9 Ethical approval 170
B.10 Informed consent 171
References 172

List of Figures

Figure 1. Effect of mild hypercapnia via rebreathing with fixed-volume dead space in a patient with OSA (AHI = 60). Repetitive obstructive apneas with associated transient EEG arousals were noted during air breathing as indicated by the repeated absence of flow despite respiratory efforts. Almost all of these obstructions and arousals were eliminated by raising $P_{ET}CO_2$ an average of 2 mmHg (left arrow) above stable, nonobstructed breathing levels in sleep. Abrupt removal of the added F_ICO_2 (right arrow) resulted in the immediate return of the cyclical obstructive apneas. On the basis of these types of findings, we raised $P_{ET}CO_2$ 2–5 mmHg via dead space rebreathing during 90–120 min of sleep in a group of patients with moderate to severe OSA and observed an average 85% reduction in AHI below air-breathing control in 17 of 21 patients [1, 2]. 8

Figure 2. Pneumotachometer (a,c) Fine mesh or (b,d) closely-packed channels help to laminarize flow, so that energy loss of the flow is due to the viscosity. The pressure drops ΔP measured with sampling lines correspond to the energy loss due to gas viscosity [59]. 15

Figure 3. Polysomnography with Central Sleep Apnea (A) and Obstructive Sleep Apnea (B). Chest effort indicated by the arrows is absent in CSA. Reprinted with permission from [77]. 18

Figure 4. The polysomnographic tracing includes electroencephalogram (EEG), electromyogram (EMG) EMGgg: Electromyogram of the genioglossus muscle (intramuscular); EMGsub: EMG of the submental muscle (surface), RESP flow, SaO_2, etc. A) The cessation and resumption of flow defines the apneic event. B) one obstructed apneic event (between the dotted vertical lines in A) is expanded to illustrate the progressive increase in inspiratory effort, pressure at the level of the epiglottis (*P*epi) and dilator muscle EMG (EMGgg) during the apnea. It demonstrates snoring on the flow tracing follow by apnea, and increases in EMG activity throughout the apneic event. Reprinted with permission of the American Thoracic Society, Copyright © 2016 American Thoracic Society. [105]. 26

Figure 5 Demonstrates SAS diagnostic parameters of interest, the types of physiological events that characterize those parameters, clinically useful sensor modalities for observing disease relevant biosignals, and classification methods commonly used to recognize SAS event patterns. 32

Figure 6 Demonstrates the high airway resistance of OSA patients causes the mid-inspiratory flow limitation. Patients without airway obstructed (CSA patients or normal people) have higher mid-inspiratory flow [189]. 48

Figure 7: *Left*: Schematic diagram of an accordion-like, 8 cm diameter collapsed bellows DS. An axial stepper motor rotates a long worm gear protruding at the near end that expands the bellows up to expanded length. The larger perforated white surround (casing) prevents the patient from contacting any motion, yet permits gas flow. *Right*: Mannequin using the device [59]. 79

Figure 8: Average CO_2 concentrations for device volumes $v = [0.5, 1.2] \times 10 - 3$ m^3 obtained from simulation. 83

Figure 9: Transient CO_2 concentration (mol/m^3) propagation in a reservoir with the volume $v = 1.2 \times 10 - 3$ m^3 at three time instances: $t = 0.5$ s (a, d), $t = 1.0$ s (b, e), $t = 2.4$ s (c, f). Subplots (a, b, c) and (d, e, f) denote the exhale and inhale processes, respectively. The inflow boundary condition is assumed at the left side of the reservoir. In subplots (a, b, c) the left side denotes the inlet of accordion-like device, and in (d, e, f), left side denotes the outlet of accordion-like device presented in figure.7 83

Figure 10: Transient CO_2 concentration (mol/m^3) propagation in a reservoir with the volume $v = 0.5 \times 10 - 3$ m^3 at three time instances: t = 0.5 s (a, d), t = 1.0 s (b, e), t = 2.4 s (c, f). Subplots (a, b, c) and (d, e, f) denote the exhale and inhale processes, respectively. The inflow boundary condition is assumed at the left side of the reservoir. In subplots (a, b, c) the left side denotes the inlet of accordion-like device, and in (d, e, f), left side denotes the outlet of accordion-like device presented in figure. 7 84

Figure 11: Transient CO_2 accumulation in an apnea treatment device with the volume of $v = 1.2 \times 10 - 3$ m^3. The plot shows the results of the mathematical model, simulation, and experiment. 87

Figure 12: Parametric analysis of the CO_2 accumulation in the apnea treatment device for different values of DS volume, RV, tidal volume, TV, and mixing efficiency, γ. The CO_2 accumulation is provided for: *top*: RV $\in$ 0.5, 1.7 L and $\gamma \in [0, 1]$, and *bottom*: RV $\in$ 0.5, 1.7 L and TV $\in$ 0.5, 1.7 L 88

Figure 13: HPS mannequin end-tidal carbon dioxide capnography. The plot shows a segment of room air breathing followed by a segment of breathing through a face mask with 150 ml DS, then an additional 300 ml DS were added to the mask and the end-tidal CO_2 was recorded. This action was repeated for total of three times. The segment with added DS shows an elevation in $P_{ET}CO_2$ 90
Figure 14: Comparison of the average CO_2 accumulation obtained from COMSOL simulation, mathematical model, experimental data and its fitted curve inside the apnea treatment device. CO_2 increased at the lower and higher volume level of added DS. At each level after adequate number of breathing cycle CO_2 level reach plateaued. 90
Figure 15: The subject sleeps using the lightweight comfortable clear plastic facemask held in place with head straps. Air flows through a rotatable elbow in the facemask and a short flexible hose. Then through an accordion like 8 cm diameter collapsed bellows. An axial stepper motor rotates a long worm gear protruding at the near end that expands the bellows to 10 times the collapsed length. The larger perforated white surround prevents the patient from contacting any motion, yet permits gas flow 97
Figure 16 The subject sleeps with the cylindrical reservoir prototype. Lung air flows from the lightweight comfortable clear plastic mask through a short fexible hose, then out the dark hole. After a significant apnea is detected, the hole automatically moves counterclockwise to lengthen dead space. We have found this device to be comfortable and does not disturb sleep. 99
Figure 17 is a flow diagram showing the interaction of one or more components of a sleep apnea therapy device according to one or more examples of embodiments. 102
Figure 18 is an electrical circuit diagram of a sleep apnea therapy device according to one or more examples of embodiments. 103
Figure 19 is a flow chart or logic diagram, illustrating one or more examples of an algorithm used to sense apnea and increase dead space, or not sense apnea and decrease dead space. 108
Figure 20 is a flow chart or logic diagram, illustrating of an algorithm used to sense apnea/hypopnea and increase dead space, or not sense them and decrease dead space. 110
Figure 21 shows observed experimental data under “control” conditions with repeated obstructive apneas. 117
Figure 22 is a chart illustrating experimental data under “low” dead space conditions (450 ml). 118
Figure 23 is a chart illustrating observed experimental data under “high” dead space concentrations (570 ml). 118
Figure 24 Sketch of parameters describing urinary flow 128
Figure 25 Abnormal flow curve sketches 128
Figure 26, VVD development requires (top) computer hardware and software, cameras, video processing, storage and transmission and (bottom) hardware for the booth, toilet, and graduated cylinder (The part where the patient actually voids (urinates) into) 159
Figure 27. A perspective view of one VVD booth setup illustrating a male patient standing ready to urinate with three cameras monitoring from the side, top, and back (cylinder view). 160
Figure 28. The software acquires the video, processes it, and displays images and flow versus time. 161
Figure 29. Bench testing setup - A balloon squeezes out a water stream directed by a tube toward a black funnel that guides the stream into a graduated cylinder sitting on a digital scale. The camera monitors the graduated cylinder and records volume versus time, which is used to derive flow versus time. The digital scale (iWeigh-002M-6D-DI100-LV1000 model by Loadstar Sensors) records weight versus time, which is used to derive flow versus time. 162
Figure 30. (a)–(c) A Bland-Altman plot showing the difference between the total voided volume measured by the VVD and the true total voided volume of a) 100 ml b) 300 ml c) 500 ml. (d)–(f) A Bland-Altman plot showing the difference between the total voided volume measured by the mass flowmeter and the true total voided volume of d) 100 ml. e) 300 ml f) 500 ml. The green lines represent the 95% confidence interval. 164
Figure 31. Flow rate versus time as measured by the VVD and scale mass flowmeter. 165

Figure 32 Screenshot of the VVD software mid-voiding displaying all three cameras, patient information, uroflowmetry results, and a live flow graph. 166

List of Tables

Table I Comparison between Breathing Monitoring Technologies 12
Table II Summary of SAS diagnostic parameters, the types of physiological events, sensor modalities, and commonly used classification methods 28
Table III Summary of data representations, classification methods, and results from empirical studies of the performance of automated approaches to scoring and SAS event recognition. 40
Table IV ResMed's fuzzy logic for phase determination 46
Table V Summary of benefits and challenges of PAP modalities. 50
Table VI Comparison of oral appliances 56
Table 7: Summary of uroflometry methods 150
Table 8 Comparison between VVD and mass flowmeter measurements of predetermined voided volume - 100*(mean ± SD)/ predetermined volume (%) 163
Table 9 Clinical testing measurements of 3 healthy volunteers. 166
Table 10 Comparison of the Uroflowmeters, simple visual examination, and VVD's features 169

Glossary

AASM	American Academy of Sleep Medicine
AHI	Apnea Hypopnea Index
ANN	Artificial Neural Network
APAP	Auto-titrating Positive Airway Pressure
APEN	Approximate Entropy
ASV	Adaptive Servo Ventilation
BiPAP	Bi-level positive airway pressure
BP	Blood Pressure
CIH	Chronic Intermittent Hypoxemia
COPD	Chronic Obstructive Pulmonary Disease
CPAP	Continuous Positive Airway Pressure
CSA	Central Sleep Apnea
CVD	Cardiovascular Disease
DFA	Detrended Fluctuation Analysis
DNN-HMM Model	Deep Neural Network--Hidden Markov
DWT	Discrete Wavelet Transform
EEG	Electroencephalogram
ECG	Electrocardiogram
EMG	Electromyogram
EOG	Electrooculogram
EPAP	Pressure during Expiration
EPR	Expiratory Pressure Relief
FIS	Fuzzy Inference System
FOT	Forced Oscillation Technique
GG	Genioglossus

GH	Geniohyoideus
GMMs	Gaussian Mixture Models
HFIS	High-frequency Inspiratory Sounds
HMM	Hidden Markov Models
HRV	Heart rate variability
IPAP	Pressure during Inspiration
LLE	Largest Lyapunov Exponent
MAAs	Mandibular Advancement Appliances
MRA	Multiresolution Analytical
NAF	Nasal Airflow
OAs	Oral Appliances
OPT	Oral Pressure Therapy
OSA	Obstructive Sleep Apnea
PAP	Positive Airway Pressure
PLMs	Periodic Leg Movements
PPG	Photoplethymography
PSG	Polysomnogram
PVDF	Polyvinylidene Fluoride
RDI	Respiratory Disturbance Index
REM	Rapid eye movement
REM sleep	Rapid eye movement sleep
RL	REM Latency
RIP	Respiratory Inductance Plethysmography
SAS	Sleep Apnea Syndrome
SE	Sleep Efficiency
SI	Severity Index
SL	Sleep Latency

SNA	Sympathetic Nerve Activity
SPLs	Soft Palate Lifters
SVM	Support Vector Machine
TEO	Teager Energy Operators
TMJ	Temporomandibular Joint
TRDs	Tongue Retaining Devices
TST	Total Sleep Time
WPF	Weighted Peak Flow

1 Chapter 1 Introduction

1.1 Objectives

Continuous positive airway pressure (CPAP) has been shown to be an effective treatment for obstructive apneas (OSA) and even some types of central sleep apnea [3-5], but positive airway pressure is not tolerated by many OSA patients and greatly underutilized by many who do use it [6]. Alternative treatment methods need to be explored. Our study will determine and explore the effectiveness of an alternative treatment of OSA in the form of incremental inspired CO_2, utilizing a unique variable rebreathe device, with no added positive airway pressure (PAP). This device was developed via the cooperative efforts of biomedical engineers and respiratory physiologists/physicians at UW-Madison.

Aim 1. To develop a comfortable medical device with no increased pressure whereby the sleep apnea patient rebreathes exhaled gas in order to raise the fraction of inspired CO_2 (F_ICO_2), measures flow vs. time, counts apneas, automatically adjusts dead space to minimize apneas, hypopneas, and records all for download.

Aim 2. To evaluate how volumetric differences in the dead space device, used for sleep apnea treatment, affects the dynamics of CO_2 accumulation in the device by means of mathematical/simulation/computational modeling and experimental approaches.

Aim 3. To determine the effectiveness of a novel automatically adjustable CO_2 rebreathe device-–without added positive pressure–as a treatment for obstructive, central and mixed-type sleep apneas.

.

Hypothesis: Based on our recent proof of principle findings revealing the effectiveness of added CO_2 [7, 8]—without the addition of positive airway pressure—in a group of OSA patients and our development of an automatically adjustable variable CO_2 device to control and minimize the effective CO_2 dose, we propose that most types of obstructive, mixed, and central sleep apneas in most predominantly OSA patients will be significantly reduced through the application of our "Smart CO_2" device with minimal to no adverse effects on sleep state stability or cardiovascular responses.

1.2 Chapters Summary

These chapters are partially based on the following publications (Papers / Patent):

- **Mehdi Shokoueinejad**, Arman Pazouki, Jake Levin, Fa Wang, Jerome Dempsey, John G. Webster. "A modeling study on CO2 rebreathing device for spleep apnea treatment by means of CFD analysis and experiment" (Accepted, JMBE, Aug 2016)
- Mulchrone, A., **M. Shokoueinejad**, and J. Webster. "*A review of preventing central sleep apnea by inspired CO2*." *Physiological Measurement* 37, no. 5 (2016): R36.
- **Shokoueinejad, Mehdi**; Fernandez, Chris R.; Carroll, Emily; Wang, Fa; Levin, Jake ; Rusk, Sam; Glattard, Nick; Mulchrone, Ashley; Zhang, Xuan; Xie, Ailiang; Teodorescu, Mihaela; Dempsey , Jerome ; Webster, John. "*Sleep apnea: a review of diagnostic sensors, algorithms, and therapies"* (Submitted *Physiological Measurement*), Oct 2016
- Webster. J., dos Santos, I, **Shokoueinejad, M**., Levin, J., Dempsey, J., Wang, F., Xie, A. "SLEEP APNEA THERAPY DEVICE THAT AUTOMATICALLY ADJUSTS THE FRACTION OF INSPIRED CARBON DIOXIDE" United States Patent Filed. 15/376,180, Dec 11, 2016
- **Shokoueinejad M**, Wang F, Webster J, Jeremy D, "The use of Auto-Titration Sleep Apnea therapy device by adjusting Inspired Carbon Dioxide"
- **Mehdi Shokoueinejad** , Rayan Alkashgari, Hisham A. Mosli, Nazeeh Alothmany, John G. Webster,"Video Voiding Device For Diagnosing Lower Urinary Tract Dysfunction". (Accepted for publication, Journal of Medical and Biological Engineering, June 2016)
- Nazeeh Alothmany, Hisham Mosli, John G. Webster, **Mehdi Shokoueinejad**, Rayan Alkashgari1, "Critical Review of Uroflowmetry Methods". (Submitted, Journal of Medical Device 2016)

The development and presentation of the following chapters is summarized below:

Chapter 2: Background provides an overview of background information regarding effectiveness of using CO_2 in treating sleep apnea. It answers the following question, Does utilizing CO_2 as a treatment for sleep apnea make sense? Furthermore, it covers proof of principle, and potential adverse effects of imposed hypercapnia

Chapter 3: Sleep Apnea diagnostic signal modalities focuses on the engineering and methods of diagnosing and detecting apneic events and presents results and accuracy of using each signal modalities (both invasive and noninvasive) to detect apneic events in OSA and CNS patients.

Chapter 4: Sleep Apnea signal processing, algorithms, and techniques the objective of this section was to investigate and review literature to cover the most commonly used and high performance techniques to implement signal processing techniques in order to detect apneic events.

Chapter 5: Current modalities for SAS Due to the complex pathophysiology of sleep apnea, several nonsurgical and nonpharmacological treatments have emerged that have proven quite effective. However, an effective and comfortable treatment option for sleep apnea has yet to be developed. This section discusses the assistive and therapeutic oral devices for sleep apneas.

Chapter 6: A review of preventing central sleep apnea by inspired CO_2. a portion of the treatments covered in chapter 5 are often noncompliant due to the side effects of current treatments. This chapter prevents a review of the current standard treatment for central sleep

apnea, and investigates the advantages and possible consequences of using inspired CO_2 as an alternative treatment option.

Chapter 7: A modeling study on inspired CO_2 rebreathing device for sleep apnea treatment by means of CFD analysis and experiment. We performed a CFD analysis using an experimental test bench. The objective of this section is to evaluate how volumetric differences in the DS device, used for sleep apnea treatment, affects the dynamics of CO_2 accumulation in the device by means of mathematical/simulation/computational modeling and experimental approaches.

Chapter 8: Conclusion and Recommendations summarizes the contributions of this dissertation and recommends future work for the use of "SmartCO_2" for evaluation of diverse potential side effects such as sleep state disruption.

2 Chapter 2 Background and Significance of using CO_2

2.1 Treatment approaches to OSA.

Based on considerable clinical investigation over the past 3 decades it is generally agreed that the occurrence of significant apneas and hypopneas during sleep plus the accompanying chronic intermittent hypoxemia (CIH) must be treated in order to reduce the occurrence of cardiovascular, metabolic, and behavioral daytime consequences [9, 10]. To this end, several treatments have been developed including the application of positive airway pressure—either via CPAP or adaptive servo-ventilation (ASV) devices, along with dental devices, to improve airway collapsibility [11], and even use of chemoreceptor stimulants such as acetazolamide [12] or inhibitors such as supplemental oxygen [1, 13]. The use of CPAP is clearly effective in OSA but not well tolerated and greatly underutilized by many patients [6]; whereas, these other approaches are consistently effective in only a minority of OSA patients and usually with a milder form of OSA. For predominantly central apneas, no single treatment—including CPAP, oxygen, acetazolamide or ASV—has been found to be effective across the majority of CSA patients and with most treatments, patient compliance is a serious problem [3, 4].

2.2 Does utilizing CO_2 as a treatment for sleep apnea make sense?

Although upper airway collapsibility is a critical component of OSA, it is now well-established that pathophysiologic characteristics such as a sensitive arousal threshold (to elicit ventilatory overshoots), high "loop gain" i.e. chemosensitivity and plant gain, and/or reduced responsiveness of airway dilator musculature to chemoreceptor stimulation are also commonly present in the majority of OSA patients [2, 14]. In turn, CO_2 has been shown to be a major regulator of airway caliber during sleep, i.e. when the "wakefulness" stimulus is removed, as evidenced by the following observations: 1) small transient reductions in $PaCO_2$—as experienced with ventilatory

overshoots which occur upon recovery from an apnea and/or via transient arousals—of 1–4 mmHg will elicit apneas and ventilatory instability during NREM sleep [15, 16]; 2) adding inspired CO_2 sufficient to increase $PaCO_2$ 1–3 mmHg removes most or all of the hypocapnic induced central apneas and the periodic breathing induced via hypoxic exposure and/or CHF, spinal cord injury, or with idiopathic central apnea [17-21]; and 3) adding inspired CO_2 increases both phrenic (linear) and hypoglossal (alinear) motor nerve activity, thereby recruiting both diaphragm and upper airway dilator muscles [22, 23].

So theoretically, increasing CO_2 should stabilize central respiratory motor output as well as improve upper airway caliber and prevent upper airway obstruction. The VA sleep lab (The John Rankin Laboratory of Pulmonary Medicine, Medical Sciences Center, University of Wisconsin-Madison, Madison) has a long history of investigating roles for CO_2 in both central and obstructive apnea: a) using brief hypoxia or mechanical ventilation to elicit ventilatory instability and transient hypocapnia in sleep caused periodic airway obstruction at the nadir of the respiratory cycle in snorers [24]; b) small increments in inspired CO_2 markedly reduced upper airway resistance and airflow limitation during sleep in snorers [25]; c) most importantly, Porf. Dempsey's team recently completed a "proof of principle" experiment demonstrating CO_2 effects in OSA patients [1].

2.3 Proof of principle: mild/moderate hypercapnia stabilizes breathing and reduces OSA!

Prof. Dempsey's team used fixed dead space rebreathing devices in 21 predominantly OSA patients (AHI = 42 ±5 events/h) in whom 92% of events were obstructive apneas. Critical airway closing pressure (*P*crit) was positive in most patients. Rebreathing CO_2 has previously been shown to be highly effective in preventing central apnea and instabilities in sleep caused by hypoxic exposure and CHF (see above), and over many months in CPAP-treated OSA patients

with “residual” central apnea, i.e. so-called “complex” sleep apnea [26, 27]. This study was the first they were aware of, other than a single case study [28], that studied added CO_2 alone as a treatment for OSA [1].

When Dempsey’s team added dead space sufficient to increase $P_{ET}CO_2$ 1–5 mmHg over 1–5 h of sleep, they found that AHI was reduced to 15 ±4% of control and most often to <10 event/h in 17 of the 21 patients (see Figure 1) [1]. Further, adding smaller amounts of inspired CO_2 during the hyperpneic phase of the apnea cycle so that transient hypocapnia was prevented and $P_{ET}CO_2$ maintained at control levels, caused a smaller reduction in AHI to 31 ±6% of control in 14 of 26 OSA patients. These data were interpreted to mean that added CO_2 had two types of effects on sleep apnea depending on the amount of added hypercapnia: 1) stabilizing respiratory motor output when transient hypocapnia was prevented and 2) recruiting upper airway muscle dilators to prevent airway obstruction at mild to moderate elevations in $P_{ET}CO_2$. While this study showed added CO_2 to be a remarkably effective treatment of even moderately severe OSA, before they could envision clinical application of this treatment, they must consider other unwanted side effects of hypercapnia.

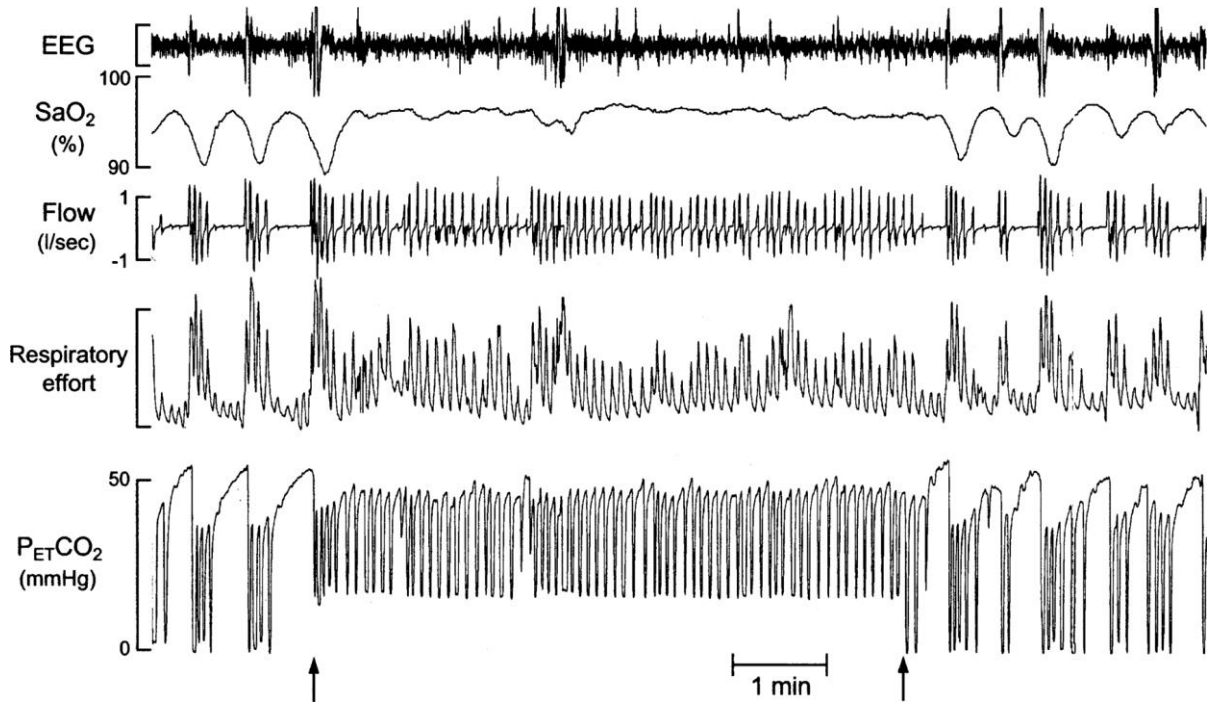

Figure 1. Effect of mild hypercapnia via rebreathing with fixed-volume dead space in a patient with OSA (AHI = 60). Repetitive obstructive apneas with associated transient EEG arousals were noted during air breathing as indicated by the repeated absence of flow despite respiratory efforts. Almost all of these obstructions and arousals were eliminated by raising $P_{ET}CO_2$ an average of 2 mmHg (left arrow) above stable, nonobstructed breathing levels in sleep. Abrupt removal of the added F_ICO_2 (right arrow) resulted in the immediate return of the cyclical obstructive apneas. On the basis of these types of findings, we raised $P_{ET}CO_2$ 2–5 mmHg via dead space rebreathing during 90–120 min of sleep in a group of patients with moderate to severe OSA and observed an average 85% reduction in AHI below air-breathing control in 17 of 21 patients [1, 2].

2.4 Potential adverse effects of imposed hypercapnia.

The chemoreceptor stimulation resulting from elevated systemic CO_2 increases both ventilation and sympathetic outflow—the latter potentially producing increased vascular resistance along with increased myocardial contraction and cardiac output. These effects are opposed by the local vasodilator actions of CO_2 on relaxing vascular smooth muscle and on eliciting bradycardia via effects on the cardiac pacemaker [29-31]. Excessive sensory input to the CNS via chemoreceptor stimulation may also elicit transient arousals thereby destabilizing sleep state [32]. In addition,

sustained hypercapnia—like hypoxia—is capable of affecting redox signaling mechanisms through production of oxidative and nitrosative derivatives [33]. Long-term cumulative effects of raising P_aCO_2 intermittently for short periods have not been studied. Acute effects have been shown primarily during wakefulness to have significant but small effects on systemic blood pressure (+1 mmHg increase in MAP per mmHg increase in $P_{ET}CO_2$) with no increases in vascular conductance [34, 35]. The effects of added CO_2 on sleep state in sleep apnea patients are mixed with increases in sleep state stability associated with $P_{ET}CO_2$ increments of <3–4 mmHg, whereas larger increases in CO_2 cause unstable sleep state [1, 19, 21, 36-38]. More detailed studies of these potential side effects of added hypercapnia throughout the night and over multiple nights in a variety of OSA patients are clearly needed to determine the effects of added CO_2 over a wide range on both sleep efficiency and cardiovascular status. Because many of the transient arousals in OSA patients are caused by apneic/hypopneic events, the degree to which added CO_2 might influence sleep state stability will depend in part upon the effect of the therapy on sleep disordered breathing.

In summary, we interpret Prof. Dempsey's proof of principle findings to mean that supplemental CO_2 could be an effective means of treating obstructive and central types of sleep apnea in most OSA patients, but there must be a means of controlling and minimizing the CO_2 dose to prevent unwanted side effects such as sleep state destabilization, excessive sympathetic activation, or inflammatory responses.

3 Chapter 3 Sleep apnea diagnostic signal modalities

This section reviews the current engineering approaches for the detection and treatment of sleep apnea. It discusses signal acquisition and processing, highlights the current nonsurgical and nonpharmacological treatments, and discusses potential new therapeutic approaches.

3.1 Introduction

An escalating 10% of the general United States population has clinically significant sleep apnea [39]. It is estimated that between 24–26% of men and 9–28% of women in the United States and Europe suffer from the disease, which is characterized by repeated periods of reduced or absent airflow that interrupt sleep [40]. Sleep apnea is categorized into three forms; obstructive sleep apnea (OSA), central sleep apnea (CSA), and the combination of OSA and CSA, constituting 84%, 0.4%, 15% of cases, respectively [41]**.** These disturbances have been shown to have significant effects on health and behavior such as cardiovascular morbidities, insulin resistance, neural injury, accelerated mortality, reduced cognitive function and poor work efficiency [40, 42]. In fact, OSA is believed to be a contributing factor to multiple devastating events such as the Three Mile Island accident, the Challenger explosion [43], and Chernobyl [44]. In addition, it can often amplify other medical conditions such as depression and schizophrenia [45, 46].

The gold standard diagnostic procedure for sleep apnea is polysomnography (PSG), more commonly known as a "sleep study". During this test, the patient stays overnight at a sleep laboratory where their respiratory and neurophysiological signals are recorded while they sleep**.** The resulting data are then analyzed by a specialist. Overall, it is a very time-consuming and expensive process as it can cost up to several thousand dollars [47-49]. Some systems are available for home-use, but it is still unclear if these machines are appropriate diagnostic tools

[50]. There is still a need for automatic systems that reliably detect apneic events, so many ongoing research efforts are concentrated on this task.

For over 25 years, the primary treatment intervention for sleep apnea has been Continuous Positive Airway Pressure (CPAP) [51], but nearly half of patients cannot tolerate CPAP and thus adherence is poor [52]. Due to the limited effectiveness of current CPAP systems, more acceptable designs for CPAP treatment and other innovations have been developed to prevent sleep apnea.

3.2 Methods to diagnose and detect apneic events

Today, the digital and computerized systems for monitoring and analyzing sleep data have replaced paper-based systems. According to the American Academy of Sleep Medicine (AASM) digital task force, systems used to diagnose and detect respiratory events encompass 5 basic and distinct processes [53]. First, the system must provide data acquisition and recording mechanisms. Second, the system must provide data viewing capabilities. Third, the system must enable the manipulation of data, in terms of visual scoring and editing of events. Fourth, the system must allow for data reduction, where epoch and event resolution data can be parametrized into useful diagnostic summary statistics for reporting. Finally, the system must enable storage and archival of relevant data and results. Despite the necessity of these systems in the clinical arena, to date, no uniform standard exists for any of these defined data processes.

According to the classification proposed by the AASM, sleep diagnostic devices could be categorized into 4 types. Type-1, standard PSG system which includes conventional biosignals, allowing acquisition of physiologic data from different organs, such as brain activity (EEG), muscle activity (EMG), eye movement (EOG), cardiac function (ECG, Heart Rate Variability), as

well as respiratory parameters such as airflow, respiratory movement/effort, and oxygen saturation. Type-2, Type-3, and Type-4 devices include a minimum of seven, four, and one signal channel of respiratory/neurophysiological biosignals, respectively [54]. Several clinically useful sensor modalities and techniques for observing relevant biosignals have been developed for the detection of respiratory events, which is described in the following section (2.a) and summarized in Table I.

Table I Comparison between Breathing Monitoring Technologies

Airflow Measurement Technology	Description	Direct or Indirect	Distinguish between OSA or CSA	Pros	Cons
Pneumotachography	Measures airflow through the pressure difference of linearized flow that is captured by a facemask	Direct	No	Considered Gold Standard, high accuracy	Wearing mask can be uncomfortable and cumbersome
Differential Pressure Sensors	Measure through pressure difference caused by an orifice that disrupts airflow captured by a facemask	Direct	No	Well characterized flow characteristics for flow calculations	Create pressure drop and resistance, a bad seal between the mask and the patient can cause erroneous measurements
Hotwire Anemometers	Measure through temperature change caused by airflow captured by a facemask	Direct	No	Fast frequency response, high accuracy, large range of measurable flows	Susceptible to patient debris, dependent on laminar flow, need a tight seal for accurate measurements
Nasal Cannula Temperature Measurements	Measure Temperature difference in nasal cannula from breathing	Direct	No	Able to be comfortably placed in nasal cannula	Slow response time, unable to accurately detect full range of flow values
Nasal Cannula Pressure Measurements	Measure pressure changes in nasal cannula from breathing	Direct	No	Correlates well with measurements from pneumotachometers	Proportionality coefficients drift over longer periods of study
PVDF	Produces linear output based on pressure and temperature changes from breathing	Direct	No	Respond to both heat and pressure, eliminates need for multiple sensors	Similar disadvantages to those of nasal cannula temperature and pressure measurement
RIP	Records changes in thoracic and abdomen cross sections through changes in self-inductance of wires wrapped around the body	Indirect	Yes	High accuracy, sensitivity and patient safety.	Calibration posture affects accuracy
IP	Measures changes in chest area through changes in electrical resistance	Indirect	Yes	Provides nonrestrictive continuous monitoring of respiratory rate	Calibration posture affects accuracy
Acoustic Monitoring	Detects breathing events through the frequency of noise produced from airflow	Indirect	No	Does not require patient contact	Does not yet accurately assess AHI indexes
FGV Sensing and Laser Sensing	Movements of chest and abdomen are monitored using lasers or light to detect cessation of breathing	Indirect	No	Does not require patient contact	Requires patient to patient calibration, and is highly dependent on patient movement

3.3 Signal and sensors for detecting and diagnosing apneic events

3.3.1 Direct and indirect measurement of airflow

Body plethysmography is considered the gold standard in the direct assessment of airflow, or tidal volume. In body plethysmography, the person is completely enclosed in a rigid constant-volume chamber. Drift of the body temperature and body movement inside the chamber can affect the pressure, volume, and flow measurement, possibly leading to a source of error [55]. Total body plethysmography accounts for changes in lung volume due to both air leaving the lungs during exhalation and gas compression from changing abdominal pressures. Although body plethysmography is considered the gold standard for airflow measurements during awake pulmonary testing, it is not feasible for sleep studies because it involves conscious patient participation. The patient must be seated upright and hold his or her mouth around the mouthpiece to fully enclose the respiratory circuit so that flow is captured and precisely measured by the plethysmograph.

Pneumotachography is the gold standard for monitoring ventilation during sleep. A flow meter is attached to a facemask which is placed on the nose and mouth [56]. The patient's airflow passes through a flow-resistive element with channels that laminarize the flow. With a laminar flow, the energy loss of the air going through the resistive element is due to viscosity. The pressure difference is measured across the resistive element to quantify the energy loss, and the flow F is directly proportional to the pressure difference: $F = \frac{\pi r^4 (P_i - P_o)}{8\eta L}$. Under laminar flow, the pneumotachometer obeys the Hagen-Poiseuille law, where r is the radius of the channel, Pi and Po are the pressures of the inlet and outlet ports, η is the viscosity, and L is the length of the

channel [57] (Fig. 1). Miscalculations of the viscosity can cause erroneous measurements of the flow.

In addition to the pneumotachometer, sensors commonly used in spirometry and ventilation monitoring include differential pressure sensors and hotwire anemometers. Differential pressure sensors operate by having a fixed orifice in the line of flow. The flow is laminar upstream from the orifice and turbulent downstream from the orifice, causing a pressure difference. Using Bernoulli's principle and known cross-sectional area of the channel, the flow is calculated from the pressure drop across the orifice.

Although differential pressure sensors are widely used in anesthesia systems, ventilators, and spirometers, they result in a high pressure drop across the orifice at high flows, which is not ideal, and are insensitive to low flows [57]. Additionally, differential pressure sensors are pressure dependent, and an unsealed respiratory circuit could cause erroneous measurements.

Hotwire anemometers are also used widely in spirometry and ventilation monitoring. Hot wire anemometers use a very fine wire electrically heated to some temperature above ambient. Air flowing past the wire cools the wire. Hotwire anemometers show great potential for medical airflow monitoring because they have a fast frequency response, high accuracy, a low pressure drop, and the ability to measure low flows and a wide dynamic range [58]. However, hotwire anemometry is susceptible to turbulent flows and debris. If placed proximally to the patient, notice should be taken to laminarize the flow and ensure debris does not affect the sensor or patient. When used in a mask for respiratory monitoring, a tight seal between the mask and the patient should be ensured to prevent leaks and cause erroneous flow measurement.

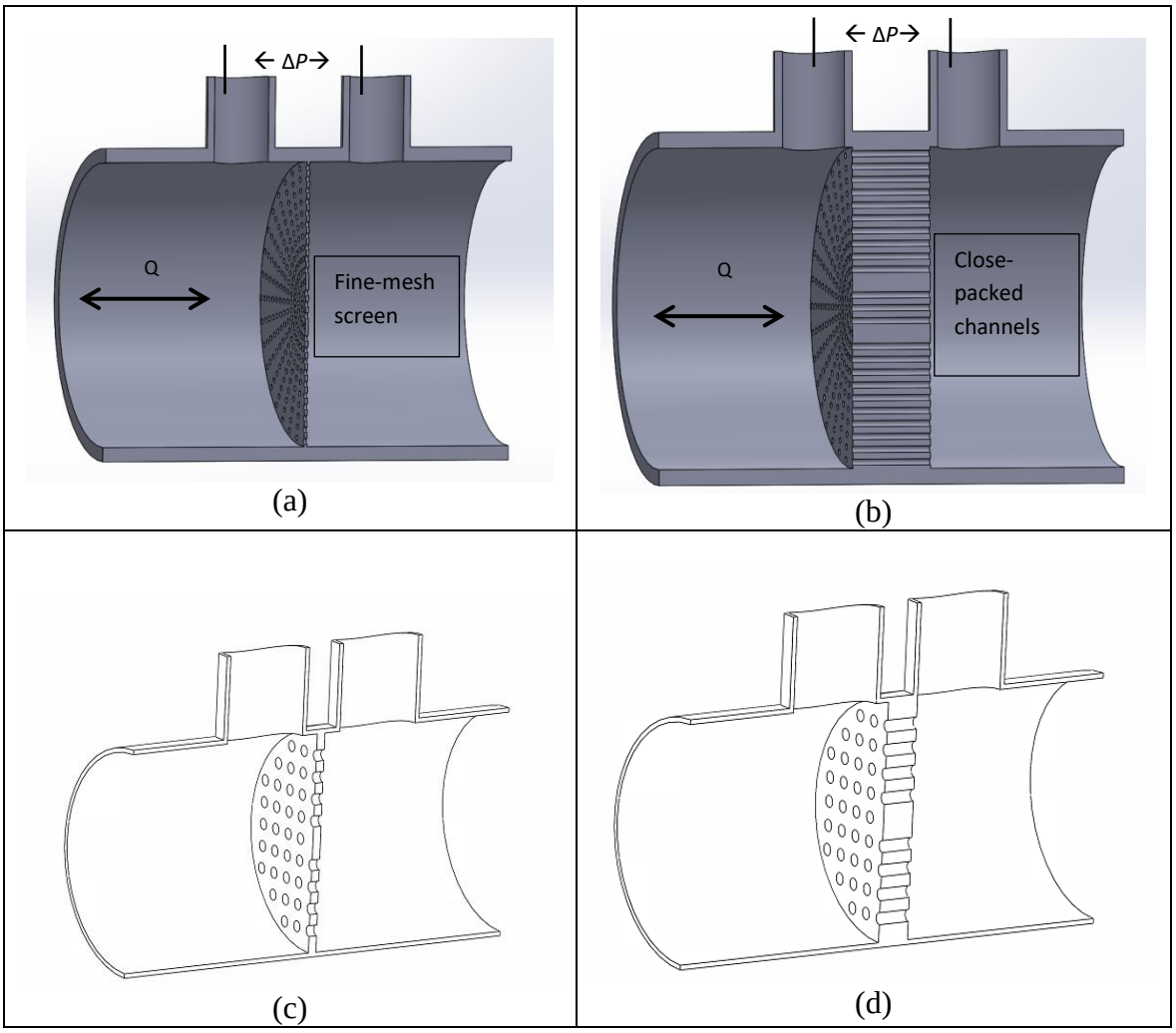

Figure 2. Pneumotachometer (a,c) Fine mesh or (b,d) closely-packed channels help to laminarize flow, so that energy loss of the flow is due to the viscosity. The pressure drops ΔP measured with sampling lines correspond to the energy loss due to gas viscosity [59].

Use of a facemask with a pneumotachometer, differential pressure sensor, and hotwire anemometer sensor is often considered bulky or uncomfortable for a patient to wear during an entire sleep study. In order to prevent disturbance of sleep and circumvent the need for patient participation for flow measurement, flow sensors have been placed in nasal cannulas or above the mouth and below the nose. When measured from a nose cannula, parameters such as humidity, end-tidal CO_2, temperature, and pressure can assess changes in flow and be used to detect apneas and hypopneas. Although thermistors in a nose cannula have been widely used to assess cessation of flow, they have a slow response time and cannot reliably detect the full range of flows that

occur during respiratory events [60-62]. Positioning of thermo-elements on the face, body positioning, and variation in sensitivity and frequency response between different sensors can cause variability which contributes to a poor relationship between air temperature and airflow [63, 64].

Alternatively, the pressure measured from a nasal cannula has shown to correlate well with patient breathing. When measuring the pressure of the nasal cannula, the measurement is linearized by computing the square root of the nasal prong pressure [65]. Several studies have compared the Apnea Hypopnea Indexes (AHI) that resulted from nasal cannula pressure measurements to scores that resulted from thermistors or chest wall movements with reported bias of the AHI ranging from $-9.6\ h^{-1}$ to $+4.6\ h^{-1}$ [66-71]. When compared with face mask pneumotachometers, the AHI score of the nasal pressure cannula had a fair correlation to that derived from pneumotachometer. However, when measured over several hours, proportionality coefficients shifted, and therefore the nasal pressure recordings did not quantitatively reflect airflow [72]. Although not quantitatively reflecting patient airflow, the nasal pressure cannula monitoring can be used to detect inspiratory flow limitation.

Polyvinylidene Fluoride (PVDF) sensors have been recently introduced for sleep respiratory monitoring. PVDF consists of a thin plastic film, that when polarized, is sensitive to both temperature and pressure changes, and produces a linear voltage output based on those changes. When compared with the traditional methods of a thermistor and nasal pressure cannula , PVDF had a near unity correlation coefficient for the four indices calculated, including apnea–hypopnea index (0.990), obstructive apnea index (0.992), hypopnea index (0.958), and central apnea index (1.0) [73]. PVDF sensors eliminate the need to have multiple sensors placed at the same location,

as they respond to both heat and pressure. However, they have similar limitations to those of thermistors and pressure sensors.

The commonly used respiratory inductance plethysmography (RIP) indirectly measures ventilation by recording changes in thoracic and abdomen cross-section. RIP measures abdomen chest movements through coiled wires wrapped around a patient's chest that carry a low-amplitude sine wave. Changes in chest and abdomen circumference alter the self-inductance of the wires, and therefore the frequency of the sine wave, which can be demodulated and processed to track changes in chest and abdomen size [74]. RIP is widely studied and regarded highly by the AASM due to its great accuracy, sensitivity, and high patient safety [75]. The wires were initially integrated into two elastic bands, one around the abdomen and one around the chest, but RIP has also been used with wires sewn into shirts, comfortably worn by patients.

With proper calibration, RIP can achieve a tidal volume measurement accuracy of 96% when compared with pneumotachography or spirometry [76]. The posture of the patient greatly affects the measurement of tidal volume; if the RIP is calibrated with the patient in the upright position, sleeping and breathing in the supine position can lead to greater sources of error. However, Gonzales et al. found that using a two-body posture calibration method can improve the error due to changing body position, with measured tidal volumes falling within 4–10% of those measured by spirometry [76].

RIP is noted for its added benefit of helping to distinguish between obstructive sleep apnea (OSA) and (CSA), as illustrated in Figure 2. During OSA, cessation of breathing occurs despite an ongoing effort to breathe, while CSA occurs when the brain does not properly send signals to the

muscles controlling respiration. During CSA, the lack of effort by the muscles in the abdomen and chest can be noted with the use of RIP, aiding distinguishing CSA from OSA.

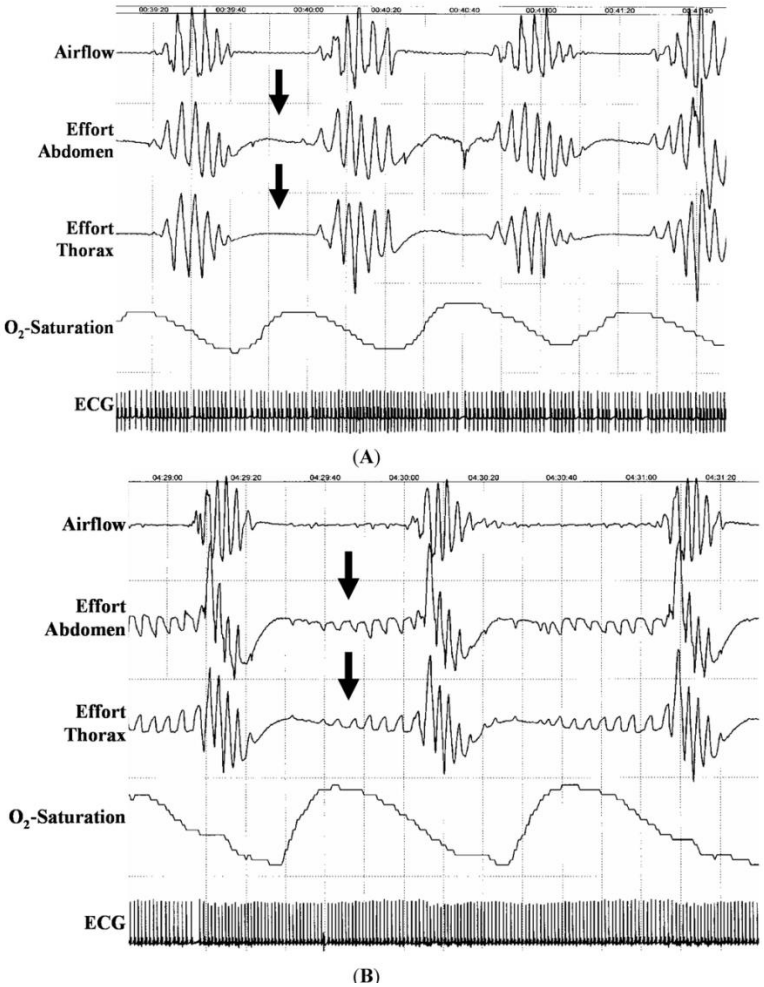

Figure 3. Polysomnography with Central Sleep Apnea (A) and Obstructive Sleep Apnea (B). Chest effort indicated by the arrows is absent in CSA. Reprinted with permission from [77].

Impedance plethysmography (IP) measures respiratory cycles by changes in electrical resistance. When volume changes within an induced electrical field, a high frequency (about 100 kHz), low level current (about 1 mA or more) is injected through electrodes placed on the chest wall. As the thoracic cross-sectional area changes during breathing, it changes the electrical resistance, which can be recorded as a change in voltage [56]. Like RIP, IP is prone to error and inconsistency due to changes in patients' posture during recording signals.

In addition to more traditional thermal and pressure sensors, acoustic monitoring has also been researched as a possible means to detect apneas and hypopneas. An acoustic sensor is used to record the signals generated from the expired air flow. These signals can be acquired in the natural sleep environment without any contact to the subject and can be used to detect breathing events, obstruction and snoring [78-80]. Children with suspected obstructive Sleep Disordered Breathing were found to produce louder high-frequency inspiratory sounds (HFIS) during sleep as well as have narrower airways [81]. The HFIS were observed using a microphone placed above the observed patient. Although the occurrence of HFIS correlated with the patient's rate of obstructive respiratory events, the HFIS intensity did not correlate well with respiratory effort as measured by an esophageal catheter [82]. This could be explained by the fact that HFIS intensity increases with high-velocity, high-turbulent flows, and some obstructive events do not have any patient airflow. While acoustic monitoring has not yet been used to accurately assess AHI indexes, acoustic monitoring has been used in the commercially available Masimo RRa® to determine respiratory rate and apneas through an acoustic sensor that adheres to patients' necks. The RRa® was found to be 3% more accurate than a capnograph when assessing respiratory rate, and had a higher sensitivity ($P = 0.0461$) when detecting cessation of breathing (≥ 30 s) [83].

In another effort to diagnose and monitor respiratory events without patient contact, fiber grating vision sensing and laser sensing have been researched. With these technologies, the positions or movements of the chest and abdomen are monitored with respect to the patient's center of gravity. Using over 100 sampling locations, respiratory events could be determined and distinction between OSA and CSA could be made [84]. However, this method requires much calibration between patients, and is highly dependent upon patient movement, which can occur during sleep.

With refinement, fiber-grating vision sensing could be used to detect sleep apnea without patient contact.

Researchers have also explored the use of off-the-shelf smart phones and applications to diagnose sleep apnea using a sonar system with frequency modulated continuous waves. The system uses the phone's speakers to emit sound waves and analyzes the reflections. The reflections from the body arrive back to the phone at different times depending on the distance from the phone, and amplitude changes due to changes in breathing are extracted. The system can even analyze breathing from two patients lying in the same bed. When placed within 1 m of the patient, the phone application can estimate respiratory rate with 99.2% accuracy. When compared with a traditional PSG, the application identified CSAs with a 0.9957 correlation coefficient, OSAs with a 0.9860 correlation coefficient, and hypopneas with a 0.9533 correlation coefficient. The system accurately predicted apneic events without patient contact, but does not provide other information provided in a traditional PSG, including patient position, visual information, and electroencephalogram signals used to determine sleep stages (REM, non-REM, and awake) [85].

3.3.2 Measurement of the concentration or partial pressure of respiratory gases

CO_2 concentration:

The concentration of respiratory gases in the blood can reflect the condition of patients' breathing patterns. While the arterial CO_2 concentration is a parameter of interest, it is expensive and invasive to monitor during polysomnography. Alternatively, capnometry is the measurement of the CO_2 concentration of exhaled air, and end-tidal PCO_2 ($P_{ET}CO_2$), is marked as an important parameter with significant correlation for apneic event detection [86]. Transcutaneous carbon

dioxide (PtcCO_2) can also be monitored. For both $P_{ET}CO_2$ and PtcCO_2 the accuracy and potential sources of error of estimating the arterial CO_2 concentration must be considered.

Monitoring of $P_{ET}CO_2$ is commonly used in pediatric patients and can be used to score apneic events. An apnea could be observed by the absence of an $P_{ET}CO_2$ peak or wave from the capnography monitor. The $P_{ET}CO_2$ is typically sampled via a sampling line connecting the nasal cannula to an external sensor, so mouth breathing or occlusion of the nasal cannula can affect the ability to monitor breathing events. Additionally, because $P_{ET}CO_2$ corresponds to the highest concentration of CO_2 within a breath rather than the flow or volume of the breath, $P_{ET}CO_2$ signals could be misleading during an inspiratory apnea if small breaths with a high CO_2 concentration continue [87].

PtcCO_2 measurement is a warm sensor placed on the surface of the skin and an electrochemical cell that determines the pH change due to CO_2 concentration. The elevated temperature of the sensor causes local hyperemia and an increased arterial blood supply below the sensor. The PtcCO_2 at the sensor is higher than the actual arterial value due to increased local blood and tissue PCO_2 and epidermal cells producing CO_2, so a correction factor is often used to determine the arterial PCO_2 from the PtcCO_2. A highly permeable membrane separates the electrochemical cell from the skin, and an Ag/AgCl reference electrode is used to measure the pH. With sensor temperatures of 42 °C, or even as low as 37 °C, a good correlation between PaCO_2 and PtcCO_2 have been reported [88].

O_2 concentration:

Oxygen concentration is also of great interest during sleep studies, because the arterial oxygen concentration may fall dramatically during an apneic event. Pulse oximetry monitors the peripheral oxygen saturation (SpO_2) by shining red and infrared light through a fingertip, ear or toe. The amount of red or infrared light that is absorbed corresponds to the concentration of oxygenated hemoglobin and deoxyhemoglobin in the blood, and therefore the oxygen concentration in the blood can be determined [56]. The SpO_2 changes during respiratory events such as apneas and hypopneas, and hypopneas are even classified as reduced airflow accompanied generally by a SpO_2 drop of at least 4%. Normal SpO_2 levels vary between patients, with normal ranges falling between 85–95% [80].

Pulse oximetry monitors are prone to error and false desaturation measurements due to motion artifact, noise, or missed readings. To reduce errors, pulse oximeters average readings and report oxygen levels every 3 to 12 s, which may cause a delay in alarms or monitoring. Notwithstanding, whether incorporated into at home monitors or used as a part of a polysomnography suite, pulse oximetry has proven to be a valuable tool in detecting and diagnosing sleep apnea. The channel typically provides summary statistics (means, minimum levels), quantifies the total time the patient experiences oxygen saturation under various thresholds and tallies the number of events where the patient experiences desaturation between 2–5% [89].

Additionally, near-infrared spectroscopy (NIRS) is a method used to continuously and noninvasively monitor cerebral oxygen concentration. NIRS uses light with wavelengths from 700 to 1300 nm to penetrate the skull to the cerebral tissue. Changes in the relative amounts of oxygenated hemoglobin and deoxygenated hemoglobin can be monitored through changes in the absorption of the light [90]. NIRS may provide an earlier warning to decreased blood

oxygenation. In a study of ten children who required episodes of apnea during laser airway surgery, cerebral oximetry indicated a 5% decrease in cerebral oximetry (rSO_2) in all patients before pulse oximeter measurements decreased by 5%. Also, in all patients, the rSO_2 decreased by 10% before the pulse oximeter measurements decreased by 10% [91]. Cerebral oximetry with NIRS provides a non-invasive measurement of oxygenation with a possibly faster response time than pulse oximetry.

Photoplethymography (PPG) is an uncomplicated and relatively inexpensive optical measurement technique that has been used to detect variations of blood volume in the microvascular bed of tissue. Using simultaneous reflective PPG and a force sensor, placed on the opposite sides of same fingertip, Keikhosravi et al showed that the photoplethysmogram signal is mainly due to volume changes not the blood compression and rarefaction induced by heartbeat [92]. Although, PPG has traditionally been used to measure oxygen saturation and heart rate determination, it has shown that its capability and usefulness is not limited to the calculation of the aforementioned physiological parameters. Active research efforts in this field are being devoted to identifying additional physiological parameters that can be extracted and measured from the PPG signal. Thus, investigation into the analysis of the PPG signal has increasingly become widespread. Ghamari proposed a mathematical model to represent the original PPG signal as summation of two Gaussian functions [93]. In the case of sleep apnea as an example, when apnea occurs, the sympathetic activity of the nervous system increases. This increase leads to vasoconstriction which directly reflects on the original shape of the PPG signal by a decrease in the signal amplitude. [94-96]

3.3.3 Measurement of electropotentials

Electropotentials are measured during sleep studies to detect SAS events and sleep patterns. Signals such as EMG, EEG, and EOG are collected during polysomnography, as illustrated in Figure 3.

A number of studies have shown that SAS events and patterns can be detected with high accuracy using only single channel ECG data. Heart rate variability (HRV) information can be obtained from the ECG signal, and using the standard deviation of the NN or RR interval of both nighttime and daytime heart beats has shown to detect obstructive sleep apnea with high sensitivity (89.7%) and high specificity (98.1%). However, using ECG as the sole parameter for sleep apnea screening has its limitations, as diseases such as diabetes, sequelae of myocardial infarction and chronic heart failure, which are often associated with OSA, can cause false negatives when screening for OSA [97, 98]. Changes in HRV due to tidal volume and breathing effort must be taken into account when processing HRV data [99]. Even when not used as the sole parameter for sleep apnea detection, ECG data are still a valuable tool used in polysomnography.

Chin and leg EMG is a traditional parameter used during polysomnography. EMG data are most often used during polysomnography to monitor sleep stages, along with EEG and EOG, because muscle tone subsides during NREM sleep and is at its lowest during REM sleep. In addition, chin electrodes are typically placed close to the Geniohyoideus (GH) and Genioglossus (GG) muscles which are pharyngeal dilator muscles and which play an important part in maintaining upper airway patency. Therefore, chin EMG can be considered a noninvasive method to assess upper-airway muscles' EMG activity shown in Fig. 3. OSA patients have been found to have significantly higher chin EMG at sleep termination, which correlates with other findings that OSA

patients have higher upper airway muscle activities than normal subjects in wakefulness [100, 101].

Lastly, surface EEG allows for detailed analysis of depth of sleep through sleep staging, as well as sleep architecture and efficiency based on phasic transitions through sleep cycles. While not required to obtain a SAS diagnosis, EEG provides a clinically useful measure of the effect of SAS respiratory pathology on the overall quality of sleep. In SAS patients, conventional parameters showed predictable decrements in total sleep time, fragmentation of sleep architecture, slow wave sleep, and REM sleep and increases in stage 1 and nocturnal awakenings [102]. Moreover, obstructive event-induced work of breathing or hypoxemia has an effect on electrocortical activity. In a study of severe SAS patients, EEG signals measured directly following apnea onset displayed average differences of 268% between initial and maximum values, and 202% between initial and final values [103]. As such, the AASM recommends three EEG derivations for scoring of sleep; including frontal, central, and occipital sensor locations F4/M1, C4/M1, O_2/M1, as well as back-up derivations: F3/M2, C3/M2, and O1/M2 [104, 105].

Electrooculogram (EOG) is used to capture the distinct sharp eye movements characteristic of REM sleep. Arousal from REM sleep is accompanied by sudden halting of rapid eye movement on EOG and increasing in muscle tone recorded on EMG.

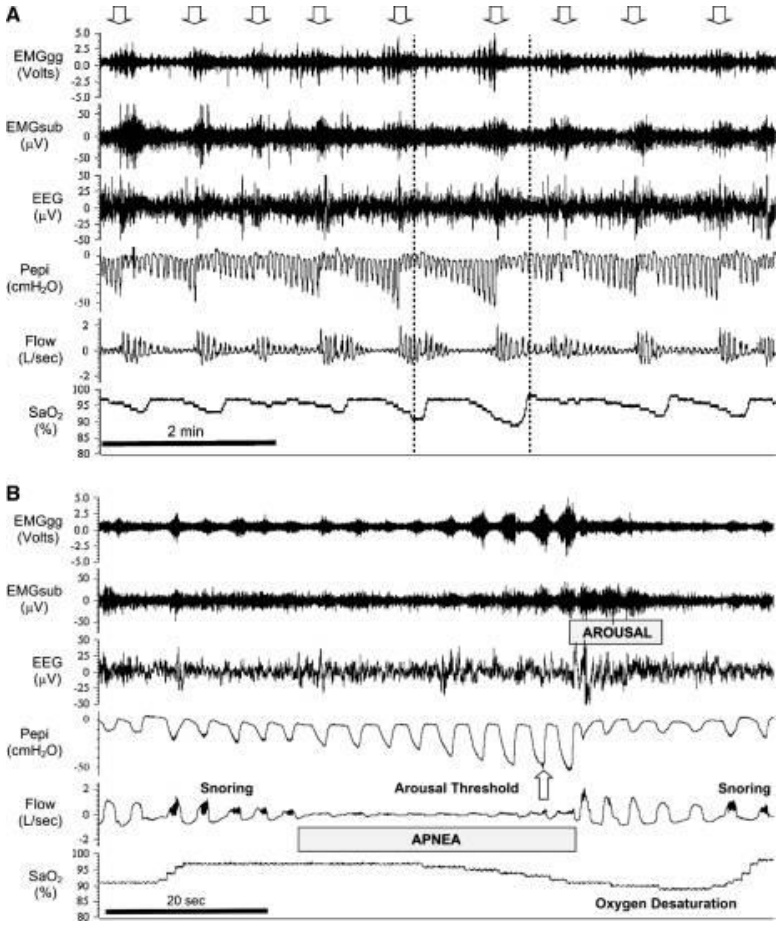

Figure 4. The polysomnographic tracing includes electroencephalogram (EEG), electromyogram (EMG) EMGgg: Electromyogram of the genioglossus muscle (intramuscular); EMGsub: EMG of the submental muscle (surface), RESP flow, SaO_2, etc. A) The cessation and resumption of flow defines the apneic event. B) one obstructed apneic event (between the dotted vertical lines in A) is expanded to illustrate the progressive increase in inspiratory effort, pressure at the level of the epiglottis (*P*epi) and dilator muscle EMG (EMGgg) during the apnea. It demonstrates snoring on the flow tracing follow by apnea, and increases in EMG activity throughout the apneic event. Reprinted with permission of the American Thoracic Society, Copyright © 2016 American Thoracic Society. [106].

3.3.4 Patients' sleeping behavior and body movements in sleep

Body position of patients during a sleep cycle is of great interest to researchers because OSA severity can vary with body position. To monitor body position, accelerometers or video recordings have been used.

Using accelerometry (or actigraphy), patient body movements can be recorded, typically with inexpensive piezoelectric sensors. Its ability to track body motion and snoring helps track

information such as sleep duration and the number of times a patient wakes during the night. Although actigraphy has lower specificity than polysomnography in identifying wakefulness in patients, its use might be preferred to polysomnography when patient monitoring spans a long duration, as it is easier for patients to comply with actigraphy monitoring than traditional polysomnography [80].

Video recordings and corresponding image processing technology have been widely used in the noncontact apnea detecting field. Many researchers correlate the PSG signals to the patient's sleeping behavior, such as body position, which is extracted from videos. In some cases, video recordings have helped to confirm diagnoses when used in conjunction with PSG signals. Even though the AHI limits may be normal, video recordings may show supplemental information about respiratory events such as head movements and arousals [73, 107-110].

Table II. Summary of SAS diagnostic parameters from PSG, types of physiological events encompassing those parameters, sensor modalities for detecting events, and classification methods, and algorithms commonly used to recognize SAS event patterns.

Table II Summary of SAS diagnostic parameters, the types of physiological events, sensor modalities, and commonly used classification methods

Diagnostic Parameters	**Characteristic Physiological Events**	**Relevant Signal and Sensor Modalities**	**Classification Methods**
Apnea-Hypopnea Index (AHI), Respiratory Disturbance Index (RDI), other Respiratory Parameters	Obstructive Apneas, Central Apneas, Mixed Apneas, Hypopneas, Respiratory Effort-Related Arousals, Oxygen Desaturations, Bradycardia, Sinus Tachycardia	Pneumotachometry, Nasal cannula pressure sensors, Thermistor, thermocouples, Polyvinylidene Fluoride, Hotwire anemometers, Respiratory inductance plethysmography (RIP), Impedance pneumography (IP), Magnetometer, Strain gages, End-tidal PCO_2, Pulse oximetry, Photoplethysmography, ECG, Audio (acoustic sensor), IR, Sonar, Video, Actigraphy,	Amplitude and Adaptive Thresholding, Fuzzy Networks, Artificial Neural Networks, Decision Trees, Ensemble Models, Nearest Neighbor Methods, Linear and Kernel SVM, Deep Neural Networks
Sleep Architecture, Sleep Efficiency (SE), Arousal Index (ArI), Sleep Latency (SL), REM Latency (RL), Total Sleep TIme (TST), Periodic Leg Movements (PLMS) Index, other Arousal and Sleep Parameters	Stage Wake, Stage REM, Stage N1, Stage N2, Stage N3, Arousals, Sleep Spindles, K-Complexes, Periodic Leg Movements, Spikes, Sharps, Vertex Wave Sharps	EEG (F4-M1, C4-M1, O2-M1, F3-M2, C3-M2,O3-M2), Chin EMG, EOG, ECG, Leg EMG, Audio, Video, Actigraphy	Autoregressive Models, Hidden Markov Models, Gaussian Mixture Models, Linear and Quadratic Discriminant Analysis, Random Forests, Regression Trees, Deep Belief Networks, Deep Neural Networks

4 Chapter 4 Sleep Apnea Signal processing, algorithms, and techniques

Once single or multichannel sleep data of sufficient quality has been acquired, subsequent analysis is needed to quantify and summarize relevant diagnostic parameters for SAS including the Apnea-Hypopnea Index (AHI), Respiratory Disturbance Index (RDI), Arousal Index, sleep architecture, and sleep efficiency. The current gold standard for obtaining these measurements is manual scoring, and typically involves a certified polysomnography technician applying visual pattern recognition techniques to the sleep data on a 30 s epoch basis. For each epoch, the technician identifies any obstructive, central or mixed apneas, hypopneas, respiratory effort related arousals, EEG arousals, oxygen desaturations, arrhythmias, periodic leg movements, the relevant sleep stage, among other physiological variables [111, 112].

This manual scoring process is time consuming, often requiring 1–2 h per Type-1 sleep study. In addition, manual scoring is prone to error and inconsistency. The AASM Inter-Scorer Reliability program enables estimation of the average epoch by epoch agreement between an individual technician's scoring to an expertly scored sample polysomnography study. The latest results indicate a 77.1% agreement on OSAs, 52.4% on CSAs, 65.4% on Hypopneas, and 82.6% on Arousals [113, 114]. A key source of variability comes from indirect measurement of respiratory airflow; thermistor on the nose, pressure measurements at the nose, and other common signals are indirect measures of airflow and breathing, and render it difficult to objectively detect hypopneas or central sleep apneas. Other factors contributing to relatively low inter-rater agreement include physiological variability between patients, data quality and noise characteristics, human fatigue, and the task complexity of analyzing hundreds of epochs of multimodal sensor data for dozens of multivariate physiological patterns.

Significant research efforts have focused on exploring computational approaches to sleep scoring, with the aim of developing automated systems that can achieve noninferior, equivalent, or superior performance relative to expert humans [115]. Multisite studies at 5 academic centers have evaluated the performance of an automated scoring system versus computer-assisted manual scoring, as well as the computer-assisted scoring agreement across sleep centers [116, 117]. Large validation studies like these have assisted in the development of commercially available systems for autoscoring [118, 119]. Yet the acceptance of these systems remains limited; in 2015, a survey of 179 sleep labs reported by ResMed showed only 14% used any form of autoscoring or computed assisted scoring as of 2015. As such, the development of broadly accepted and utilized computational approaches to scoring remains an open research challenge.

This section provides an overview of the fundamental algorithmic and signal processing techniques employed to automate the detection of apnea related physiological events. In particular, we discuss the application of amplitude based analysis, time-frequency and wavelet based transformations, nonlinear transformations, autoregressive models, and recent machine learning approaches to identify apneas, hypopneas, and sleep stages in single and multichannel polysomnography data settings. This discussion is by no means comprehensive, and seeks to give readers a sense of the classes of tools at hand. For additional information, we refer the reader to a review on computer-assisted diagnosis specific to apnea-hypopnea event detection [120], a comparative review of automated sleep staging algorithms [121], and a review specific to artificial neural network applications for sleep scoring [122].

4.1 Signal processing and data representations

A common framework through which we can consider the problem of recognizing SAS related patterns in physiological data involves two general concepts—data representations and models. Data representations can be defined as abstract reformulations of the original raw signal data that aim to exhibit desirable analytical properties for classification, such as being more discriminative between disease and normative classes, better conditioned, lower in dimensionality, sparser, among others. Models then operate on these resulting data representations, and estimate or predict the corresponding class label for each representation. In the context of automated approaches to sleep scoring, each data representation typically represents a single epoch of sleep data, while the applied models output which, if any, of the aforementioned apnea related events are found within that epoch.

The process of obtaining data representations involves applying techniques from fields including signal processing, pattern recognition, data mining, feature engineering, and machine learning to single and multichannel polysomnography data shown in Fig. 4. The sections below discuss some common data representation techniques that have exhibited promising performance for respiratory and neural event detection in empirical studies.

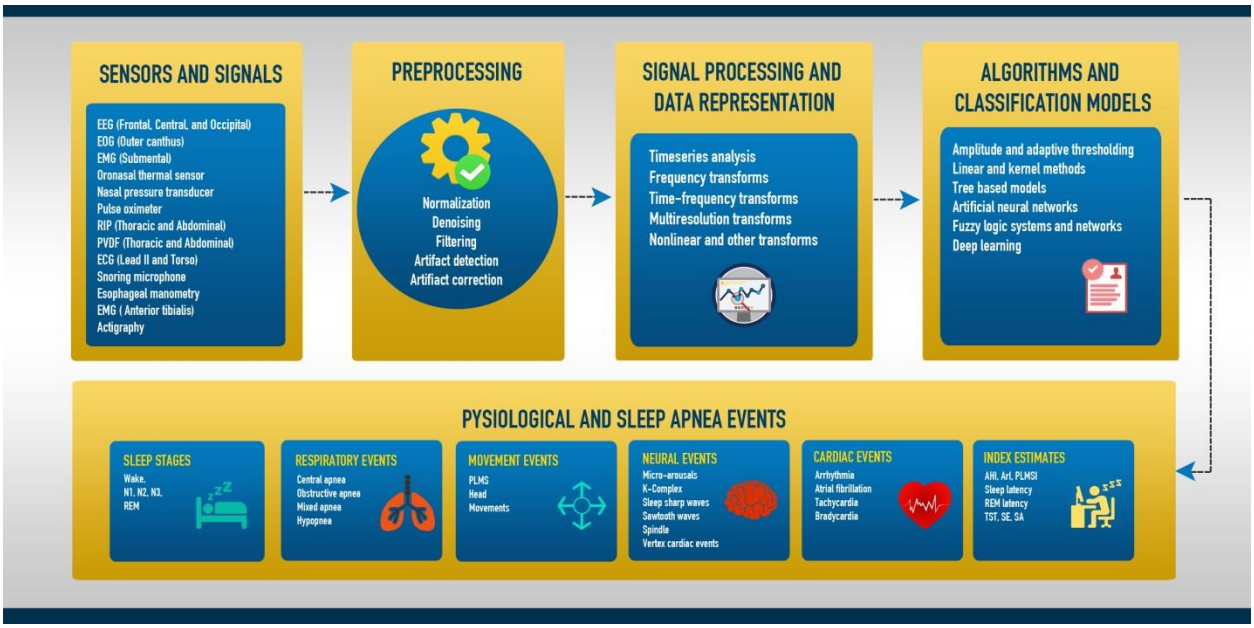

Figure 5 Demonstrates SAS diagnostic parameters of interest, the types of physiological events that characterize those parameters, clinically useful sensor modalities for observing disease relevant biosignals, and classification methods commonly used to recognize SAS event patterns.

4.1.1 Time-frequency based transforms

Time-Frequency domain transformations are among the most popular techniques for producing data representations for apnea and hypopnea detection problems. This approach commonly involves computing sufficient statistics such as mean, variance, skewness, kurtosis, variation and others on the data in the frequency or another transform domain, and supplying these summary level statistics to an adaptive model for detecting apnea and hypopnea events [123, 124]. For sleep staging, frequency power spectrum, power ratio, spectral frequency, duration ratio, spindle ratio, sws ratio, relative spectral band energy, harmonic parameters, itakura distance, and interdependency measures have also been effective [125, 126].

4.1.2 Multiresolution and wavelet based transforms

Multiresolution analytical (MRA) techniques, like the Discrete Wavelet Transform (DWT), have also demonstrated promising performance for sleep apnea event detection [124, 127] and sleep staging [128, 129] in both single and multichannel settings. These techniques commonly involve an orthonormal decomposition of the signal data into some Wavelet basis, whereby summary statistics can be computed at multiple levels of resolution. In the multiscale setting, additional informative parameters like Multiscale Entropy have been incorporated for effective single channel sleep staging [129]. Sleep data tend to exhibit greater sparsity in the Wavelet domain than the original, so this technique can be used to compress the dimensionality of epoch representations in cases where there are few epochs for analysis and the modeling system becomes underdetermined.

4.1.3 Nonlinear and other transforms

Epoch by epoch data representations have been generated using nonlinear and other transformation procedures to classify respiratory and neuronal signals with some success. Largest Lyapunov Exponent (LLE), Detrended Fluctuation Analysis (DFA) and Approximate Entropy (APEN) have been used to estimate OSA severity [130]. Analysis of ECG signals enables the extraction of information on both heart rate and the rate of respiratory inspiration and expiration. Cardiorespiratory coupling techniques explore the interplay between these derived heart and respiratory rate signals by analyzing their covariance structure, a measure of how the correlated variables change together. In the single ECG channel setting, nonlinear cardiorespiratory coupling dynamics were extracted based on recurrence quantification analysis to identify apnea and hypopneas [131]. The Choi–Williams distribution, Hilbert–Huang Transform, as well as nonlinear spectral techniques including bispectral analysis, nonlinear higher order spectra, the scattering

transform, and reflection coefficients produced by a lattice filter representation of a recursive autoregressive process have been used for classifying sleep stages with comparable accuracy to human experts [124, 132, 133]. Some recent work has applied unsupervised machine learning approaches to apnea hypopnea detection, including particle swarm feature optimization paired with 1-nearest-neighbor classification methods with robust performance [134].

4.2 Algorithms and classification models

Models and classifiers take an individual feature vectors or representations and outputs either continuous or discrete class labels. For sleep scoring, the data representations are typically vectors that correspond to a single 30 s epoch of polysomnography data. These vectors are used as inputs, while class labels for each epoch include normal breathing, apnea events, hypopnea events, and the relevant stage of sleep. The available classifiers range in complexity from simple models with a small number of static parameters such as adaptive thresholds, to architectures composed of hundreds of millions of tunable parameters as in the case of deep learning. The key aspect of machine learning classifiers is that their core models can be adaptively parameterized through a training optimization procedure that seeks to minimize the prediction error on available data while maximizing the generality to unseen data. In this sense, all models discussed here with data-adaptive parameters whose performance improves with experience could be understood in a machine learning context. This section of the review discusses specific algorithmic approaches for the classification of SAS patterns in single or multichannel PSG data.

4.2.1 Amplitude and adaptive thresholding

Some studies proposed an amplitude-based thresholding algorithm while their method is including nasal airflow (NAF), Forced Oscillation Technique (FOT), and/or abdominal breathing

signals [135]. There have been many studies showing the amplitude-based thresholding of different respiratory signals for online detection of the apneic events. Studies show that online automated apneic detection would be efficient when incorporating two or more different respiratory derivations. Taha et al, presented detection of hypopnea and cessation in breathing by analyzing the oxyhemoglobin saturation level combined with RIP. Further classification of apnea into central, mixed, or obstructive was achieved based on the presence of abdominal breathing effort. The algorithm was able to detect 93.1% of the manually detected events [136].

Other studies investigated amplitude-based and breath-by-breath ways for offline detection by using a forced oscillation technique FOT and nasal mask pressure signal time series [137]. The method is based on pressure amplitude, FOT amplitude and baseline extraction. Then, these features were compared with defined thresholds which lead to detection and classification of hypopneas as well as obstructive, mixed, and central apneas [137]. In addition, adaptive thresholding has been used with Teager Energy Operators (TEO) and other R-wave detection methods to predict OSA and CSA events from single channel ECG [131].

4.2.2 Linear and kernel methods

Linear and kernel methods have been utilized for pattern recognition for SAS applications due to their simple implementation, theoretical soundness, and broad extendibility. First and second order autoregressive techniques have used model sleep phasic transitions as autoregressive processes. Autoregressive models such as these have been employed to utilize single channel EEG data for the estimation of epoch-by-epoch sleep stages [138] [139]. Another popular machine learning method is Support Vector Machine (SVM). Vapnik and Al-Angari used SVM classifiers with linear and second-order polynomial kernels to evaluate the classification of

normal and apneic events using the respiratory signals, thoracic and abdominal, combined with ECG and oxygen saturation signals [140, 141]. The best performance of their implemented algorithm was achieved when features of available respiratory and oxygen saturation data sets were used. In the subject experiment, the polynomial kernel had distinct improvement in the oxygen saturation accuracy as the highest accuracy of 95% was achieved by both the oxygen saturation (Sensitivity: 100%, Specificity: 90.2%) and combined-features (Sensitivity: 91.8%, Specificity: 98.0%). However, uses of long data sets need long training time which is considered a disadvantage of the SVM. Theoretical and empirically-driven development of new kernel methods which are well suited to the recognition of SAS related events is an open area of ongoing research.

4.2.3 Tree based models

Tree based models have grown more popular in SAS event detection literature for their numerous desirable properties including robustness to noisy signal data, built in feature selection mechanisms, and human interpretability. Prior work includes using C4.5 decision trees to estimate OSA severity from Nasal cannula flow, thoracic belt movement and blood oxygen saturation [130]. In another study, decision trees were evaluated against the performance of neural network, auto neural, regression to identify apnea and hypopnea events from single channel ECG [131]. Moreover, regression trees or random forests with single channel EEG were used to perform sleep staging [142, 143]. In the multichannel setting, hierarchical decision trees have been used to invoke rule-based learning methods to perform reliable sleep staging [139].

4.2.4 Artificial neural networks

The use of an artificial neural network (ANN) approach is known as a predictive tool for sleep apnea. The validity of neural networks in sleep apnea has been investigated since the late 1990s [144]. Several other papers since then have reported the use of ANN and variants, including two-stage feedforward networks and neural-fuzzy networks [124, 145]. Studies have demonstrated the diagnostic performance of OSA prediction tools based on an ANN by using the PSG signal as reference [146].

Varady et al. presented neural network apnea and hypopnea online detection which is based on the analysis of NAF and/or RIP. This method can serve as a basis of an on-line respiration monitoring system. From the respiratory signal the instantaneous respiration amplitude and interval signals were derived and four feedforward ANNs were investigated [147]. In this article, the signal processing techniques (both time- and frequency-based) have been used to extract the feature and quantify respiratory events over each channel. Then, extracted features were grouped into reasoning units. Finally, the reasoning units were evaluated by a fuzzy inference system (FIS) to characterize them as each of three breathing type, apnea, hypopnea, and normal [148].

4.2.5 Fuzzy logic systems and networks

In 1965, Zadeh devised fuzzy logic to mimic decision making process in computing [149]. The use of fuzzy logic in medical research is now found in many disciplines, such as sleep-disordered breathing. Nazeran and Al-Ashmouny proposed a fuzzy logic-based algorithm to emulate human level decision-making. Their fuzzy inference algorithm used three input variables derived on a breath-by-breath basis from respiratory airflow measurements in order to produce a “severity index” (SI) quantifying the degree of SAS [150, 151]. Studies have demonstrated the usage of fuzzy logic to process the normalized area and the standard deviation of consecutive 3 s intervals

of baseline adjusted and rectified airflow signal to detect apnea and hypopnea in OSA patient data with an overall correct detection rate of 83% across all patients [150]. Overall, FIS has been shown to improve the decision making process in the epidemiology of sleep disorders. There have been many short term studies showing usage of other classifier algorithms which use multichannel signals for sleep apnea detection which are discussed in the next section.

4.2.6 Deep learning

Deep learning is an active subfield of machine learning whereby the feature extraction and selection process is incorporated directly in the feature learning process. In the context of SAS event detection, deep learning algorithms can be applied directly to raw signal data on an epoch by epoch basis, and adaptively derived data representations that optimize the statistical differences between nonapnea and apnea epochs. In the signal channel ECG setting, Kaguara employed Stacked Autoencoders with Deep Multilayer Perceptron classifiers to robustly recognize apnea events, even with the computational and energy constraints of mobile computing trained Deep Belief Nets to perform sleep staging on multichannel neural signals with high accuracy [152]. In this approach, Hidden Markov Models (HMM) were used as a postprocessing step to accurately capture the transitions between sleep stages probabilistically. Zhang applied Sparse Deep Belief Networks to raw multichannel EEG data to provide staging of sleep phases [153]. In another series of studies researchers showed the highly successful application of parallel multi-state HMMs with generative models, such as Gaussian Mixture Models (GMMs) or discriminative models, such as Deep Neural Networks (DNNs) for describing the posterior probability of HMM states in real time detection of a wide range of acoustic events under high noise conditions [154]. These approaches are appealing, because they enable practitioners to avoid the expertise and time intensive process of iterative, manual feature extraction.

4.2.7 Low dimensionality Total variability based approaches

Having a large enough training material is a necessary prerequisite for training an accurate GMM- or Hybrid Deep Neural Network--Hidden Markov Model (DNN-HMM) based classification systems. In another set of studies, researchers have shown that similar accuracies can be achieved using i-vector based approaches introduced by Dehak et al., in which the acoustic features are mapped to a lower dimensional total variability space where the necessary information for a target classification task can be found [155]. I-vectors provide a low-dimensional representation of feature vectors that can be successfully used for classification and recognition tasks. Presenting the acoustic events in the low-dimensional total variability space, ensures that for representing a new acoustic feature only a small number of parameters need to be estimated. To achieve this total variability space needs to encapsulate as much as possible of the super vectors in its restricted number of dimensions. This approach has been successfully used for acoustic event and speaker's acoustic characteristic classification in studies proposed by Najafian et al. [156]. It is interesting to measure their success in sleep apnea detection task using corresponding acoustic features where the amount of data is limited and applying deep learning based approaches is not possible.

Table III Summary of data representations, classification methods, and results from empirical studies of the performance of automated approaches to scoring and SAS event recognition.

Prediction Type	Signal Modalities	Data Representations	Classification Methods	Main Results	References
Apnea Events	ECG and Accelerometer	DWT Based Features	Decision Tree	Classification F1 Score 91.4%	[127]
Apnea Events	ECG	Raw Signals	Deep Neural Network with Stacked Autoencoders	90% Detection Accuracy	[157]
Apnea Events	ECG	Statistical Time-Frequency features	R-wave detection methods including adaptive thresholding and Teager Energy Operators (TEO)	Significant differences in Normal, OSA, and CSA HRV spectral ratios	[123]
Apnea, Hypopnea Events	ECG	Dynamic coupling based on recurrence quantification	Neural network, autoneural, regression, decision tree and ensemble models	88.06% Detection accuracy	[131]
Apnea, Hypopnea Events	ECG	Statistical DTW Based Features	Two-staged feedforward Neural Network	Detection accuracy 94.84% for OSA and 76.82% Hypopnea	[124]
Apnea, Hypopnea Events	RIP, Oxygen Saturation	Raw Signals	Amplitude Thresholding and AASM Rules	93.1% Detection accuracy	[136]
Apnea, Hypopnea Events	Single-channel airflow record	square-law, Hilbert-based, and modified envelope detectors	Adaptive thresholding	82% – 95% Cohen's coefficient of agreement	[158]
Apnea Severity	Nasal cannula flow, thoracic belt movement, SpO_2	Largest Lyapunov Exponent, Detrended Fluctuation Analysis, and Approximate Entropy	C4.5 Decision Trees	74.2% Accuracy dividing patients into severity groups	[130]
Sleep Stages	Single EEG channel	Autoregressive modeling and multiscale entropy	Linear Discriminant Analysis	88.1% Sensitivity, Kappa coefficient 0.81	[126]
Sleep Stages	Single EEG channel	Choi–Williams distribution, CWT, and Hilbert–Huang Transform	Random Forest	83% Detection agreement, Kappa coefficient 0.76	[143]
Sleep Stages	Single EEG channel	Reflection coefficients	Gaussian Observation Hidden Markov Model	80% Approximate detection accuracy	[145]
Sleep Stages	Savitzky-Golay filtered Single EEG channel	DWT Based Features	Regression Trees	75% Detection accuracy	[129, 143]
Sleep Stages	EEG	Relative Spectral Band Energy, Harmonic Parameters, and Itakura Distance	Autoregressive Modeling and Neuro-fuzzy Classification	--	[159]
Sleep Stages	EEG	Bispectral analysis techniques	Second-order AR model	96% Agreement SWS, 95% Agreement REM	[160]
Sleep Stages	EEG	Nonlinear higher order spectra	Gaussian Mixture Model	88.7% Detection accuracy	[161]
Sleep Stages	Multichannel EEG	Sparse and collaborative representations of classical time-frequency features	Extreme learning machine	81.1% Detection accuracy	[162]
Sleep Stages	Multichannel	Raw Signals	Sparse Deep Belief Net	91.31% Detection	[153]

	EEG			accuracy	
Sleep Stages	EOG and EEG	DWT with Relative Wavelet Energy	ANFIS based Neurofuzzy Classifier	97.4% Detection accuracy	[128]
Sleep Stages	EEG (C4−A1), chin EMG	Shannon entropy, sample entropy, hurst exponent	Artificial Neural Network	82% Detection accuracy for deep and paradoxical sleep	[142]
Sleep Stages	EOG, EMG, EEG	Frequency power spectrum, power ratio, spectral frequency, duration ratio, spindle ratio, SWS ratio	Rule based methods, Hierarchical decision tree	86.68% Detection agreement, Kappa coefficient 0.79	[139, 163]
Sleep Stages	EEG, EMG, EOG	Raw Signals	Deep Belief Networks with Hidden Markov Model	--	[152]
Sleep Stages	EEG, EMG, EOG, and ECG	Linear spectral measures, interdependency measures, and nonlinear measures of complexity, entropy	Quadratic Discriminant Analysis	74% Detection accuracy	[125]

4.3 Discussion and Conclusion

To sum up, a rich library of methods has been developed and validated in prior work for the automated detection of obstructive and central apneas, hypopneas, sleep stages, among other pathophysiological patterns in polysomnography signals. Contributions have included a collection of signal processing and representational learning methods that seek to expose useful structure in PSG data by exploiting a variety of time, frequency, multiresolution, and other nonlinear transformation techniques. Paired with detection algorithms and adaptive classification models, these elements are combined in modern diagnostic hardware and software systems to enable time savings and benefits to reproducibility in the clinical setting.

A combination of statistical, information theoretic, signal processing, machine learning, techniques are used to reduce and summarize different representations of multivariate signal data. Common statistical measures alone do not always elucidate discriminative and underlying structure of interest in data, and can be supplemented with techniques including entropy, other complexity measures, factorizations of the original data, among other feature extraction methods to achieve robust and accurate classification performance [128]. Exploratory data analysis of data

in different transform domains may be useful and important to the development of new methods. Domain expertise and computational methods may be applied to produce novel features and phenotypes that have an interpretable physiological basis, and may be investigated and validated to improve the understanding of the biological basis for sleep apnea.

Examples from prior work of simple classification modules have similarly demonstrated good performance, such as envelop tracking of single channel airflow signals with adaptive thresholding for 93.1% apnea detection accuracy [158]. While humans seek to interpret scoring rules such as the AASM or R&K guidelines quantitatively, the ultimate output of the scoring process is based on visual perceptual reasoning and is therefore qualitative in nature and prone to disagreement unrelated to chance. With that, accurate performance has been validated with machine learning methods, such as kernel SVM and random forests, that may adaptively incorporate a degree of high-dimensional data that may be suited to modeling and emulating the human visual pattern recognition process with greater generalizability to noise characteristics, physiologic variability, and expected human disagreement that are inherit to manual analysis of sleep signals [141, 143]. Methods like these work well for a broad class of general applications, and may be tested during exploratory analysis side-by-side with simple models, like linear regression, to provide a sense of the benefit of more complex, high-dimensional, or adaptive models.

Other research areas show promising potential to advance the field of computational and algorithmic approaches to SAS detection and diagnosis. First, deep learning techniques have been identified as an area of significant potential to increase the efficiency and productivity of the engineering design process, as well as having shown very promising performance and accuracy in preliminary sleep applications [152]. However, a significant disadvantage of deep learning is the

lack of interpretability in both the features and models, which may consist of nonlinear interactions between hundreds of thousands or hundreds of millions of tunable parameters. Physiological models that better exploit and model the causal structure underling PSG data may inform high performance simple models that are highly interpretable. However, physiological systems are highly dynamic and complex, and therefore may be hypothesized to be well modeled by systems with hundreds of thousands or millions of parameters than to be characterized by simple models such as linear or histogram-based learning algorithms. Theoretical advances in the statistical basis for deep learning, nonconvex optimization, and physiological modeling together may allow for a rich class of models that are both highly performant and accurate, as well as and highly interpretable from a clinical and physiological perspective. Moreover, there are several research efforts to validate new and existing methods for automatic SAS event detection. A significant critique of existing validation studies lies in the size of the dataset analyzed, and therefore the statistical power and reproducibility of the described performance. Larger scale validation studies, involving multiple sites, device modalities, and thousands of normative and SAS effected patients would greatly assist in directing the field with generalizable algorithms and computational methods that are safe and effective in clinical practice for a broad class of patients and sleep disorders [164]. In development of our algorithm for "Smart CO_2" device, we used amplitude and adaptive theresholding (4.2.1) methods discussed in Fig. 20.

Chapter 5 Current treatment modalities for SAS

Due to the complex pathophysiology of sleep apnea, several nonsurgical and nonpharmacological treatments have emerged that have proven quite effective. However, an effective and comfortable treatment option for sleep apnea has yet to be developed. This section discusses the assistive and therapeutic oral devices for sleep apneas.

4.4 Assistive devices

A positive airway pressure (PAP) device usually consists of three major parts: a positive pressure generator; a nasal or oral interface such as a mask; and a tube connecting the two parts. The pressure generator is a fan or turbine which is used to apply external pressure to the patient's upper airway. PAP devices are normally divided into four different types which are summarized in Table V and discussed shortly along with their major advantages, features and target patients [165-171].

4.4.1 Types of PAP device

The first developed PAP device, continuous positive airway pressure (CPAP), delivers constant pressure for the whole night, which requires manual titration in the laboratory before use. CPAP is the basic type of PAP machine, invented by Colin Sullivan in 1981 [172], and has been widely accepted as the gold standard for treatment of OSA [173]. CPAP is effective at eliminating apneas and hypopneas [174, 175]. The major problem for CPAP is that over 40% of the patients with OSA are noncompliant with the treatment [173, 176]. Several components were added to the CPAP device to improve the adherence such as chin straps, mask re-fitting, and humidification for the tube [177]. While effective at treating OSA, CPAP may not suppress CSA, particularly in patients with heart failure [178], causing search for alternative treatment options.

The second developed, Bi-level positive airway pressure (BPAP) delivers a higher pressure during inspiration (IPAP) and a lower pressure during expiration (EPAP), which decreases the effort for the patients to breathe. A flow sensor detects the timing to change from EPAP to IPAP. IPAP and EPAP usually range from 4 to 30 cmH_2O [111]. Other parameters, such as inspiration time, pressure rise time, and flow trigger sensitivity are set by the technician [179].

The third PAP device, auto-titrating positive airway pressure (APAP) provides adjustable pressure to maintain airway patency, and gives appropriate response to the respiratory events. APAP can improve sleep quality for most of the patients when compared to the traditional CPAP device which cannot adjust the pressure when leaks occur. However, due to excessive increases in pressure in the case of mask/tube leakage, potential risk may arise. And some patients may be sensitive to the pressure changes, and thus feel less comfortable with APAP [180].

The final PAP device, adaptive servo ventilation (ASV) provides patients steady, minute ventilation based on the measurement of patient breaths. Although initially used in CSA patients [180], a 2015 study SERVE-HF involving 1,325 patients showed that while ASV was efficacious in treating CSA, it had no significant effect on a broad spectrum of functional measures including quality-of-life measures, 6-minute walk distance, or unplanned hospitalization for worsening heart failure. In contrast to smaller studies and meta-analysis, a significant increase in both cardiovascular mortality and all-cause mortality was observed in the ASV group. A first possible explanation for this trial failure is that CSA is a compensatory mechanism for heart failure. The second hypothesis is that PAP device may impair the cardiac function for some patients [181]. While theoretically feasible, these hypotheses have no experimental basis, and based on the many adverse effects of CSA on CHF pathophysiology, further research is needed to understand why the SERVE-HF study failed.

4.4.2 Current PAP technology

In addition to the types of the PAP devices, this section discusses current continuous technological advances that aim to improve the patient's comfort, adherence, and clinical benefits which could be categorized as, respiration phase detection, ventilation estimation, CSA distinguishing, humidifiers, expiratory pressure relief, ramp, and automatic start and finish.

Determining the respiration phase is essential for auto PAP devices to apply future expiratory pressure relief and inspiratory flow limitation. ResMed's devices employ Fuzzy logic to separate the whole respiration cycle into 9 different phases described in Table IV, which is based on the respiration flow rate direction and the volume of flow [182]. Respironics's devices divide the respiration cycle into fixed time segment (64 ms). To estimate the total duration of respiration cycle, Respironics records and analyzes the history inspiration time and expiration time data [183].

Table IV ResMed's fuzzy logic for phase determination

Flow	Rate of change	Fuzzy phase
Zero	Increasing	Start inspiration
Small positive	Increasing slowly	Early inspiration
Large positive	Steady	Peak inspiration
Small positive	Decreasing slowly	Late inspiration
Zero	Decreasing fast	Start expiration
Small negative	Decreasing slowly	Early expiration
Large negative	Steady	Peak expiration
Small negative	Increasing slowly	Late expiration
Zero	Steady	Expiratory phase

To quantify a patient's breath quality, different companies employ different algorithms to estimate ventilation. A weighted peak flow (WPF) method which averages the weighted peak flow over a current period of time [184, 185] has a good noise rejection to estimate the ventilation. ResMed measures long term average ventilation (for example, the instantaneous ventilation is averaged within a 100 s interval by a low pass filter). The target ventilation is taken as 95% of the long term average ventilation [186].

Airway patency detection could distinguish CSA from OSA. Two methods are used to detect airway patency: cardiogenic pulsation testing [187] and device-generated pressure oscillation testing [188]. The first method tries to detect the cardiogenic flow, which is the airflow induced in the lungs. It is related to the proximity of the lungs and the heart during sleep. Based on analysis of a large number of clinical cases, researchers concluded that no cardiogenic oscillation was shown in OSA with a specificity of 100%, thus it could be a good indicator of CSA [189, 190]. The second method, applies an oscillatory pressure waveform to a patient's airway. This waveform induces an airflow signal. Figure 5 shows that patients with OSA (airway obstructed) have lower mid-inspiratory flow than CSA patients. This indicator, compared with the pre-set threshold, helps the device to distinguish CSA from OSA [188].

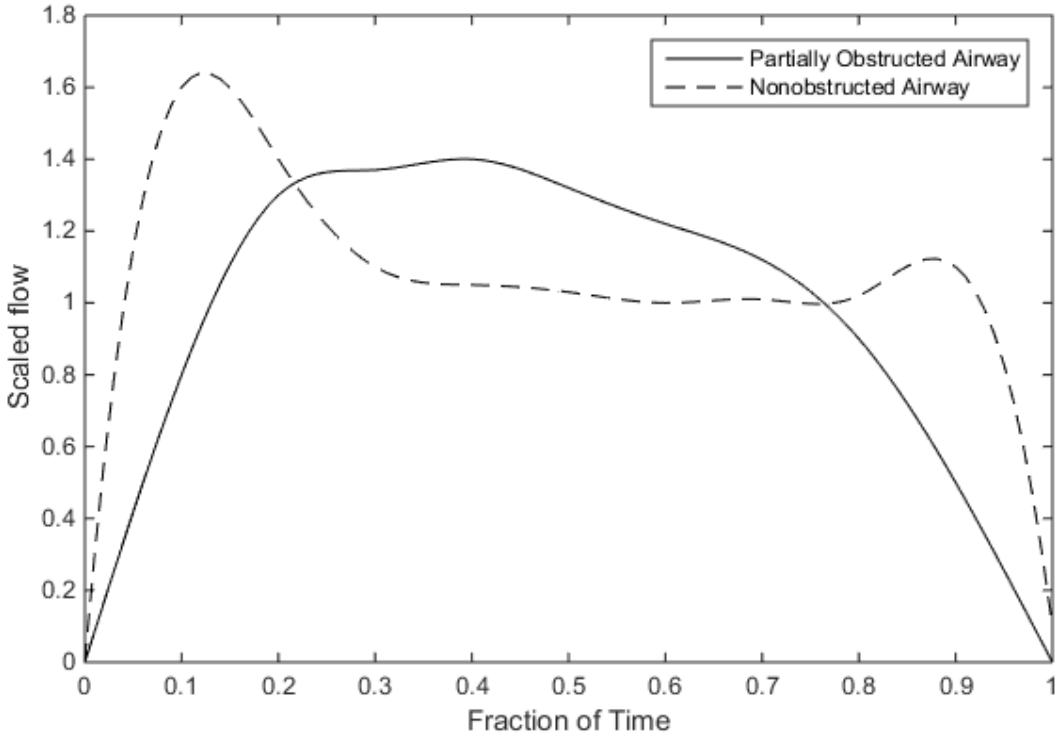

Figure 6 Demonstrates the high airway resistance of OSA patients causes the mid-inspiratory flow limitation. Patients without airway obstructed (CSA patients or normal people) have higher mid-inspiratory flow [191].

Several methods have been developed to increase patient's comfort on PAP. Humidifiers increase the humidity of inhaled air. They most often are heated, and consist of a water chamber and a heating plate. To get desirable humidification of air, temperature sensors at the heating plate or humidification at the tube are necessary to control the production of water vapor. Higher humidification of inhaled air helps to reduce nasal irritation and congestion [192]. If bedroom temperature is much cooler than the heating temperature, water may condense in the tube or mask, which is called "rainout". Insulation of the PAP hose can prevent condensation. Also, a heated hose could also benefit the user's comfort, which could increase humidification and eliminate "rainout".

To aid patients' exhale against CPAP, the expiratory pressure relief (EPR) feature was introduced. With EPR, when the patient exhales, the flow generator device detects the beginning of exhalation, and then adjusts the motor speed to drop treatment pressure, thus reducing the breathing effort. Generally, EPR is set from 0 to 3 cmH_2O and should not drop below 4 cmH_2O.

The ramp feature reduces the uncomfortable feeling of sudden air pressure increase. It works by gradually increasing pressure over a defined time range. Commonly this time is around 15–20 min. ResMed's AutoRamp fixes the starting pressure and keeps tracking the state of the patients' sleep. When patients have fallen asleep, the pressure increases gradually until it reaches the preset pressure. It determines the state of sleep by detecting the breath stability or the occurrence of sleep events. Respironics smart ramp increases the speed of ramp if hypopneas or obstructive apneas are detected [193].

Some PAP devices automatically start working when the machine senses airflow from breathing, which indicates that the patient is wearing the mask. If the machine senses very high airflow for a certain period of time (e.g. 1.5 s) this indicates the machine is working incorrectly and will automatically turn off.

The summary of benefits and challenges of PAP modalities are presented in Table. V. In summary, PAP devices are extremely effective when used correctly; however, their major challenge remains the patients' intolerance and nonadherence.

Table V Summary of benefits and challenges of PAP modalities.

Types of PAP device	Benefits	Challenges	Target	Features	Typical models
CPAP	Less expensive, CPAP Fixed pressure setting does not require monitoring	Relative high pressure, less patient comfort, low compliance	OSA patients	Fixed pressure by manual titration	AirSense 10 CPAP, System One CPAP devices ICON™+ Novo, IntelliPAP®
BPAP	Significant and comparable decrease in respiratory effort [165, 168]	ventilation was associated with patient -machine asynchrony; does not offer any significant clinical benefits over CPAP	OSA patients nonresponsive or nontolerant of CPAP	Bi-level pressure by manual titration	System One bi-level devices,IntelliPAP Bilevel S®
APAP	Improved sleep architecture, reduced treatment pressure, low pressure leak, less side effects [169-171]	Costly; it has no better ability to eliminate respiratory events or to improve subjective sleepiness	OSA patients and home testing patients	Adjustable pressure	Airsense 10 AutoSet,System One auto devices, ICON™+ Auto, IntelliPAP
ASV	Greater benefit for CSA-CSR patients for improved respiratory disturbances, oxygen desaturations, and arousals [166, 167]	Costly, no significant effect on quality-of-life measures, observed significant increase in cardiovascular mortality [181]	OSA and respiratory insufficiency patients with central apnea, periodic breathing such as Cheyne-Stokes respiration (CSR), or complex apnea	Pressure support	AutoAdjust®

4.5 Therapeutic oral devices

4.5.1 Oral appliances

Oral appliances (OAs) or intraoral devices (ODs) which aim to treat OSA by physically altering the mandible, tongue, or soft palate during sleep to prevent the collapse of upper airway muscles that is characteristic of OSA [194]. ODs are growing in popularity, as they are found to be more comfortable than CPAP and have higher adherence rates. However, ODs tend to be a secondary form of treatment for OSA to CPAP as CPAP has a higher efficacy; ODs are recommended when a patient becomes noncompliant to CPAP [195]. Yet, there is no predictive effectiveness ability for ODs since they have been shown to either help, hinder, or not alter sleep apnea in patients.

There are three types of ODs: Soft Palate Lifters (SPLs), Tongue Retaining Devices (TRDs), and Mandibular Advancement Appliances (MAAs or oral appliances). MAAs are by far the most used ODs today to combat OSA. MAAs operates by holding the mandible in an anterior position to physically open up the airway. When the mandible is kept anteriorly to its normal position, the MAA prevents the mandible from receding into the oropharynx and blocking the airway. TRDs hold the tongue forward in the mouth to prevent it from receding into the airway, while SPLs hold the soft palate in place to prevent collapsing in the airway. With the main airway kept open during sleep, OAs prevent apneic episodes [194].

4.5.2 Types of oral devices

Mandibular advancement appliances (MAA)

MAAs have many different designs but are fairly consistent in their effectiveness. MAAs are fixed in the mouth by attaching them to one or two dental arches. They can be molded using dental impressions obtained at the dentist's office or use thermoplastics that can be molded at the clinic. Depending on the MAA, the mouth can be left opened during sleep while other designs keep it closed. Tubes and holes can be used to allow for pressure relief or oral breathing. Some MAAs combine with posterior additions to retain the tongue or hold up the soft palate. All MAAs rotate the mandible downwards and protrude the mandible into an anterior position to create an increase in the upper oropharyngeal airway [196].

Material choice and construction can vary across MAAs. They may be made from a custom molding using plaster casts [197] or wax interocclusal records. More recently, there have been MAAs that can be customized by using a thermoplastic, removing the need for time-intensive molds to be made. Possible material choices include soft elastomers [197], acrylic [198], and soft

polyethylene [199] among others. MAAs may be fixed in the oral cavity by hugging the dental arches [198] or by being molded to the teeth [199]. Keeping the lower mandible in the proper position has been achieved by using screws [198], plastic flanges for biting, and U-shaped springs [199].

The major concern with using MAAs is determining how far protruded the mandible needs to be, to reduce the AHI to an acceptable level while preventing temporo-mandibular joint pain. Previously, to determine the correct mandible placement, the MAA was set as far forward as tolerable by the patient and then a polysomnography was performed to determine the effectiveness, and repeated until the minimal protrusion was found. Titration protocols have been developed to determine the correct protrusion level, but no common consensus has yet been reached. With current titration protocols call for adjustments to be made over weeks in the clinic or remotely at the patient's home instead of having multiple arousals during the night in a sleep lab, obtaining the proper jaw placement has become more effective. Tsai found an absence of apneas of participants at 64% using this protocol [200].

Tongue Retaining Device (TRD)

Tongue retention devices are the second most utilized form of OA, as they can be both a stand-alone appliance or in combination with MAAs. TRDs utilize negative pressure to secure the tongue [201]. The negative pressure can come from either a stand-alone vacuum device that connects to a plastic mouthpiece that provides suction, or a plastic bulb that fits in between the teeth [194, 202]. TRDs have lower efficacy rates and compliance rates than their MAA counterparts, making them less common to treat OSA. TRDs can be used in conjunction with MAAs or stand-alone if there are dental issues with using MAAs.

Soft Palate Lifter (SPL)

Soft palate lifters presently are rarely used. SPLs are the most uncomfortable OA since they operate on the most posterior region of the mouth, next to the uvula. SPLs are secured by a mouth guard or retainer along the maxilla with a plate or rigid planar extrusion from the posterior side, supporting the soft palate. This device has not been shown to be effective against OSA nor tolerable by patients [203].

Oral Pressure Therapy (OPT)

A newer approach to oral treatment of sleep apnea is by use of Oral Pressure Therapy (OPT). Oral pressure therapy uses a vacuum in the mouth to pull the soft tissues forward and prevent collapse. By using negative pressure in the mouth, the soft palate and tongue are held forward when the muscles would normally relax and allow for airflow to continue through the nose. While this approach still requires an external device, it tends to be quieter than CPAP and is less obstructed by being able to use a small mouth guard versus a mask [204].

4.5.3 Comparison of oral appliances to CPAP

MMAs have a role as alternative treatment strategies for OSA. Since CPAP has been proven to be the most effective method of treatment for OSA, it is the first-line treatment strategy. If the patient cannot tolerate CPAP due to side-effects, the next course of action may be to use OAs. OAs are used only for mild cases of OSA, as for more severe cases of OSA CPAP is still the better option. Also, OAs are not effective against central sleep apnea. When considering using OAs, it is important to establish what is causing the OSA and determine if oral adjustments can possibly treat the cause. Furthermore, dental factors have to be considered when using OAs. If there are issues with any dental structures from teeth to the temporomandibular joint (TMJ), OAs

therapy might not be possible, as common side effects of OAs are teeth discomfort and TMJ pain [205].

Oral Appliances have promise as a main treatment for sleep apnea for patients who can't tolerate CPAP. OAs have been shown to greatly reduce or eliminate snoring in almost all patients according to bed partners and patients. The effectiveness of OAs also proves attractive, with relatively high rates in reduction of AHI. The side-effects for both MAAs and TRDs are mild and can be overcome with continued use of the device. Compliance rates for OAs tend to be higher than CPAP, which supports the use of OAs when patients don't comply with CPAP [196]. Although oral appliances are not as effective as CPAP in reducing sleep apnea, snoring, and improving daytime function, they have a definite role in the treatment of snoring and mild sleep apnea.

4.5.4 Comparisons between intra-oral devices

MAA versus OPT

OPT also has a role in treatment of OSA, which can be considered as alternative therapy for sleep apnea. MAAs have a high compliance rate and are effective at treating mild OSA making them the first choice for ODs. OPT can be used as a secondary option if the patient does not tolerate MAAs. OPTs were found to have a 90% compliance rate after 3 months and had a 53% reduction in AHI over the night in patients with mild-severe OSA. These results suggest that OPT could be used as alternative treatment for a small subset of the sleep apnea population who are nonusers of other forms of ODs or CPAP [206]. There has been no direct comparison between MAAs and OPTs.

MAA versus TRD

When comparing MAAs to TRDs, it was found that MAAs were favored and performed better than TRDs. After three weeks, MAAs had a compliance rate of 86.4% whereas TRDs of 36.4%. MAA was favored over TRD by 90.9% of patients and eliminated snoring in 40.9% of patients versus 27.3% for TRD. MAAs were also ripped out of the mouth during sleep less often than TRDs, 9% vs. 86.4%, respectively [201].

4.5.5 Compliance/Adherence issues of oral devices

While compliance rates are high for oral devices, the main reason for discontinued use often deals with the perception of the device's effectiveness. Wearers of OAs most frequently use their devices because of complaints from their bed partners about snoring. Since the patients tend to only have a mild form of sleep apnea, they experience few daytime symptoms. This lack of daytime symptoms can lead the patient to not realize they have sleep apnea or that it has been dealt with and they stop usage. With no bed partner to detect snoring, or if they stop noticing it, the patient might stop using their treatment device even if it is comfortable. This can lead to lower compliance rates for sleep apnea patients, even though they are pleased with their devices [194].

Compliance rates for OAs have had difficulty in being accurately described due to various reasons for discontinued use. Since OAs are used to treat mild forms of OSA, patients can discontinue use even though they still have sleep apnea because they do not realize it. This leads to variations in studies about how many patients continue compliance with their devices over time as between different studies the use different lengths of follow-up and definition of compliance. For instance, three different studies had a compliance rate of 100% for 3 to 21 months, 75% after 7 months, and 52% after 3 years [196].

Side effects for OD can be common, but are relatively mild and tolerable, especially when compared to CPAP. Possible adverse effects for MAA were found to include jaw discomfort, TMJ pain, dryness of mouth, and slight shifting of the teeth. Similar side effects were also found with TRDs, being dryness of mouth, excess salivation, and soft tissue irritation [201]. For SPL, the side effects were more severe and have led to lower compliance rates. They are: gagging, soft tissue irritation, and choking [203]. Comparison of oral appliance is summarized in Table VI.

Table VI Comparison of oral appliances

Device	Method	Effectiveness	Compliance	Side effects	Comparison against CPAP	Reference
Mandibular Advancement Appliance	Hold mandible forward to open airway using intraoral appliance	68.2%	50–100%	jaw soreness, mouth dryness	less effective, higher compliance	[194, 201]
Soft Palate Lifter	Prevent soft palate collapse into airway	minimal	25%	gagging, soft tissue irritation, and choking	less effective and less compliance	[203]
Tongue Retaining Device	Retain tongue to prevent obstruction	45.4%	36.4%	Excess salivation, dryness of mouth, soft tissue irritation	less effective, similar compliance	[201]
Oral Pressure Therapy	Provide suction to hold soft tissue in place	~50%	48%	soft tissue irritation	less effective, similar compliance	[204]

4.5.6 Inspired CO_2

Another potential method for controlling abnormal breathing abnormalities is the use of inspired CO_2. Since the early 1980s, several studies have shown that the constant inhalation of CO_2 can help prevent apneas [207-211]. It is believed that breathing in low CO_2 concentrations can help prevent periodic reductions in P_aCO_2. By preventing these levels from falling below the apnea threshold, the number of breathing cessations can be reduced. However, handling all the equipment for exogenous CO_2 can be cumbersome in a household setting, and the benefits towards sleep quality are still debated [210, 212, 213]. Another method of increasing CO_2, is the addition of extra dead space. Dead space is the portion of the airway passages that does not contribute to gas exchange (i.e. trachea and bronchi). It has been shown that the Apnea-Hypopnea Index (AHI) can be decreased by the addition of as little as 400–600 ml of dead space [7, 8, 214]. Though there are possible adverse effects to the cardiovascular system [214], CO_2 rebreathing has been shown to be highly effective in preventing central apnea and instabilities in sleep caused by hypoxic exposure and CHF, and over many months in CPAP-treated OSA patients with “residual” central apnea, i.e. so-called “complex” sleep apnea [215, 216]. Xie et al. reported the first experimental study that tested added CO_2 alone as a treatment for OSA [7]. The detailed review on others studies will be covered in section Chapter 7.

4.6 Discussion and conclusions

In summary, tremendous research and engineering efforts have been applied to design and optimize tools that enable the study and understanding of physiological substrates that characterize sleep apnea syndrome. These efforts have contributed to the advent of a broad class of signal and sensor modalities that can be administered clinically, individually or in combination,

to provide reliable measures for SAS diagnosis. With this, an extensive collection of computational and signal processing methods has been proposed and evaluated to automate the identification of SAS disease patterns. Once diagnosed, patients benefit from a growing array of therapeutic techniques and technologies that continue to evolve with ongoing research and development.

Despite this significant progress in our understanding of SAS, as well as development and refinement of diagnostic and therapeutic tools, the epidemiological problem of sleep apnea and its impact on population health, productivity and healthcare costs, continues to grow. It is estimated that between 18 and 22 million Americans suffer from SAS , 80–90% of adults suffering from SAS remain undiagnosed and untreated, and costs of untreated SAS may double a patient's medical expenses mainly due to increased CVD risk and mortality [217]. Motivated by the scale of this growing problem, significant remaining research challenges must be addressed to reach the unaddressed SAS population and ensure access to efficient and effective care. As such, this review concludes with a discussion of open research and engineering challenges for signal, sensor, and computational approaches to SAS detection, as well as the development of new therapeutic methods.

First, there is a significant opportunity to improve the detection and understanding of SAS phenotypes through research on new and improved diagnostic signal and sensor modalities. Complex patients suffering from a combination of SAS along with comorbid neurological and cardiopulmonary conditions indeed require a Type 1 supervised nocturnal polysomnography study. For these patients, attended in-lab PSG remains the gold standard for diagnosis because the controlled environment allows for expert application and monitoring of biosensors, acquisition of a larger quantity and variety of signals, and helps to ensure high quality and fidelity of diagnostic

data. However, with 26% of persons age 30–70 estimated to suffer from sleep apnea, these complex cases represent a significant minority of the total affected population [39]. At-home sleep studies decouple the acquisition of diagnostic SAS data from the equipment, personnel, and capacity constraints of physical sleep labs, offering a faster and lower cost pathway for the majority of patients. Nonetheless, Type 1 in-lab sleep studies account for the vast majority of diagnostic tests for patients of all suspected severity levels conducted each year. Therefore, research that aims to improve signal and sensor technology for at-home sleep studies, such that it more closely reproduces the quality, quantity, and comprehensive variety of controlled in-lab sleep studies is paramount. In doing so, we hypothesize that acceptance of at-home sleep studies can be improved among clinicians, while allowing for more convenient and inexpensive testing options for patients. Moreover, increasingly noninvasive and noncontact sensor modalities promise the potential for ongoing at-home monitoring of SAS patterns and sleep quality, to inform preventive care and treatment optimization.

Second, research focused on computational and signal processing methods for SAS pattern identification offers potential to introduce significant efficiencies into the clinical diagnostic workflow. The scoring of sleep studies represents a critical step in the SAS diagnostic process, whereby the collection of relevant disease patterns is reduced to clinically relevant diagnostic parameters including AHI, RDI, and others. Today, an estimated 86% of sleep centers don’t use any form of either computer assisted or automated scoring, despite the availability of clinically validated commercial systems. A common hypothesis for the slow clinical acceptance of these systems is the complex, repetitive, and genuinely ambiguous nature of the event scoring task, where, for example, even expert scorers on average agree 52.4% on CSAs and 65.4% on Hypopneas [114]. With these factors in mind, additional research is needed to create automated

scoring methods, algorithms, and software that can overcome the barriers to clinical acceptance with improved sensitivity and specificity towards the expert human standard. To advance this research, open data formats and interoperability standards will be required to enable both retrospective and prospective evaluations of new computational, signal processing, and algorithmic methods.

Finally, development of new treatment techniques and deeper investigations into the alterations in physiological mechanisms are needed. It is well understood that patient compliance with PAP devices is very low, with over 40% of patients with OSA being nonadherent to CPAP, and many patients regularly adherent for a small fraction of their total sleep time [176]. Oral appliances have shown significant benefits in this regard for mild OSA sufferers, but do not offer the same efficacy as PAP for moderate to severe OSA, CSA, or complex comorbid patients. Moreover, the recent SERVE-HF study indicated not only that ASV therapy did not significantly improve many quality of life indicators, but resulted in an observed increase in cardiovascular and all-cause mortality in CSA patients [181]. It is clear that new alternative devices that are more comfortable, tolerable, and better accepted by patients are needed to truly achieve an improved sleep quality. For CSA and complex comorbid patients in particular, more research and greater knowledge of disease alterations to sleep physiology are needed, to understand which, if any, of the expressed physiological symptoms may in fact be beneficially acquired compensatory mechanisms that present as seemingly pathological, but assist in patient homeostasis and systemic preservation through nonobvious pathways. These and other alternative and improved therapies are critical to effectively treat the growing SAS population.

In conclusion, sleep apnea is a significant and rapidly growing problem at the societal scale, for which tremendous scientific and engineering effort has been applied to understand and develop

diagnostic and therapeutic tools. This work has led to an array of validated signal and sensor modalities for acquiring, storing and viewing sleep data; a broad class of computational and signal processing approaches to detect and classify SAS disease patterns; and a set of distinctive therapeutic technologies whose use cases span the continuum of disease severity. This review provides a current perspective of the classes of tools at hand, along with a sense of their relative strengths and areas for further improvement. These engineering contributions have defined our understanding of sleep science and pathology, and cannot be understated. However, diagnosing and treating the large and growing unaddressed SAS population remains a paramount challenge. Future work in improved at-home signal acquisition systems, new noninvasive and noncontact sensor modalities, sensitive and specific computational approaches to automate sleep scoring, and open interoperable sleep data formats show significant promise to increase the efficiency and accuracy of SAS diagnosis. These, paired with research into comfortable therapeutics that improve adherence, and safer, better understood treatment alternatives for severe and complex comorbid patients, will enable a transformative difference in sleep, quality of life, productivity, and reduce healthcare costs for tens of millions of patients globally.

5 Chapter 6 A review of preventing central sleep apnea by inspired CO_2

This chapter is partially based on the following publication [50]:

Mulchrone, A., **M. Shokoueinejad**, and J. Webster. "*A review of preventing central sleep apnea by inspired CO2.*" *Physiological Measurement* 37, no. 5 (2016): R36.

5.1 Abstract

Although almost completely unknown half a century ago, sleep disorders are gaining recognition as major issues to public health due to their growing prevalence and dire societal consequences. Despite being linked to several infamous catastrophic events such as Chernobyl, it is estimated that 90% of suffers fail to get diagnosed and receive treatment, and a significant portion of the ones that do are often noncompliant due to the side effects of current treatments. This chapter prevents a review of the current standard treatment for central sleep apnea, and investigates the advantages and possible consequences of using inspired CO_2 as an alternative treatment option.

5.2 Introduction

Although almost completely unknown half a century ago, sleep disorders are becoming a growing health problem. The prevalence and burden of sleep disorders are often overlooked, but their effects are starting to cause notice. There are currently over 80 unique sleep ailments discovered by the International Classification of Sleep Disorders (ICSD), and each has their own treatment plan [218, 219]. Some of the most common sleep disturbances include central nervous system hypersomnias, circadian rhythm sleep disturbances, insomnia, sleep-disordered breathing, and sleep-related movement disorders [220].

The health effects of these sleep disorders cover a wide range of effects from simple daytime sleepiness, which is very nonspecific and common to many disorders [221], to more severe effects such as an increased risk of cardiovascular disease and stroke [222]. Approximately 35-40% of people in the United States stuffer from daytime drowsiness [223], which has been shown to lead to reduced cognitive function, higher prevalence of motor vehicle accidents [224-226], poor work efficiency [227-229], and is a significant cause of mortality and morbidity [223]. It has even been linked to several infamous catastrophic events such as Chernobyl [223], the challenger explosion, and the Three Mile Island accident [230]. As a result, these diseases are now being recognized as major issues to public health due to potentially severe societal consequences [229]. Moreover, insufficient or poor quality sleep can influence one's mental status, reducing mental function. This decrease in compliance compounds chronic disease treatment and can aggravate mental conditions such depression and schizophrenia [231, 232]. However, sleepiness is not necessarily always the result of having a sleep disorder. It can also be the consequence of a large sleep debt due to irregular work and/or sleep schedules [229].

5.3 Diagnosis

The gold standard for the diagnosis of a sleep disorder requires an overnight stay at a sleep laboratory, where the patient is evaluated with a polysomnogram [233, 234]. This is more commonly known as a 'sleep study'. The full-night polysomnograms (PSG) are expensive and time-consuming. They require both an open bed at the sleep study center, which can have limited availability due to long waiting lists, and a number of specialists to administer the test and interpret the data [233]. Patient expenses can range anywhere from approximately $800 [235], to several thousand dollars [229, 236, 237]. There are many sleep recording systems available on the market for home use. They aim to reduce the financial costs in order to reach out and appeal

to a larger population; however, in order to cut costs the total number of recording parameters are also reduced [233, 238]. Examples of these devices include the type II Sleepscan Netlink Traveller (Bio-Logic Systems, United States of America); the type II Vitaport-4 PSG (TEMEC Instruments, Netherlands); the type IV Visi Grey Flash (Stowood Scientific Instruments, United Kingdom); and the single-channel EEG type IV BioSomnia (OBS Medical, United Kingdom). These devices range from a single-channel data recording system to a 40 channel system [239]. However, there is debate whether or not these systems work accurately enough to serve as a diagnostic tool. A patient with no medical guidance or technical training has a greater probability of incorrectly placing the sensors, which can lead to inconclusive or misleading results [233]. Even if the data are acquired correctly, there is still a long waiting period to have the results analyzed due to a lack of readily available, trained specialists [240]. Some reject that these home portable sleep monitoring systems are cost advantageous [241]. On the other hand, there are groups that deem that these systems show very good diagnostic accuracy and are an excellent alternative to in-laboratory PSG. They claim that patients are more comfortable, which produces better sleep efficiency [236]. With the rising trend of risk factors such as obesity, sleep disorders are becoming more common [242-244]. Over the last few years, the number of patients being successfully diagnosed and treated has drastically increased [229], but it is still estimated that up to 90% of those affected fail to get diagnosed and receive treatment [245].

5.4 Sleep Apnea

One prevalent sleep disorder is sleep apnea; it affects individuals of all ages and is often under-diagnosed [246, 247]. This disease is characterized by breathing that repeatedly stops and starts. The patient undergoes intermittent cessations of breathing (apnea) or periods with reduced airflow (hypopnea) [233, 248]. However, sleep apnea can be further categorized into either obstructive

sleep apnea (OSA), or central sleep apnea (CSA). Patients with obstructive sleep apnea typically experience a complete or partial block of the upper airway, despite respiratory effort. On the contrary, central sleep apnea is characterized by a lack of drive to breathe [233, 249]. Interruptions in respiration, regardless of cause, can lead to insufficient ventilation and consequently compromised gas exchange. Arterial oxygen levels begin to decline while carbon dioxide levels climb [233]. Obstructive sleep apnea will not be further discussed in much detail in this article; instead, it will mainly focus on central sleep apnea.

5.5 Heart Failure

Central sleep apnea is extremely common in patients that also suffer from congestive heart failure (CHF) [250]. Heart failure, a subdivision of cardiovascular disease, is characterized by the progressive weakening of the heart wall. As the condition advances, the heart becomes too weak to eject all the blood from the ventricles, which leads to a decrease in cardiac output and an increase in ventricular filling pressures [251]. Over time, the declining cardiac output will fail to meet the body's metabolic needs for oxygen, and the increasing end-diastolic left ventricular volume will cause a buildup of pressure back to the lungs. These alterations in the Starling forces result in excess filtration out of the capillaries [252]. Ultimately, these pressures lead to increased alveolar fluid in the interstitial space, also known as edema. This pulmonary congestion puts patients at increased risk of developing central sleep apnea due to oxygen's poor solubility [253-255].

In the United States, heart failure is the leading cause of mortality and morbidity; one out of every eight death certificates mention heart failure as a primary or secondary cause of death. It also is the most frequent cause of hospital admissions in patients over 65 years old [251, 256]. Over 5.8

million Americans are affected, and 825,000 new diagnoses are being made each year. Readmission rates for such patients exceed 50% within six months, resulting in estimated direct and indirect annual costs of over $39 billion in the United States alone. This amount is vastly underestimated, as it only accounts for cases in which heart failure was the primary diagnosis. Due to the increasing occurrence of biomedical risk factors such as obesity, hypertension, diabetes, and an aging population, the number of people in the United States affected by heart disease is estimated to increase 46% by 2030, with projected annual costs escalating to over $69.7 billion [256, 257]. As many as 50% of patients with heart failure suffer from breathing disorders, the most common being central sleep apnea [258-260]. As the prevalence of heart failure continues to rise, so will conditions such as sleep apnea. New methods for sleep disorder detection and treatment are needed in order to keep up with the number of people suffering from these diseases.

5.6 Current Treatments

Continuous positive airway pressure (CPAP) is the current gold standard treatment for obstructive sleep apnea. It is also used for patients with central sleep apnea, and has been shown to be especially beneficial for people also suffering from heart failure [261]. At night, the patient wears a mask over their nose and mouth, through which an air blower forces air into the nasal passages. It proves a constant and continuous pressure, but this can be adjusted. CPAP has been shown to attenuate central sleep apnea, improve nocturnal oxygenation levels, and improve the ejection fraction. They are moderately effective when used correctly, but due to side effects, approximately 30–35% of patients are intolerant or noncompliant. These side effects can include skin abrasions, bruising, chafing, abdominal cramping, chest discomfort, and nasal congestion or dryness [11]. Even compliant patients typically use it for less than the optimal duration necessary

to prevent adverse outcomes; anywhere from 29–83% of patients use the CPAP for less than four hours per night. Studies have demonstrated a dose dependent relationship with CPAP use and symptom improvement and lowered mortality [262], and failure to use the device for even a single night can permit the reemergence of daytime sleepiness or neurobehavioral deficits [6]. Studies have also shown lowered norepinephrine levels and improvements in the 6 min walk test with use of a CPAP [263]. This standard test is used to evaluate the integrated response of the pulmonary, cardiovascular, and circulatory systems, in addition to neuromuscular control and muscle metabolism; however, it cannot provide the relative contributions of each of these systems [264, 265]. Overall, CPAP has been shown to reduce some of the negative pathophysiologic consequences of CSA, but it is unclear whether these improvement are due to the elimination of CSA itself or due to the CPAP improving cardiac function [266].

Another treatment method for CSA is the adaptive servo-ventilation machine (ASV). It is very similar to the CPAP machine in that it also delivers pressurized room air into the patient's nose and mouth through a mask. However, the major difference is that ASV therapy uses an algorithm in order to support regular breathing. It is sensitive enough to detect significant reductions or pauses in the breathing rhythm, and fluctuate its pressures in order to support each individual breath. Several studies have shown that ASV is superior to CPAP in patients with heart failure with respect to sleep quality, decrease in heart failure events, and that it may contribute to the prevention of increased mortality rates [267, 268] . However, the effectiveness and safety of this treatment method is currently under debate. It has been shown to be ineffective in patients with sleep apnea that is complicated by chronic opioid therapy [269], as well as possibly increasing the mortality rate of individuals with chronic heart failure in conjunction with a reduced left ventricular ejection fraction (LVEF $\leq$ 45%) [270] [271]. However, some groups argue that there

was substantial nonadherence to the study protocol regarding the patients' use of the ASV and that carefully monitored trials should be encouraged to further investigate the effectiveness of ASV in heart failure patients (Bradley [263].

Even though it has been over a century since pathological Cheyne-Stokes breathing was shown to be abolished by the administration of excess CO_2 [272], the potential systemic consequences of hyperventilation and sympathetic overactivation that could make this a less attractive treatment option are still being studied [21, 213]. One study reported that the overall numbers of sleep-related arousals were not reduced and overall sleep quality was not altered, even though static CO_2 delivery reduced the number of oscillations in ventilatory parameters [37]. It is possible that the excess CO_2 could be directly stimulating the cortex, or reducing the cortical arousal threshold.

5.7 Chemical Control of Breathing

Chemoreceptors are sensory receptors responsible for transducing chemical signals into action potentials that the brain can interpret and regulate. There are two main classes, the peripheral chemoreceptors (located in the aortic body on the transverse aortic arch and on the carotid body on the common carotid artery) and the central chemoreceptors (which are located on the ventrolateral surface of the medulla oblongata in the central nervous system) [273]. Together they are responsible for regulating the body's pH, P_aO_2, and P_aCO_2 levels within their physiological set points. The central chemoreceptors are unable to respond to plasma changes in H+ as the peripheral chemoreceptors can, since H+ is unable to pass the blood-brain barrier. Instead, these neurons measure the pH change of the cerebral spinal fluid (CSF) due to $PaCO_2$. The CSF acidity is influenced solely by changing carbon dioxide level, which is able to pass through the blood-brain barrier. As the CO_2 diffuses across, it reacts to form carbonic acid which

quickly dissociates into bicarbonate and hydrogen ions, effectively decreasing the local pH. Due to its influence on pH levels, PaCO$_2$ is very closely monitored through a negative feedback mechanism to a set point of approximately 5.3 kPa, or 40 mmHg in a healthy individual [273].

The respiratory system is able to compensate for small deviations in plasma pH by altering the respiratory rate. An increase in PaCO$_2$, for example, will be sensed by the chemoreceptors and the patient will undergo a period of hyperventilation, resulting in the excess exhaling of CO$_2$, which is present in the blood. Even a small rise can recruit upper airway dilator muscles in order to prevent airway obstruction [274, 275]. However, these ventilation output changes can vary greatly between various individuals and with different diseases [249]. An individual with high chemosensivity will over respond to these small changes in chemical stimuli and continue to hyperventilate until the PaCO$_2$ falls below the eupneic level and the pH becomes too basic. They then will begin to hypoventilate in order to retain CO$_2$ and decrease pH back to normal. Individuals suffering from CSA and heart failure typically present with increased sensitivity to CO$_2$ [276]. The mechanism responsible for this heightened chemosensitivity is believed to be increased sympathetic activity, as measured by urine [277, 278], plasma [277], direct skeletal muscle activity, and norepinephrine levels [253]. Similarly, low chemosensitivity can be just as destabilizing, as severe blood gas disturbances can occur before a respiratory response is observed [249]. All individuals, healthy or otherwise, are susceptible to breathing cessation if the PaCO$_2$ falls below a threshold denoted as the apnea threshold. This threshold is typically about 2–6 mmHg below the eucapnic sleeping PaCO$_2$ levels [249, 279].

5.8 Inspired CO$_2$

The use of CO_2 to stabilize periodic breathing abnormalities has been investigated since the early 1980s [207]. Since then, several other studies have reported that use of constant CO_2 inhalation was able to help prevent apneas so long as enough CO_2 was administered [21, 25, 209, 210]. It is believed that chemoreceptor oversensitivity is the mechanism resulting in the periodic reductions in $PaCO_2$ below the apnea threshold that causes the cessation of breathing in central sleep apnea. It is not known if this is triggered mainly by the peripheral or central chemoreceptors [21], but it is hypothesized that breathing in low concentrations of CO_2 at night can eliminate these apneas. This alternative therapy, if successful, would provide a new treatment for patients where CPAP had failed, or was intolerable.

There have been many short term studies showing that inspired CO_2 has been successful in treating in CSA patients with CHF [21, 38], without CHF or any other apparent cardiovascular adverse effects [19, 20], idiopathic central sleep apnea (ICSA) [20], and Cheyne-Stokes breathing (CSB) [21]. Overall breath-to-breath oscillations of $PaCO_2$ stabilized, as well as pH and overall breathing rhythm [280], as well as overall CSA symptoms [37]. However, the delivery system from exogenous CO_2 is quite cumbersome and not easy to manage in a household setting. Some reports even show that increased CO_2 inspiration does not improve sleep quality (which is most commonly due to the tight face mask) [38], has no reduction in the number of arousals during sleep [37], and may lead to increases in sympathetic excitation [281].

Other studies have been performed investigating ways to increase CO_2 without the use of CO_2 tanks. One possible alternative is adding additional dead space. Dead space is the volume of airway passages (such as the trachea and bronchi) that contain air that does not reach the alveoli, where it must reach if it is to contribute to gas exchange. By adding a mask attached to a small cylinder, less carbon dioxide is exhaled in each breath and the total distance to the lungs is

increased; in other words, dead space is added. The rebreathing of this carbon dioxide induces moderate hypercapnic (increased CO_2) conditions. The addition of approximately 400–600 ml of dead space has been shown to decrease the Apnea-Hypopnea Index (AHI) (which is represented by the number of apnea and hypopnea events per hour of sleep), decrease the number of arousals, improve sleep quality [19], and stabilize breathing patterns [282]. However, there may be adverse effects to adding dead space. This includes fatiguing already compromised respiratory muscles, and inducing sympathetically driven responses such as vasoconstriction, tachycardia, and increased myocardial contractility. Overworking the heart may lead to an increase in morbidity [19].

Furthermore, some other clinical studies have reported the effect of low concentrations of inhaled CO_2 in a group of preterm infants with apnea. The premature infants can respond to CO_2 inhalation with an overall decrease in total pulmonary resistance, which allows them to achieve greater airflow. Saif Al-Saif et al found that low concentrations of CO_2 (0.5%-1.5%) decreased the total number and the duration of apneas, a mild increase in the minute ventilation, and improved oxygenation [283]. Moreover, they suggest that a 0.8% CO_2 concentration in preterm infants is at least as effective as theophylline in describing AHI [284].

5.9 Conclusions

In summary, the number of sleep apnea diagnoses is rapidly increasing each year due to more awareness and better detection instruments. The prevalence of this disease is going to keep increasing as heart failure, to which is it closely tied with, continues to plague more of the human population, particularly in developed countries that have increased life expectancies. The current gold standard for the treatment of sleep apnea, CPAP, does not always work with patients with

central sleep apnea and a significant portion of those it would help refuse to utilize it due to its side effects and an inability to sleep with the mask. There have been several promising studies showing that inspired CO_2 (either directly inspired through exogenous tanks or by increasing the total dead space) can help reduce the AHI and improve sleep quality compared to CPAP. However, there are several potential adverse effects associated with inspiring CO_2 that have not been fully explored. The initial results from the short trails is promising, but larger studies are needed to determine the long-term efficacy and safety of inspired CO_2 as a possible treatment for CSA.

6 Chapter 7 A modeling study on inspired CO_2 rebreathing device for sleep apnea treatment by means of CFD analysis and experiment

This chapter is partially based on the following publication [285]:

Mehdi Shokoueinejad, Arman Pazouki, Jake Levin, Fa Wang, Jerome Dempsey, John G. Webster. "A modeling study on CO2 rebreathing device for spleep apnea treatment by means of CFD analysis and experiment" (Accepted, JMBE, Aug 2016)

6.1 Abstract

We present the device design, simulation, and measurement results of a therapy device that potentially prevents sleep apnea by slightly increasing inspired CO_2 through added dead space (DS). The rationale for treatment of sleep apnea with CO_2 manipulation is based on two recently reported premises: (i) preventing transient reductions in $PaCO_2$ will prevent the patient from reaching their apneic threshold, thereby preventing "central" apnea and instabilities in respiratory motor output; and (ii) raising $PaCO_2$ and end-tidal CO_2, even by a minimal amount, provides a strong recruitment of upper airway dilator muscles, thereby preventing airway obstruction. We have also provided the simulation results, obtained from solving the Navier-Stokes (NS) equations within the device volume. Therein, the NS equations are coupled with a convection-diffusion equation that represents the transport of CO_2 in the device, thus enabling the transient simulation of CO_2 propagation. Using this procedure, a prototype of variable volume dead space reservoir device was designed. Volumetric factors influencing carbon dioxide increases in the added reservoir (open-ended DS) were investigated. The maximum/minimum amount of CO_2 concentration were obtained for the maximum/minimum device volume; 3.4 and 2.4 mol/m^3 for the DS volumes of 1.2 and 0.5×10^{-3} m^3, respectively. In all case studies, the CO_2 buildup reached a plateau after approximately 20 breathing cycles. The experimental measurement results are in

agreement with the simulation and numerical results obtained using the proposed simplified modeling technique, with a maximum relative error of 3.5 %.

Nomenclature

Parameter	Definition
P_aCO_2	Atrial Pressure of Carbon Dioxide in Arterial Blood
$P_{ET}CO_2$	End tidal CO_2
x_{O_2}	Concentration of O_2
x_{CO_2}	Concentration of CO_2
$x_{O_2,1}$	Chamber O_2 concentration before inhale
$x_{O_2,2}$	Chamber O_2 concentration after inhale
$x_{O_2,3}$	Chamber O_2 concentration after exhale
$x_{O_2,in}$	Inlet air O_2 concentration
$x_{CO_2,2}$	Average CO_2 concentration after inhale
$y_{O_2,1}$	Average inhale air O_2 concentration
$y_{O_2,2}$	Average exhale air O_2 concentration
$c_{n,1}^{ave}$	Average CO_2 concentration after inhale where *n* is the breathing cycle number
$c_{n,2}^{ave}$	Average CO_2 concentration after exhale in n^{th} breathing cycle
v_b	Air velocity at the inlet boundary
TV	Tidal Volume
RV	Reservoir Volume
γ	Main reason to introduce γ in the equations is to (*i*) account for imperfect mixing in small volume, e.g. due to undeveloped flow; and (*ii*) account for any unforeseen parameter that can affect the mixing of CO_2 and fresh air.

6.2 Introduction

Sleep apnea, where breathing stops repeatedly and interrupts sleep, leading to significant cardio-vascular morbidities, insulin resistance, neural injury, heart attack, irregular heartbeat, and accelerated mortality. These effects of sleep apnea lead to a decrease in quality of life and productivity. Sleep apnea may increase the risk for accidents while working or driving.

One possible treatment for sleep apnea is the use of inspired CO_2. Since the early 1980s, several studies have shown that the constant inhalation of CO_2 can help prevent central sleep apneas (CSA) [59, 207-211]. Even obstructive sleep apnea (OSA) patients with extremely collapsible

airways responded positively to the CO_2 treatment Most of these results were obtained during periods of 1 to 6 h of CO_2 therapy during the night [7].

Although upper airway collapsibility is a critical component of OSA, it is now well-established that pathophysiologic characteristics such as a sensitive arousal threshold (to elicit ventilatory overshoots), high "loop gain" i.e. chemo-sensitivity and plant gain, and/or reduced responsiveness of airway dilator musculature to chemoreceptor stimulation are also commonly present in the majority of OSA patients [2, 14]. In turn, CO_2 has been shown to be a major regulator of airway caliber during sleep, i.e. when the "wakefulness" stimulus is removed, as evidenced by the following observations: 1) small transient reductions in $PaCO_2$--as experienced with ventilatory overshoots which occur upon recovery from an apnea and/or via transient arousals—of 1–4 mmHg will elicit apneas and ventilatory instability during NREM sleep [15, 16]; 2) adding inspired CO_2 sufficient to increase $PaCO_2$ 1–3 mmHg removes most or all of the hypocapnic induced central apneas and the periodic breathing induced via hypoxic exposure and/or CHF, spinal cord injury, or with idiopathic central apnea [17-21]; and 3) adding inspired CO_2 increases both phrenic (linear) and hypoglossal (alinear) motor nerve activity, thereby recruiting both diaphragm and upper airway dilator muscles [22, 23].

So theoretically, increasing CO_2 should stabilize central respiratory motor output as well as improve upper airway caliber and prevent upper airway obstruction. It is believed that breathing in low concentrations of CO_2 can help prevent periodic reductions in $PaCO_2$. By preventing these levels from falling below the apnea threshold of $PaCO_2$, the number of breathing cessations can be reduced. However, handling all the equipment for exogenous CO_2 can be cumbersome in a household setting, and the benefits towards sleep quality are still debated [210, 212, 213]. Another method of increasing CO_2, is the addition of extra DS. Dead space is the portion of the

airway passages that do not contribute to gas exchange (i.e. trachea and bronchi). It has been shown that the Apnea-Hypopnea Index (AHI) in CSA and OSA patients can be decreased by the addition of as little as 400 to 600 ml of external DS [7, 8, 214]. A study showed that 17 of 21 OSA patients subjected to mild to moderate levels of rebreathing their own CO_2 during sleep eliminated most of their sleep disordered breathing [7]. This study used a "fixed" volume rebreathing device worn using a full face mask.

These findings by using DS raised the question of how rebreathing of exhaled gas affects subsequent CO_2 accumulation/concentration rate change. In addition to the experimental study of such problems, computer simulation provides an alternative way of validating the DS-based experiment by considering a range of parameters that affect the CO_2 concentration, thus allowing for the analysis of a larger group of subjects. Unfortunately, the literature is void of any computational modeling. At the very best, a mathematical modeling of the CO_2 accumulation in closed spaces is provided in [286]. This model; however, is not extendable to the current study since the apnea treatment device considered herein is an open end volume.

The present study aims to investigate the effects of DS volume on CO_2 concentrations through simulation and experimentation. The aim is to propose, quantify, and validate the CO_2 accumulation in the proposed device designs. The remainder of the document is organized as follows. Section 7.3 elaborates on the design of the device that is used to treat the sleep apnea. A computational approach is explained and adopted in section 7.4. The simulation and experiment results for various device volumes are provided in section 7.4. A mathematical model to capture the CO_2 accumulation in the open-volume apnea treatment device is discussed in section 7.5. Section 4 provides further discussion of the results.

6.3 Device design

A variable volume DS reservoir device was designed for the purpose of validating the mathematical model formulated in this study. The design of our device incorporated an automatic variable DS volume, different from previous models which involved a fixed volume. Our device's main criterion was to allow for incremental adjustments in length to vary the DS present in the device. The varied DS volume's objective is to create different CO_2 concentrations inside the device's reservoir for rebreathing. The CO_2 concentration is measured at different volume intervals to determine the effect of DS volumes on CO_2 concentrations.

A generic embodiment of the device consists of a mask to cover the wearer's mouth and nose, the mask is connected via a flexible tube to a variable sized reservoir that has an inlet, connected to the tube, and an outlet which is open for fresh air ventilation. The distance between inlet and outlet is adjustable. The main feature of this device is the variably sized reservoir. Different physical devices can be constructed to create this variably sized reservoir that has an adjustable length between the inlet and outlet. One such embodiment of the reservoir consists of a worm-gear driven bellow tube to position its base which allows the contraction and expansion of a constant diameter cylinder to a desired volume.

The embodiment's external housing and threaded disc, pictured in Fig. 7, were fabricated using 3D printing. The motor was mounted to the left side of the housing using screws. The worm gear was attached to the motor via a hole on the left wall. The threaded disc that acts as the outlet for the DS was then screwed halfway down the shaft. A plastic bellow was stretched over the threaded disc and secured to a lip at the left wall of the device that encompasses the inlet hole. With the internal components assembled, a top to the housing was screwed on the right side of the

device, closing the reservoir and centering the worm gear with a ball bearing in the top. An Arduino processor was then mounted in an electronics box and screwed to the housing to process the sensors and control the motor.

The device controls the CO_2 concentrations by moving the threaded disc and changing the DS volume. By varying the volume of the DS, exhaled CO_2 builds up in the DS and does not get recycled into the ambient surroundings. The exhaled CO_2 mixes with ambient air in the DS to raise the CO_2 concentrations in the rebreathed DS. Once the user inhales, the excess CO_2 from the DS raises the CO_2 concentration in the user. CO_2 levels in the user are fluctuated by adjusting the amount of DS present for inhalation. The longer the DS, the more CO_2 that can accumulate without being ejected from the device during exhalation. When the device records a hypopnea from the patient with the device's sensors, it actuates the motor and drives the worm gear to incrementally advance the threaded disc for expansion of the DS. As more hypopneas occur, the device will keep incrementing the threaded disc until apneas discontinue. If a hyperpnea occurs, then the device will retract the threaded disc and reduce the volume of DS the user rebreathes. This retraction will continue until no hypo-/hyperpnea occur, at which point the device will maintain the current DS volume.

Figure 7 shows the device used for this study. Exhaled breath from the wearer comes in through the inlet on the top left side of the device and enters the DS. The DS is defined as the volume of the threaded container from the plate that connects to the open air to the plate that connects to the flexible breathing tube. The threaded disc (approximately center on Fig. 7) contains an outlet for airflow and a threaded hole that interfaces with a central worm gear (center shaft with threads in Fig. 7. A motor located below the inlet drives the worm gear that results in a translation of the threaded disc to either expand or contract the DS (an expansion would be moving the threaded

disc to the right as seen in Fig. 7). The DS is contained within a larger cylindrical casing that contains square holes for the air exchange and prevents interference from external objects to the moving internal parts.

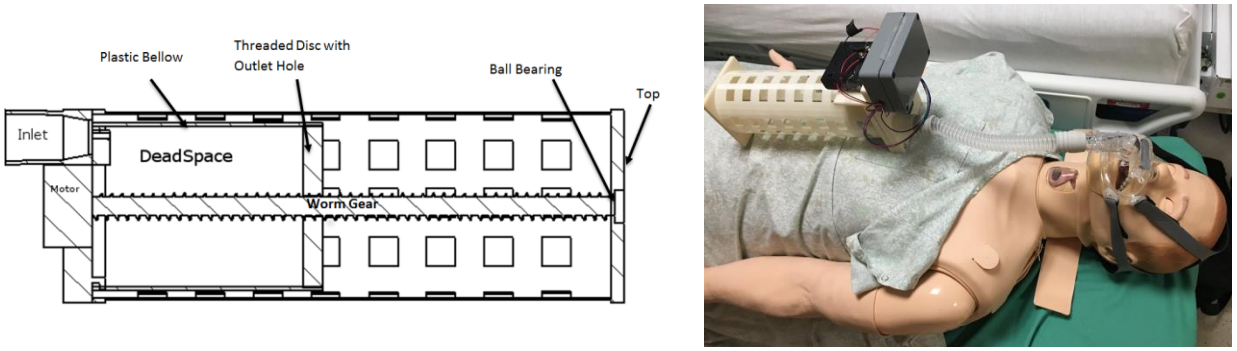

Figure 7: *Left*: Schematic diagram of an accordion-like, 8 cm diameter collapsed bellows DS. An axial stepper motor rotates a long worm gear protruding at the near end that expands the bellows up to expanded length. The larger perforated white surround (casing) prevents the patient from contacting any motion, yet permits gas flow. *Right*: Mannequin using the device [59].

6.4 Analysis

6.4.1 Numerical Simulation

To further investigate the accumulation of the CO_2 in the rebreathing device, a numerical simulation of the transport of diluted species was conducted herein. The governing equation of the transient air flow in the device can be explained by Navier-Stokes (NS) and Continuity equations

$$\rho \frac{\delta u}{\delta t} + \rho(u.\nabla)u = \nabla.[-pI + \mu(\nabla u + (\nabla u)^T)] \qquad (1)$$

$$\nabla.u = 0\,, \qquad (2)$$

where $u,\ p, \rho$ and μ are the fluid velocity, pressure, density, and viscosity, respectively. The convection-diffusion of the CO_2 is expressed by [287]

$$\frac{\delta c_i}{\delta t} + \nabla.(-D_i \nabla c_i) + u.\nabla c_i = R_i\,, \qquad (3)$$

where c_i and $R_i$are the CO_2 concentration and source/sink; $R_i = 0$ in the current study due the absence of chemical reaction. D_i is the diffusivity (also called diffusion coefficient), such as mass diffusivity for particle motion. The value of diffusion coefficient D for the diffusion of CO_2 in fresh air is 0.166 cm^2/s at 310.15 T/K [288]. Equation (3) is coupled to the NS equations given in Eqs. (1) and (2).

Due to the negligible amount of CO_2 in the fresh air (< 0.04 %) and stationary condition before breathing, a uniform zero initial CO_2 concentration,$c_o = 0$, and zero velocity were assumed in the device. The outflow boundary conditions for velocity and concentration were modeled as

$$[-pI + \mu(\nabla u + (\nabla u)^T)]n = -p_0 n\,, \qquad (4)$$

$$Dn_{.i}\,\nabla c_i = 0\,, \qquad (5)$$

where p_0 is the ambient pressure.

The COMSOL software [289] was leveraged to model the CO_2 propagation explained by Eqs. (1–5). A breathing cycle was then modeled as two separate simulations to mimic the inhale and exhale processes individually. The difference of the two simulations was in the inlet concentration boundary condition as explained below:

Inhale: An inflow air with the CO_2 concentration $c = 0$ mol/m^3, i.e. that of the fresh air, and velocity $v_b = 0.35$ m/s in form of a step function was applied to the simulation [290]. At the end of the simulation, the average CO_2 concentration, $c_{n,1}^{ave}$, was measured inside the reservoir, where n is the breathing cycle number.

Exhale: An inflow concentration $c = 20.95 - (1 - \frac{5}{21})c_{\mathrm{n},1}^{\mathrm{ave}}$ [286] and velocity v_{b} was considered. The average CO_2 concentration of the reservoir, $c_{\mathrm{n},2}^{\mathrm{ave}}$, was measured at the end of the process.

Zero initial velocities were considered inside the reservoir for both Inhale and Exhale cycle. The initial concentration for each cycle was the final average concentration of the previous cycle; that is, for the breathing cycle n, $c_{\mathrm{n},2}^{\mathrm{ave}}$ and $c_{\mathrm{n},1}^{\mathrm{ave}}$ were assigned as the initial concentration of the Inhale and Exhale, respectively.

Fluid and concentration equations, Eqs (1–3) were solved simultaneously (fully coupled). In terms of modeling, a Reynolds-Averaged Navier-Stokes (RANS) with a $K - \epsilon$ model is used. The linear system constructed from the FEM discretization was solved using an iterative Backward Differentiation Formula (BDF-2) method at each time step until the convergence was achieved (on average around 7–9 iterations). The simulation consisted of multiple (20) breathing cycle with independent inhale and exhale simulation in each cycle (total of 40 simulations). The inlet and outlet boundary conditions were implemented using Dirichlet (for velocity and concentration) and Neumann (for pressure). The compute time to execute 40 simulations was around 18 h on a PC with an Intel I7 processor and 64 GB RAM.

In the simulation of the exhale, the inlet condition, i.e. where the exhale air entered the chamber, had a fixed velocity which was obtained from the exhale air volumetric rate in an average human (500 ml/cycle which represents the tidal volume). More specifically, we set the inlet velocity equal to 0.3 [m/s].

Similarly, the exhale concentration was fixed; the value of exhale CO_2 was calculated based on the average concentration of O_2 in inhale: $c = 20.95 - (1 - \frac{5}{21})c_{\mathrm{n},1}^{\mathrm{ave}}$ [286] where c_{ave} is the

average inhale concentration (mol/m^3) and (1–5/21) is a typical rate of O_2 consumption in one breathing cycle. The value of c_{ave} was estimated by averaging the chamber CO_2 concentration at the beginning and end of one inhale cycle. Finally, the pressure boundary condition was applied using Neumann boundary where pressure gradient was zero in the direction of the boundary. The simulation procedure for the inhale was the same as that of the exhale and the velocity and pressure boundary conditions were similar to those of the exhale. The CO_2 concentration at the inlet, i.e. where the air enters the chamber, was the same as that of the fresh air (almost zero).

As for the initial condition, we used zero velocity and atmospheric pressure in the reservoir. The value of the concentration depended on the history of the breathing through the device, i.e. the number of the simulation in the sequence of breathing cycles: at any certain simulation, we set the initial CO_2 concentration the same as that calculated from the last breathing subcycle (inhale or exhale).

We used variable mesh length (smaller elements at the wall, larger at the center) with a growth rate of 1.2 normal to the wall. The reason for doing this was to improve the quality of the wall boundary condition. We used the COMSOL meshing tool. Overall, the model was discretized using about 40000 Tetrahedra, Pyramid, and Prism elements, please see Fig. S1. Table S1 includes details about the mesh used in the computational study, such as type of elements, number of elements, and mesh quality metrics.

Two device dimensions, with DS volumes equal to $v = [0.5, 1.2] \times 10^{-3}$ m^3, were investigated. For each device $n = 20$ breathing cycles were simulated using the Inhale and Exhale procedures explained before. As shown in Fig. 8 the plateau of the average CO_2 buildup occurs before the 20th breathing cycle. Figures 9 and 10 capture the concentration development in

device designs associated with the maximum and minimum volume for three time steps: $t = 0.5, 1.0, 2.4$ s. A breathing cycle is assumed to take about 4.8 s, which is equivalent to 2.4 s exhale or inhale time.

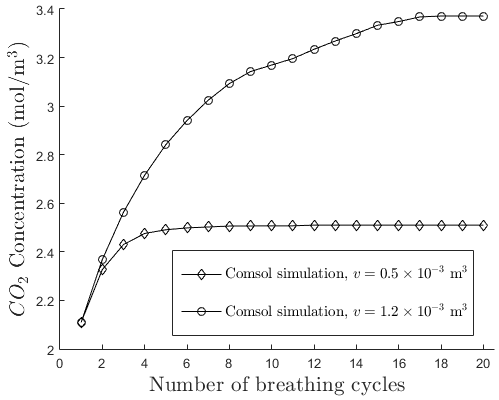

Figure 8: Average CO_2 concentrations for device volumes $\boldsymbol{v} = [\mathbf{0.5}, \mathbf{1.2}] \times \mathbf{10^{-3}}$ m^3 obtained from simulation.

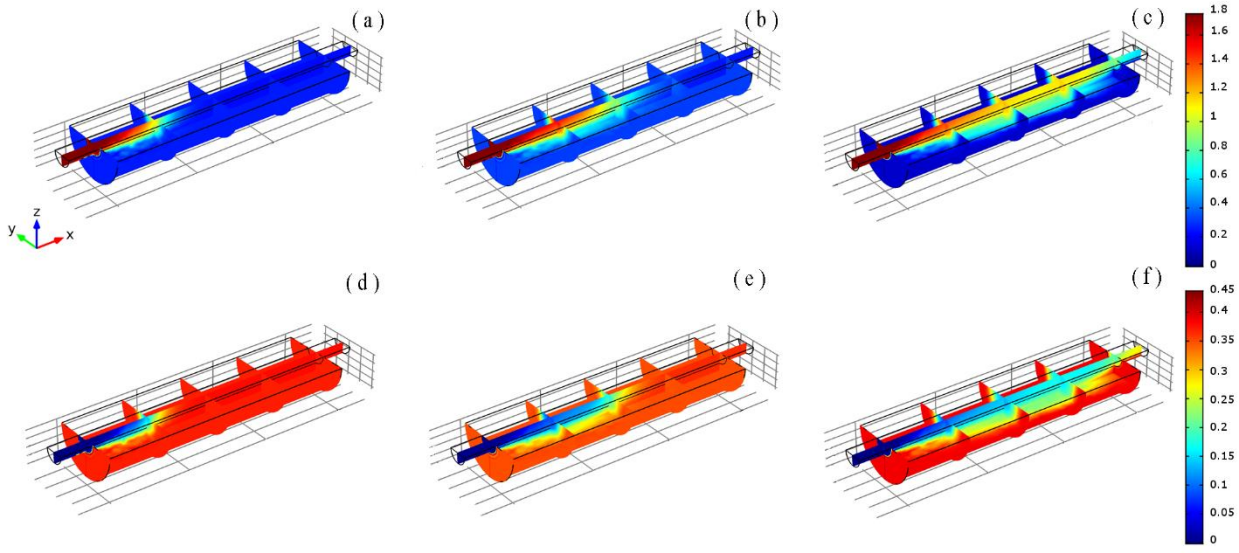

Figure 9: Transient CO_2 concentration (mol/m^3) propagation in a reservoir with the volume $\boldsymbol{v} = \mathbf{1.2} \times \mathbf{10^{-3}}$ m^3 at three time instances: $\boldsymbol{t} = \mathbf{0.5\ s}$ (a, d), $\boldsymbol{t} = \mathbf{1.0\ s}$ (b, e), $\boldsymbol{t} = \mathbf{2.4\ s}$ (c, f). Subplots (a, b, c) and (d, e, f) denote the exhale and inhale processes, respectively. The inflow boundary condition is assumed at the left side of the reservoir. In subplots (a, b, c) the left side denotes the inlet of accordion-like device, and in (d, e, f), left side denotes the outlet of accordion-like device presented in figure.7

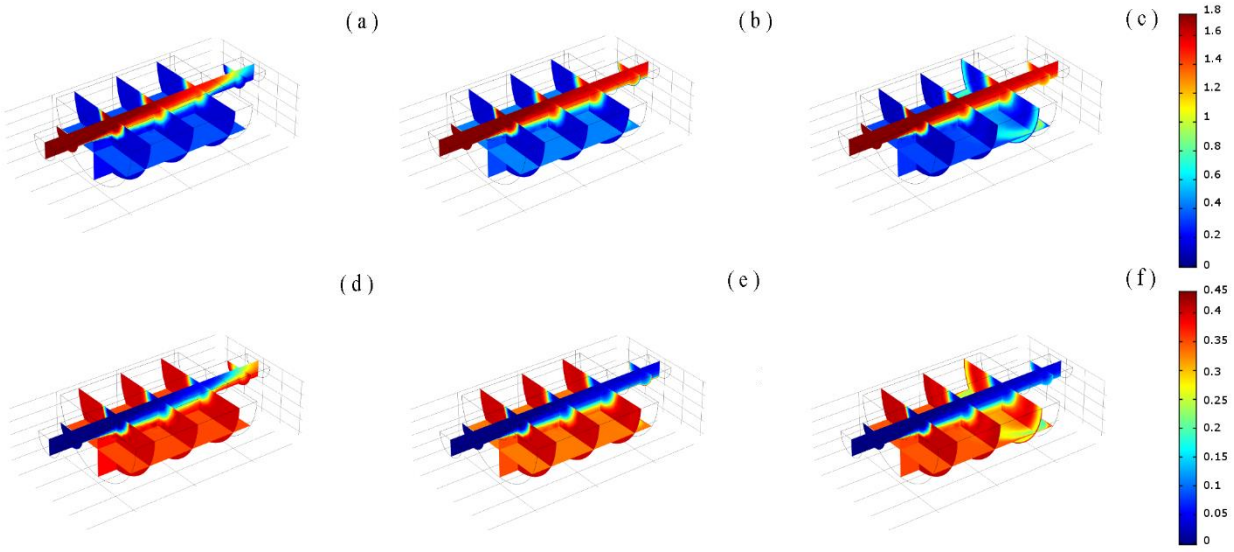

Figure 10: Transient CO_2 concentration (mol/m^3) propagation in a reservoir with the volume $\boldsymbol{v = 0.5 \times 10^{-3}}$ m^3 at three time instances: t = 0.5 s (a, d), t = 1.0 s (b, e), t = 2.4 s (c, f). Subplots (a, b, c) and (d, e, f) denote the exhale and inhale processes, respectively. The inflow boundary condition is assumed at the left side of the reservoir. In subplots (a, b, c) the left side denotes the inlet of accordion-like device, and in (d, e, f), left side denotes the outlet of accordion-like device presented in figure. 7

6.4.2 Experimental Study Model

A pediatric human patient simulator (HPS) mannequin, Fig. 7.right, was used to simulate ventilation to measure the CO_2 accumulation in a reservoir for two volumes of $v = 0.5 \,\&\, 1.2 \times 10^{-3}$ m^3.The mannequin 'breathed' with tidal volume 500 ml and expired CO_2 concentration of 5% = 2.11 (mol/m^3). End-tidal CO_2 ($P_{ET}CO_2$) and level of CO_2 were recorded using a CARDIOGRAPH® by Respironics monitoring system.

6.4.3 Mathematical Modeling

To further simplify the numerical studies, a mathematical model may be used to evaluate the accumulation of CO_2. A similar effort was made in [286] to evaluate the accumulation of CO_2 due to rebreathing in a confined space. Therein, the CO2 accumulation was formulated as

$$x_{O_2,2} = \left[(\mathrm{RV} - \mathrm{TV})x_{O_2,1} + \mathrm{TV}\left(1 - \frac{5}{21}\right)x_{O_2,1}\right]/\mathrm{RV} \quad (6)$$

$$x_{CO_2,2} = \left[8.83\,\frac{\mathrm{mol}}{\mathrm{m}^3} - x_{O_2,2}\right], \quad (7)$$

where x_{O_2} and x_{CO_2} are the concentration of O_2 and CO_2 in mol/m^3, respectively; TV is the tidal volume which is assumed to be 4.5×10^{-4} m^3; and RV is the reservoir volume in which the rebreathing occurs. Equations (6) and (7) predict a continuous increase in the CO_2 to its maximal value, i.e. 8.83 mol/m^3. Our proposed device is an open-space reservoir with a hole to allow for outflow of expired air and inflow of fresh air. Therefore, Eqs. (6) and (7) are not suitable for the current study. A model is proposed herein to describe the CO_2 accumulation inside an open-space reservoir. By allowing a reservoir connection to the ambient air, the CO_2 concentration in each breathing cycle can be obtained in a procedure explained below.

The average O_2 concentration in the chamber after an inhalation, $x_{O_2,2}$, is obtained from its value before inhalation $x_{O_2,1}$ as

$$x_{O_2,2} = \left[(\gamma\mathrm{TV})x_{O_2,\mathrm{in}} + (\mathrm{RV} - \gamma\mathrm{TV})x_{O_2,1}\right]/\mathrm{RV}, \quad (8)$$

where $x_{O_2,\mathrm{in}}$ is the inlet air O_2 concentration, which is equal to 8.83 mol/m^3 in standard air condition. Equation (8) relies on the flow incompressibility which implies that the inflow and outflow volumes are both equal to TV. Due to an imperfect mixing of the inlet with the reservoir air, part of the inlet air,$(1-\gamma)$TV, leaves the reservoir without mixing with the reservoir air. Another part, γTV, flows towards outlet after mixing with the reservoir air. The coefficient γ can have a value in the range [0, 1], with $\gamma = 1$ denoting a perfect mix. The main reason to introduce

γ in the equations is to (i) account for imperfect mixing in small volume, e.g. due to undeveloped flow; and (ii) account for any unforeseen parameter that can affect the mixing of the CO_2 and fresh air. Therefore, the average O_2 concentration,$y_{O_2,1}$, experienced during inhalation can be obtained as

$$y_{O_2,1} = 0.5\gamma\left(x_{O_2,1} + x_{O_2,2}\right) + (1-\gamma)x_{O_2,in}\,. \quad (9)$$

Similar procedure is followed during exhalation. The exhale O2 concentration, $y_{O_2,2}$, where

$$y_{O_2,2} = y_{O_2,1}\,(1-\tfrac{5}{21}), \quad (10)$$

is mixed "imperfectly" with the chamber in a similar fashion

$$x_{O_2,3} = \left[(\gamma TV)y_{O_2,2} + (RV - \gamma TV)x_{O_2,2}\right]/RV\,, \quad (11)$$

where $x_{O_2,3}$ is the O_2 concentration at the end of a breathing cycle. The O_2 reduction value in rebreathing was assumed to be 5/21, which is for a healthy subject. This value may change slightly between patients. The breathing procedure formulated by Eqs. (8) to (11) is then repeated, given the initial $x_{O_2,1}$ concentration at the beginning of the breathing is the one obtained at the end of the previous cycle, i.e. $x_{O_2,3}$. We assume that the flow rate during the inhalation and exhalation are similar; therefore, parameter γ has the same value in Eqs. (8), (9), and (11).

Figure 11 shows the CO_2 accumulation in a device with RV = 1200 ml, where it is assumed that the mixing of the inflow and reservoir air is complete (γ = 1). A good agreement with the experimental data was obtained for the small device when γ = 0.5. We conjecture that the imperfect mixing of the CO_2 and fresh air in the small device due to undeveloped flow causes imperfect mixture and calls for $\gamma < 1$. This is shown in Fig. 10 where the bulk of the flow is around pipe center line.

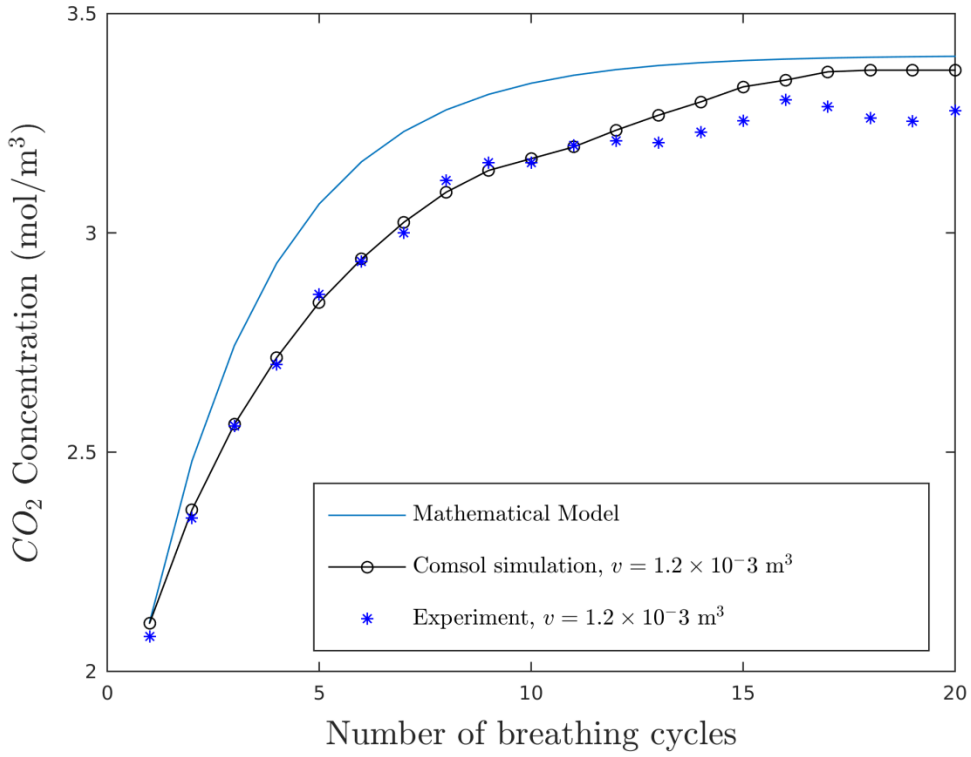

Figure 11: Transient CO_2 accumulation in an apnea treatment device with the volume of $\boldsymbol{v = 1.2 \times 10^{-3}}$ m^3. The plot shows the results of the mathematical model, simulation, and experiment.

The mathematical model and experimental results demonstrate the CO_2 buildup in the proposed device. We use this model to investigate the change of the CO_2 buildup when the environment condition changes to ensure that an excessive CO_2 concentration will never happen. To this end, we conducted a series of tests in the design domain defined by $\gamma \in [0, 1]$,TV $\in [0.3, 0.8] \times 10^{-3}$ m^3 and RV $\in [0.5, 1.7] \times 10^{-3}$ m^3. We found no situation where the CO_2 concentration exceeds 3.5 mol/m^3, see Fig. 12.

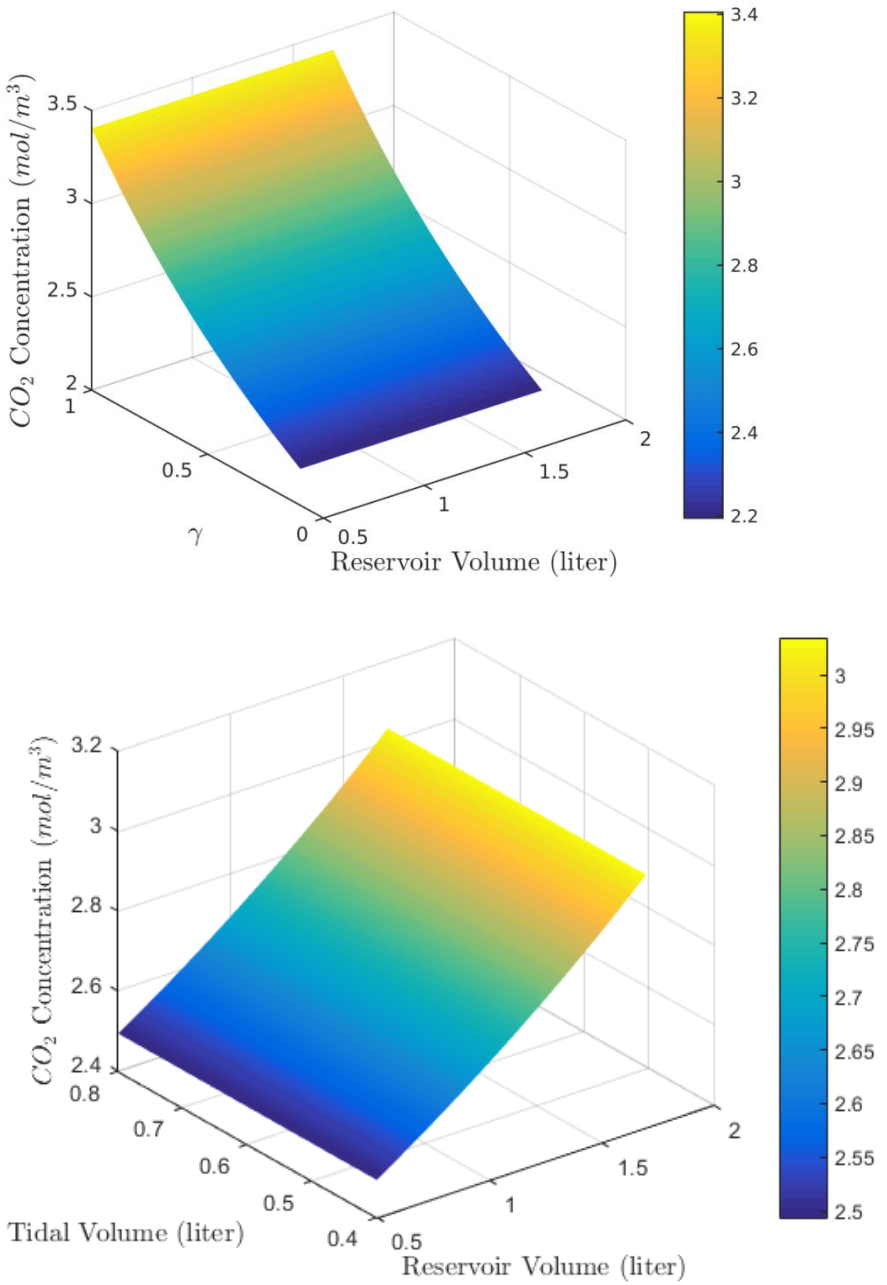

Figure 12: Parametric analysis of the CO_2 accumulation in the apnea treatment device for different values of DS volume, RV, tidal volume, TV, and mixing efficiency, $\boldsymbol{\gamma}$. The CO_2 accumulation is provided for: *top*: $\mathbf{RV} \in [\mathbf{0.5}, \mathbf{1.7}]$ L and $\boldsymbol{\gamma} \in [\mathbf{0}, \mathbf{1}]$, and *bottom*: $\mathbf{RV} \in [\mathbf{0.5}, \mathbf{1.7}]$ L and $\mathbf{TV} \in [\mathbf{0.5}, \mathbf{1.7}]$ L

The mathematical model provided to capture the CO_2 accumulation relies on the perfect mixing of the exhale air with the DS air. This condition is satisfied when the DS volume is large enough and the flow reaches a fully developed condition. However, when the DS volume is small, a great portion of the inlet air passes through the device without mixing with the existing air, see Fig. 10.

To account for this, we assumed that the mixing coefficient for small volumes changes linearly with the DS volume until it reaches its maximum at 1.2×10^{-3} m^3.

To summarize, a variable volume DS reservoir device was designed, constructed and tested. The result of this test was achieved through exposing the mannequin to inhaled gas from a CO_2 reservoir; a process that increased end-tidal CO_2 ($P_{ET}CO_2$) during normal breathing Fig. 13. Based on previous studies [59], this adjustable variable volume device may permit the use of minimal amount of dead space (and therefore minimal increase in CO_2 to eliminate significant numbers of apneas, thereby providing an opportunity for apnea elimination without side effects of "excessive" hypercapnia as described in Khayat et al study [214].

The experimental and simulation values of the CO_2 concentration for two device designs with minimum and maximum DS volume, $v = [0.5, 1.2] \times 10^{-3}$ m^3, are captured in Fig. 14. For both device volumes, the concentration values measured experimentally and computationally agree well. Additionally, confirmed by those tests, the CO_2 concentration can be adjusted by changing the DS volume.

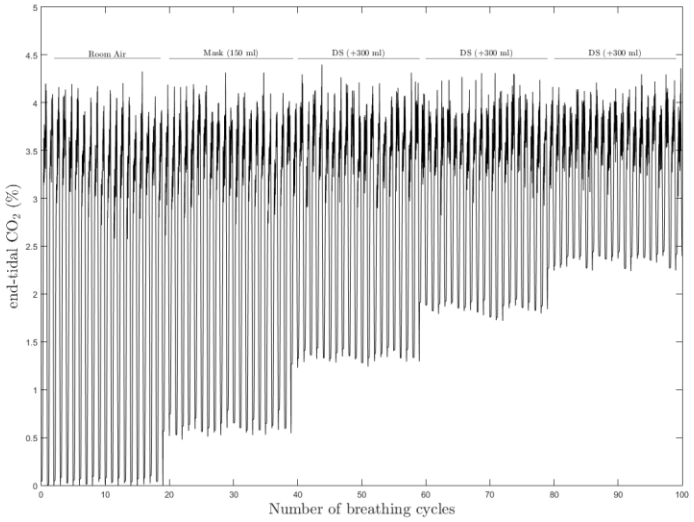

Figure 13: HPS mannequin end-tidal carbon dioxide capnography. The plot shows a segment of room air breathing followed by a segment of breathing through a face mask with 150 ml DS, then an additional 300 ml DS were added to the mask and the end-tidal CO_2 was recorded. This action was repeated for total of three times. The segment with added DS shows an elevation in $P_{ET}CO_2$

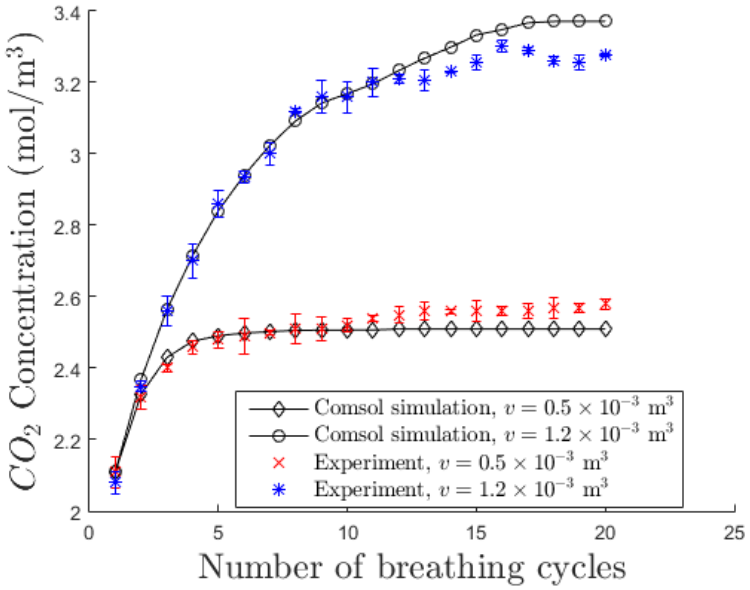

Figure 14: Comparison of the average CO_2 accumulation obtained from COMSOL simulation, mathematical model, experimental data and its fitted curve inside the apnea treatment device. CO_2 increased at the lower and higher volume level of added DS. At each level after adequate number of breathing cycle CO_2 level reach plateaued.

6.5 Discussion

The dead space device has been used in several studies since the 1980s which incorporates the rebreathing of exhaled air to induce moderate hypercapnic conditions in systemic circulation [7, 59] have recently demonstrated in a small cohort of OSA patients that breathing from a CO_2-enriched reservoir eliminates most apneic events in obstructive and central sleep apnea patients [7]. However, none of those aforementioned studies provide a model to study the behavior of CO_2 inside the DS device. To back up the experimental studies conducted on the breathing mannequin, the rebreathing process was numerically simulated. The simulation tool can provide a priori knowledge of the CO_2 accumulation for the rebreathing DS device. Furthermore, a mathematical model was provided to analyze, more efficiently, the CO_2 accumulation. The model was used to run three parametric studies (RV, TV, and γ) to ensure that excessive CO_2 accumulation is avoided. Suggested mathematical models can assess the CO_2 rebreathing device function for further study.

The merit of numerical modeling approach is to quantify the mixing pattern of the CO_2 in the device and analyze the CO_2 accumulation, through a wide range of input parameters and patient data. This study was conducted to evaluate and provide a better understanding of the transient CO_2 propagation and the mixing of the inflow and reservoir air. A series of validation scenarios using a combination of experiment and simulation were conducted for different DS volumes. We conjecture that a similar simulation technique may be used to study the problems that involve human exhale air in different apparatus.

The limitation of the study is that we did not collect qualitative or quantitative data on a human subject, subject comfort, or subject breathing effort using the device. Furthermore, for each device

design study, the geometry needs to be built in the software, and an appropriate mesh selected. The re-meshing of the reservoir may require a long processing time. More refined mesh increases the computation time exponentially since it also demands a small time step.

6.6 Conclusions

We designed, fabricated, and tested a relatively inexpensive, inspired CO_2 rebreathing device for the purpose of sleep apnea treatment. We performed a CFD analysis and an experimental test bench. This study was conducted to evaluate how volumetric differences in the DS device, used for sleep apnea treatment, affects the dynamics of CO_2 accumulation in the device by means of mathematical/simulation/computational modeling and experimental approaches. I led the team to have tested the accuracy of this device by providing a model to study the behavior of CO_2 inside the DS device. A breathing mannequin, with mechanics similar to patients, was used to simulate respiration for testing. The mannequins quantified, via mathematical modelling, the dynamics of CO_2 mixing between the inflow gas and dead space air. The main advantage of this proposed variable DS device is to elicit highly predictable (±3.5% error) alveolar $PaCO_2$ levels by changing the reservoir DS, thereby ensuring that excessive CO_2 accumulation would not occur during rebreathing. The use of suggested mathematical models can assess the CO_2 rebreathing device function for further study in the respiratory system and devices.

6.7 Supplementary Material

This section further demonstrates and explains the details and mesh type associated with the implementation of the finite element method. Table S1 includes details about the mesh used in the computational study, such as type of elements, number of elements, mesh quality metrics,

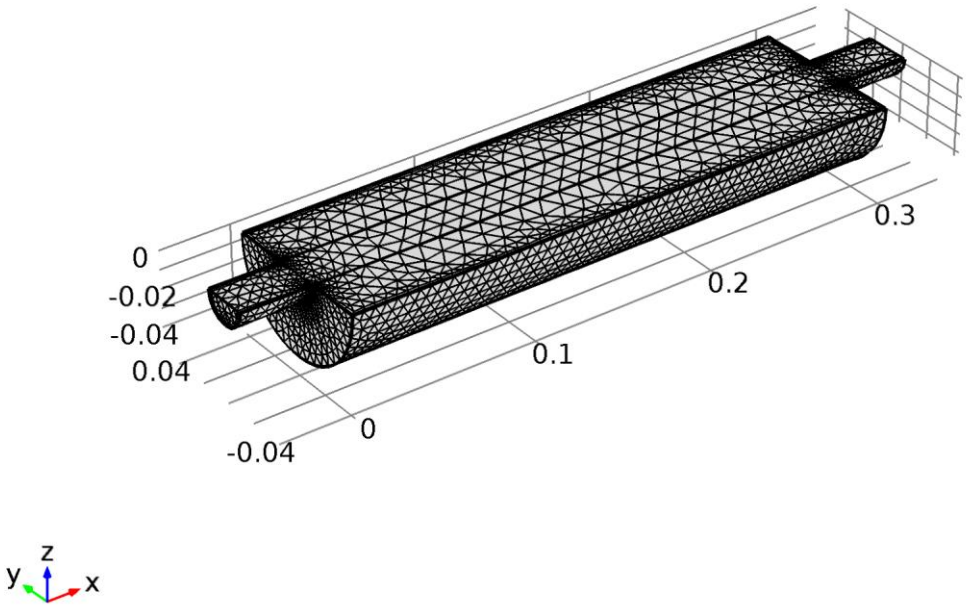

etc.

Figure S1: Demonstrates the mesh used in the computational study

Table S1: Mesh statistics' details about the mesh used in the computational study [289]

Description	Value
Minimum element quality	0.02965
Average element quality	0.5922
Tetrahedral elements	30302
Pyramid elements	186
Prism elements	7562
Triangular elements	6136
Quadrilateral elements	352
Edge elements	487
Vertex elements	18
Maximum element size	0.00608
Minimum element size	0.00182
Maximum element growth rate	1.2

7 Chapter 8 Low Cost Sleep Apnea Therapy Device "Smart CO_2 Device" for Use in Home

This chapter is partially based on the following publication [291], John Webster developed core material and Jason Hunt revised the material below, which he submitted to the US Patent Office:

- Webster. J., dos Santos, I, **Shokoueinejad, M**., Levin, J., Dempsey, J., Wang, F., Xie, A. "SLEEP APNEA THERAPY DEVICE THAT AUTOMATICALLY ADJUSTS THE FRACTION OF INSPIRED CARBON DIOXIDE" United States Patent Filed. 15/376,180, Dec 11, 2016

7.1 Abstract

Due to the complex nature of sleep apnea, and the human body, neither an effective nor comfortable treatment option for sleep apnea has been developed. Accordingly, the inventions described herein are a successful and novel alternative to current sleep apnea therapies, including CPAP therapy. The sleep apnea therapy device disclosed herein incorporates the rebreathing of exhaled air to induce moderate hypercapnic conditions in systematic blood circulation. Advantageously, it eliminates apneic events in obstructive, central, and complex sleep apnea patients.

7.2 Introduction

Generally, the sleep apnea therapy device is composed of a comfortable silicone rubber facemask that covers the mouth and nose, and flexible tubing that attaches to the anterior port of the mask. Moreover, this device counts apneas and automatically increases or decreases dead space to minimize apneas, and then sends reports to the clinician.

Accordingly, a device for reducing apnea is provided. A device for reducing sleep apnea is also disclosed which automatically increases inspired carbon dioxide by changing a volume of rebreathed exhaled air. The objective is to create different CO_2 concentrations inside the device's reservoir for rebreathing. In one or more examples, the CO_2 concentration is measured at different volume intervals to determine the effect of dead space volumes on CO_2 concentrations.

More specifically, the device disclosed and shown in the Figures includes an inlet configured to accept exhaled air from a user of the device. The exhaled air comprises exhaled CO_2. A sensor is provided, configured to detect an apneic event. A gas reservoir is also provided, configured to

adjust dead space volume. The device includes at least one exit hole for expelling the exhaled air from the user of the device. A control unit is also provided which is configured to automatically adjust the dead space volume between the inlet and the at least one exit hole in response to the apneic event detected by the sensor. The control unit analyzes data, record data, upload data, and transmits data obtained.

Disclosed herein is a sleep apnea therapy device that does not suffer from the problems of existing apnea therapies, and in particular CPAP machines. The device automatically adjusts the fraction of inspired carbon dioxide available to the user of the device to prevent sleep apnea. The disclosed device requires no blower, no increased pressure, and for these and other reasons should be more widely accepted by patients.

A method for reducing apnea is further disclosed. The method includes providing a sleep apnea therapy device as described, identifying an apneic event with the sleep apnea therapy device, and adjusting the dead space volume of such device so as to reduce apnea in a patient.

These and other features and advantages of devices, systems, and methods according to this invention are described in, the following detailed sections.

7.3 Materials and Methods

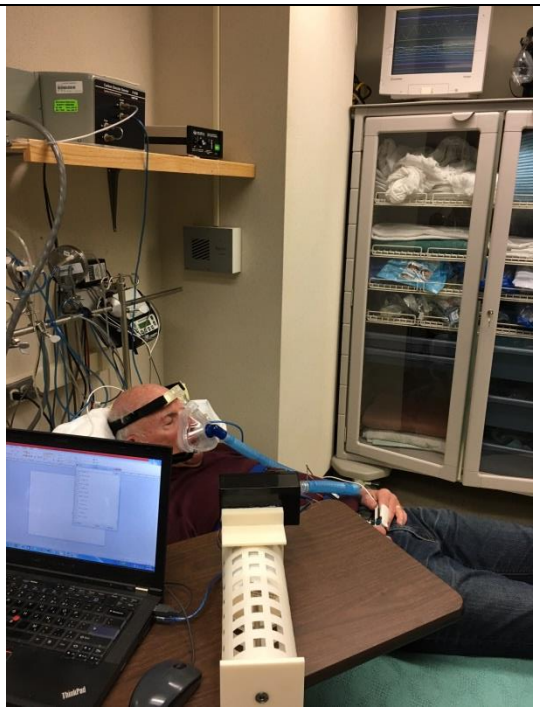

Figure 15: The subject sleeps using the lightweight comfortable clear plastic facemask held in place with head straps. Air flows through a rotatable elbow in the facemask and a short flexible hose. Then through an accordion like 8 cm diameter collapsed bellows. An axial stepper motor rotates a long worm gear protruding at the near end that expands the bellows to 10 times the collapsed length. The larger perforated white surround prevents the patient from contacting any motion, yet permits gas flow

Accordingly, a device for reducing apnea is provided. More specifically, a sleep apnea therapy device shown in Fig. 15 is provided which is configured to automatically adjust dead space volume. Generally, as shown in Fig. 15, the sleep apnea therapy device includes a mask to cover the wearer's mouth and nose. The mask is connected via a flexible tube to a variable sized reservoir that has an inlet, connected to the tube, and an outlet which is open for fresh air ventilation. The inlet is configured to accept exhaled air from a user of the device. The exhaled air comprises exhaled CO_2. The distance between the inlet and outlet is adjustable. In order to accomplish the adjustable distance forming the dead space volume, the sleep apnea therapy device includes a variably sized reservoir. Namely, a gas reservoir is provided, configured to adjust dead space volume as more fully described herein below. The device, and in particular the reservoir, includes at least one outlet or exit hole for expelling the exhaled air from the user of the device.

A sleep signal sensor, or more than one sensor, may be provided, configured to detect an apneic event. A control unit or controller is also provided which is configured to automatically adjust the dead space volume between the inlet and the at least one exit hole in response to the apneic event detected by the sensor.

To this end, the inlet is composed of a facemask which covers the mouth, the nose, or both the mouth and nose of a user of the device. Example facemasks are shown in Figs. 15. As can be seen in the Figures, the facemask is composed of a body contoured to cover the mouth and/or nose of the user. The facemask may be disposable / replaceable. The facemask may be rigid or flexible, or semi-flexible. For example, the facemask may be made out of a semiflexible plastic material. The facemask may also optionally include a cushioned surface around its outer edge, which may provide for additional user comfort. In one or more alternative examples of embodiments, the sleep apnea therapy device utilizes existing nasal masks (or nasal tubes) used in some forms of CPAP therapy (see Fig. 15). Generally, the facemask allows for breathing to occur through either the mouth or nose, subject to an increased volume of rebreatheable dead space, and an increased level of comfort.

The device and in particular the mask utilizes stability straps, which are intended to hold the device (specifically the facemask) in the same location at the patient's/user's/wearer's nose and/or mouth for the entire length of time worn by the user. For example, the facemask, in one or more examples of embodiments, includes one or more head straps which attach to the facemask and are configured wrap around a portion of the user's head. The head straps may be fixed in length, or may be variable in length, and in one or more examples of embodiments, the head straps may be elastic or may have a degree of elasticity.

Advantageously, the mask increases dead space while minimizing the effort needed to breathe. Second, as the sleep apnea therapy device does not require increased pressure, it allows for more comfort in the mask during overnight wear (e.g., eliminating the increased pressure used in many CPAP therapies).

Figure 16 The subject sleeps with the cylindrical reservoir prototype. Lung air flows from the lightweight comfortable clear plastic mask through a short fexible hose, then out the dark hole. After a significant apnea is detected, the hole automatically moves counterclockwise to lengthen dead space. We have found this device to be comfortable and does not disturb sleep.

.

Referring to Figs. 15 and 16, in one or more examples of embodiments, the facemask is joined to the gas reservoir by a flexible hose or tube , which couples to the entrance hole or aperture or inlet on the reservoir (see Fig. 16). More specifically, the mask is connected via a flexible tube to the variable sized reservoir inlet. The flexible hose or tube is hollow and permits the transfer of gas (e.g., is a conduit), in particular CO_2 between the user and inlet and reservoir. The tube or hose may be disposable/replaceable. Preferably the flexible hose or tube is tightly secured and/or sealed to prevent the entry exit of gas from said connections.

Figure 15 shows that the fixed device is adjustable by extending it to increase dead space. The device is battery driven because it makes infrequent adjustments. The device records lung flow and detects apnea by a built in D6F-V03A1 velocity sensor. When the apnea detector detects more than the threshold number of apneas (i.e. ≥10 s of zero air flow) or hypopneas (i.e. over 50–60% decrease in air flow) at a rate of > 5/h, the computer increases the dead space (for example in 50 ml increments). When the computer detects less than the threshold number of apneas, it decreases the dead space. Thus the device adapts to different patients, to a change in physiology from beginning sleep to deeper sleep, to changing airway collapsibility, to changing sleep postures, etc. Most importantly this adjustable device will permit use of the minimal amount of dead space (and therefore minimal increase in $P_{ET}CO_2$) to eliminate significant numbers of apneas, thereby providing an opportunity for apnea elimination without side effects of "excessive" hypercapnia. Based on our experience with CO_2 therapy to date, we expect our variable deadspace approach to eliminate all central apneas and hypopneas and most obstructive apneas in most sleep apnea patients—requiring <3 mmHg increase in $PaCO_2$ achieved via the variable rebreathe ("Smart CO_2") device. However, our experience also tells us that airway obstruction in some severe OSA patients will not be eliminated via our CO_2 treatment. Fig. 16 shows the assembled cylindrical reservoir prototype. The facemask covers the mouth and nasal region and allows for the attachment of adjustable, rebreathable dead space volumes. From the mask a plastic elbow can rotate left and right. Then a short flexible plastic hose connects to the larger cylinder. A stepper motor rotates the dark disk hole that can be seen at 10 o'clock. The motor can drive the hole from 10 o'clock counterclockwise. At 2 o'clock there is a baffle from the wall to the center. Thus deadspace beween hose and the top disk hole increases as the top

disk rotates from 10 o'clock to 12 o'clock. Above the disk with the dark hole is a perforated cover that prevents the patient from contacting any motion, yet permits gas flow.

In this concept, there is a wide cylindrical volume that has a stationary wall and a moving wall attached to a lid that rotates. The lid that closes the top of the reservoir would have the only breathing hole located immediately before the moving wall. To automatically adjust the CO_2 concentrations, the lid rotates counterclockwise about a center shaft that moves the rotating hole away from the breathing tube attachment and thus increases the deadspace. As the volume increases there will be a larger amount of CO_2 present since there is more space for the gas to reside and accumulate in between breaths. To decrease the amount of CO_2 the lid rotates in a clockwise direction, which will bring the hole closer to the breathing tube attachment and decrease the volume of dead space.

The mask increases dead space while minimizing the effort needed to breathe. Second, it allows for more comfort during overnight wear by eliminating the increased pressure used in many CPAP or servoventilator therapies. It utilizes the existing nasal mask (or nasal tubes) used in some forms of CPAP therapy. This device allows for breathing to occur through either the mouth or nose, subject to an increased volume of rebreathable dead space, and an increased level of comfort. Furthermore, this device is extremely feasible and very user friendly.

The device is capable of forcing the apnea patient to rebreathe exhaled gas. These designs can be implemented by a lightweight plastic construction located near the face mask and battery driven so there is no pressure blowing into the patient making the device uncomfortable, no long tubes to external fans, and no power required from the wall.

Additionally, in one or more examples of embodiments a filter (not shown) may be provided between the facemask and the variable reservoir. The filter may be provided to filter exhaled breath from the wearer before entering the tubing or reservoir and dead space as well as inhaled breath by the user.

In one or more alternative examples of embodiments, a single mixing valve could be replaced by two or more valves (not shown), which may be used to permit rebreathing dead space gas at the optimal time prior to breathing fresh air. For example, Giannoni *et al* (2010) [292] has shown that squirting 100% CO_2 at the optimal time during the inhalation phase reduces voluntary induced apneas in normal subjects while maintaining the average $P_{ET}CO_2$ near normocapnic levels. A similar approach, whereby the automated system delivers CO_2 at the optimal time to the patient / user may be used. Such an approach may minimize the arousal that may result from continuously elevated CO_2.

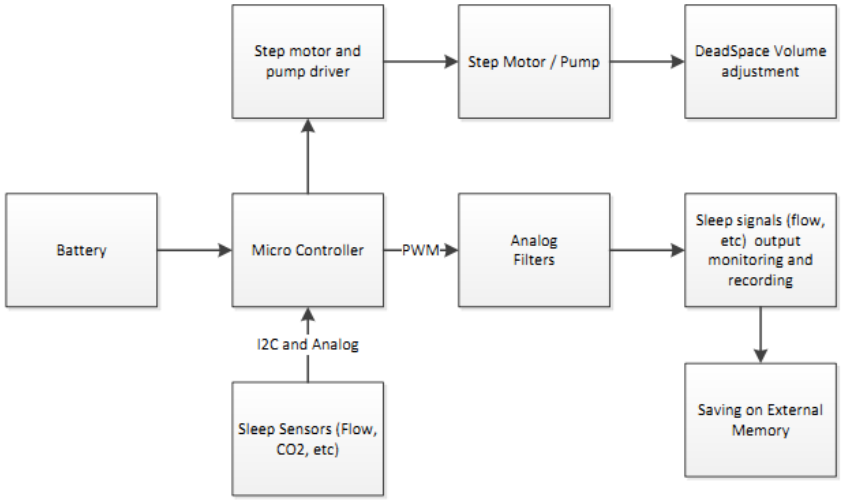

Figure 17 is a flow diagram showing the interaction of one or more components of a sleep apnea therapy device according to one or more examples of embodiments.

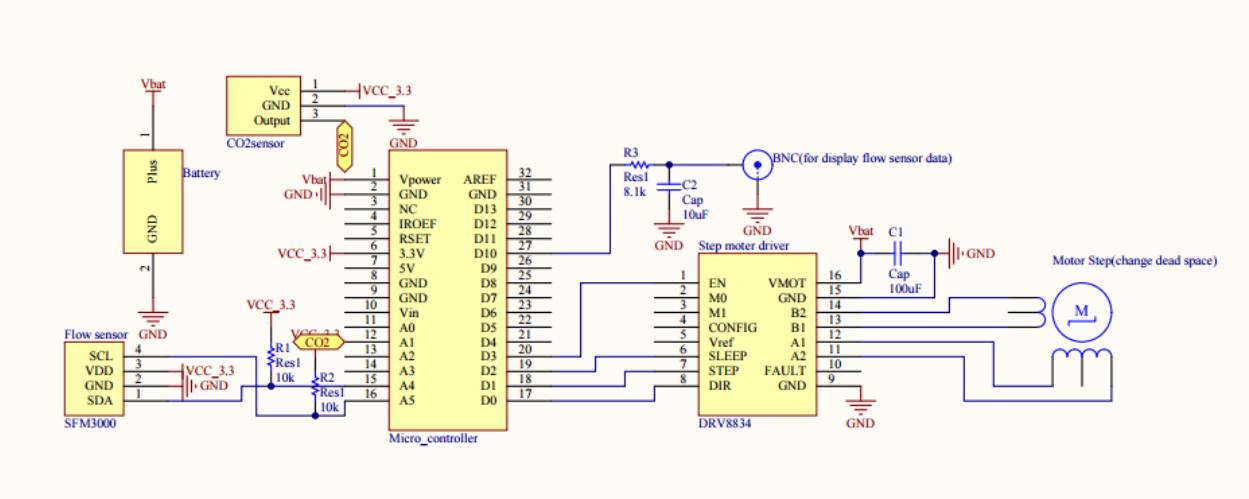

Figure 18 is an electrical circuit diagram of a sleep apnea therapy device according to one or more examples of embodiments.

As indicated, a sensor in Fig.17 and Fig. 18 is provided on or within the sleep apnea therapy device which is configured to detect an apneic event. One sensor or a plurality of sensors may be provided and used. More specifically, the sleep apnea therapy device includes one or more sensors provided in the airstream that measure the flow rate of each breath of the wearer in order to provide feedback to guide the amount of dead space volume available for rebreathing. As shown in Figs. 17 and 18, one or more sensors may be provided on or near the facemask or exit opening of the facemask, or alternatively in the flexible tube. In one or more examples of embodiments, the sensor(s) is a pulse oximeter, a thermal sensor, an optical sensor, a flow sensor, a velocity sensor, or a sound sensor, or the like, or combinations of the foregoing. Accordingly, apneas may be detected, for example by pulse oximetry, or a thermal flow sensor (such as hot wire anemometer), or an optical sensor (such as that detects movement of a drag sensor), or a flow sensor (such as a pneumotachometer). While specific examples of devices and locations are provided, variations thereon may be acceptable without departing from the overall scope of the present invention.

The sleep apnea therapy device disclosed in one or more preferred embodiments uses a feedback process and system using one or more sensors, as indicated above, which are in communication with a controller inside, on, or proximate the device. The sensors are directly connected (wired) to the controller shown in figure 18. The sensors and control are used, for example, to: **(1)** accelerate the sleep apnea healing process by stimulation of chemoreceptors which are sensitive to CO_2 levels at or near the apneic threshold; **(2)** prevent the apneic events by providing adaptable, controlled exposure of exhaled CO_2 for different patient requirements; **(3)** monitor the curing process for symptoms of both obstructive and central sleep apnea; **(4)** operate as an independent device with no required CO_2 tank; and/or **(5)** relay the information wirelessly to a central location for storage and interpretation by a physician. While specific examples are provided above, variations thereon or additions thereto may not depart from the overall scope of the present invention.

As indicated, a control unit or controller is provided which is configured to automatically adjust the dead space volume between the inlet and the at least one exit hole in response to an apneic event detected by a sensor. To this end, the control system or controller of the sleep apnea device is configured to analyze data, record data, upload data, and/or transmit data, as well as combinations of the foregoing. In one or more particular examples of embodiments, the controller is configured to analyze data as a function of time, upload data as a function of time, and/or transmit data as a function of time, as well as combinations of the foregoing. Generally, when the apnea sensor detects more than a threshold number of apneas per hour, the controller increases dead space volume within the sleep apnea therapy device reservoir; and when the apnea sensor detects less than a threshold number of apneas per hour, the controller decreases the

dead space volume within the sleep apnea therapy device reservoir. Thus, the device adapts to different patients/users, to a change in physiology from beginning sleep to deeper sleep, etc.

The control unit (Fig. 18) in one or more examples of embodiments is a microcontroller, or includes a non-transitory computer readable storage medium having stored thereon a computer program for controlling the adjustable dead space volume of the reservoir. The computer program has and executes a set of instructions that instruct the device to perform or execute one or more of the following steps: (a) identify an apneic event; and (b) adjust the dead space volume. In one or more examples of embodiments, the apneic event may be an apnea or a hypopnea, or the apneic event may be the absence of an apnea or a hypopnea. In addition to the foregoing, the control unit or controller may download data versus time. Likewise, the control unit may have a means to communicate data, and may therefore transmit data to a remote location (and may receive data from a remote location).

The control unit or controller automatically adjusts the dead space volume from a first dead space volume to a second dead space volume. In one or more further examples of embodiments, the control unit automatically adjusts the dead space volume from a second dead space volume to a first dead space volume. The second dead space volume in one example is larger than the first dead space volume. However, the first dead space volume may be larger than the second in another example of embodiments. According to the examples of embodiments described herein, the adjustment to the dead space volume results in a change in the inspired CO_2.

As indicated, in one or more examples of embodiments the system and/or method may be implemented by a microcontroller, a computer system, or in combination with a computer system. The computer system may be or include a processor. The computers may be electronic devices for use with the methods and various components described herein and may be

programmable computers which may be special purpose computers or general purpose computers that execute the system according to the relevant instructions. The computer system or portable electronic device can be an embedded system, a personal computer, notebook computer, server computer, mainframe, networked computer, workstation, handheld computer, as well as now known or future developed mobile devices, such as for example, a personal digital assistant, cell phone, smartphone, tablet computer, and the like. Other computer system configurations are also contemplated for use with the communication system including, but not limited to, multiprocessor systems, microprocessor-based or programmable electronics, network personal computers, minicomputers, smart watches, and the like. Preferably, the computing system chosen includes a processor suitable in size to efficiently operate one or more of the various systems or functions or attributes of the communication system described.

After the sensors detect the presence or absence of certain attributes in the sample, the data could be passed to the microcontroller and/or a linked computing device. The microcontroller or computing device may receive information from the one or more sensors. The microcontroller or computing device may analyze the data and apply certain recommendations or instructions.

Referring to Fig. 18, an electrical circuit diagram of one or more examples of a controller is shown. As can be seen, a microcontroller is coupled to various devices. While one microcontroller is shown, in one or more examples of embodiments, more than one microcontroller may be used. As seen in Fig. 18, a sensor, such as a flow sensor or more than one flow sensor (e.g., two or more) which detect moving air and/or detect apnea, is in electrical communication with the microcontroller such that it may communicate such detected data to the microcontroller. A CO_2 sensor may also be provided to detect CO_2 concentration and be in electrical communication with the microcontroller for measurement thereof. In one or more

examples of embodiments, two or more CO_2 sensors may be provided. A driver (or more than one driver) is also in electrical communication with the microcontroller and is in electrical communication with a motor to drive or power the motor. As described herein, the motor drives the variable volume dead space adjustment mechanism (discussed above) and thereby changes the dead space within the gas reservoir. A connector is also provided in electrical communication with the microcontroller and also in electrical communication with a display to send signals to a display for display of desired data to a user or physician. One or more batteries are also provided to supply power to the system. Of course, other sources of power, such as but not limited to AC power, may also be used in place of a battery without departing from the overall scope of the present invention.

Referring to Fig. 17, a flow diagram is provided showing generally the various hardware components of the device and corresponding interaction. As can be seen, the controller may be a microcontroller which executes software to operate the various functions of the sleep apnea therapy device disclosed herein. The microcontroller is powered by battery. As can also be seen in Fig. 18, various sleep sensors are in communication with the microcontroller. These sleep sensors may communicate with the microcontroller via, for example 1^2C and analog communication, although variation thereon will not depart from the overall scope of the present invention. The microcontroller may process the signal from the sleep sensor through analog filters, which provide sleep signal output that is monitored and recorded, and which may be saved in an external memory (of course internal memory may also be used without departing from the overall scope of the present invention)—to this end, the system may be in communication with a storage medium for the storage of data as described above. The microcontroller also communicates with a step

motor and/or pump driver which drive the step motor and pump so as to adjust the variable volume adjustment mechanism used for dead space volume adjustment, various examples of which were previously described herein.

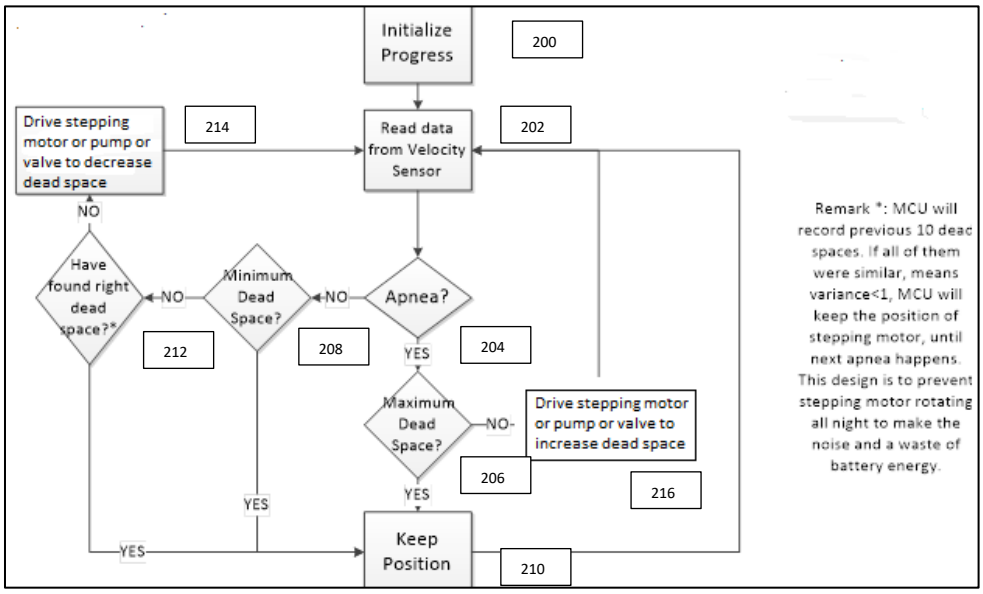

Figure 19 is a flow chart or logic diagram, illustrating one or more examples of an algorithm used to sense apnea and increase dead space, or not sense apnea and decrease dead space.

As indicated, the microcontroller executes simplified instructions provided by software. Fig. 19 illustrates a flow chart of an algorithm used to sense apnea and increase dead space, or not sense apnea and decrease dead space. First, the system or software of the control is initialized (Block 200). The control reads data received from a sensor (Block 202) contained in a portion of the sleep apnea therapy device 100 (e.g., within the dead space, which may be in or on or near the facemask) to determine whether an apnea occurred (Block 204). If an apnea occurred, then the control or system determines whether the device is positioned for maximum dead space (Block 206). If the maximum dead space condition does not exist, then the control or system determines whether the minimum dead space condition exists (Block 208). If the minimum dead space

condition exists, then the system keeps or maintains position (Block 210) and returns to reading data from the sensor (Block 202) and repeats the process. If the minimum dead space condition does not exist, then the control or system queries whether the right/correct dead space has been found for treatment of the patient (Block 212). For example, the microcontroller may record a number of previous dead spaces (e.g., 10 dead spaces). If all of them are similar (e.g., a mean variance less than 1), then the microcontroller may maintain the position of the stepping motor (and dead space) until an apnea occurs, returning to Block 202 and repeating the process. If the system has not found the right dead space, then the control engages a stepping motor or pump or valve to drive it so as to decrease the dead space (Block 214). The system then returns to reading data from a sensor (Block 202) and repeats the process.

Continuing with Fig. 19, as indicated, if after an apnea is detected a maximum dead space condition exists, then the control keeps or maintains the position of the gas reservoir (Block 210), and returns to reading data from the sensor (Block 202) and repeats the process. If the maximum dead space condition (or position) does not exist, then the control instructs/activates a stepping motor or pump or valve and drives the motor or pump or valve to increase dead space in the sleep apnea therapy device (Block 216). The system then returns to reading data from the sensor (Block 202) and repeats the process. Advantageously, the control described prevents the stepping motor from rotating all night, making constant noise, and wasting energy. Fig. 19 shows that the device counts the number of apneas and if too high, automatically increases dead space. However, the device is not limited to this embodiment. For example, if the number of apneas is near zero, it automatically decreases dead space.

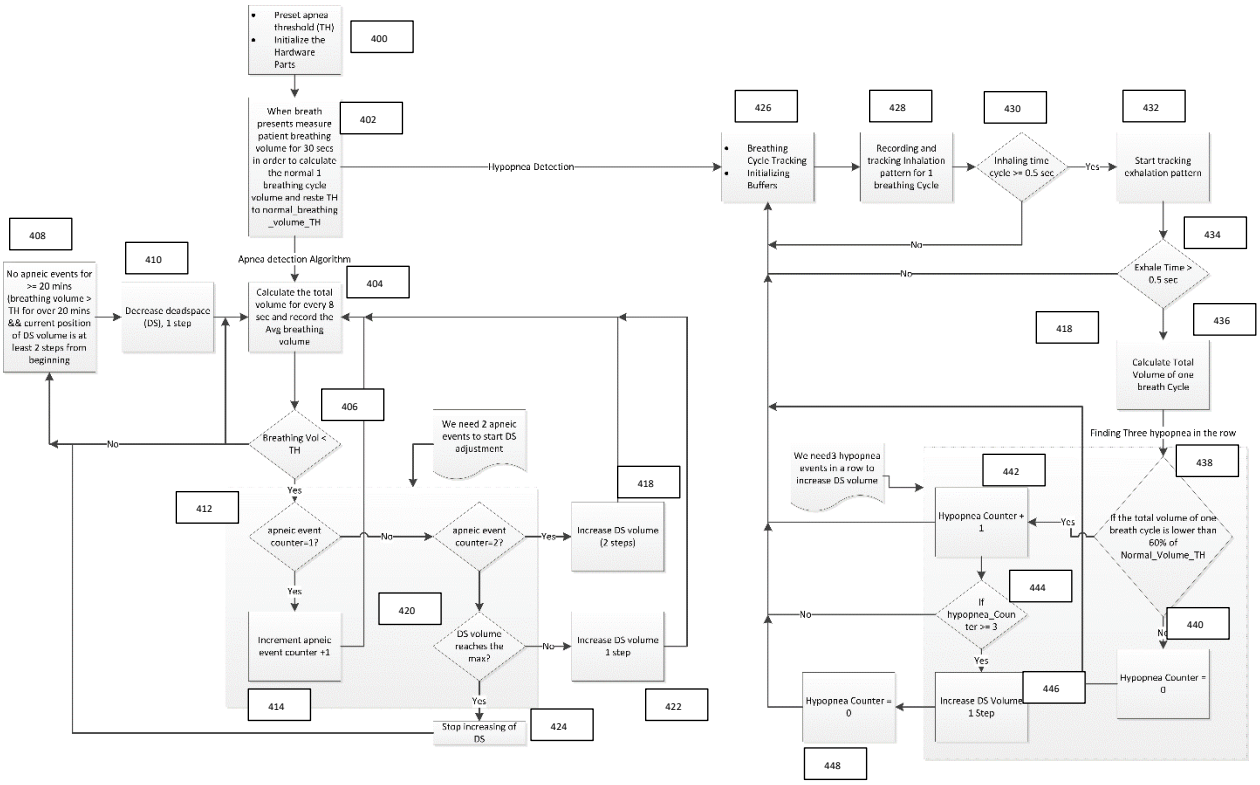

Figure 20 is a flow chart or logic diagram, illustrating of an algorithm used to sense apnea/hypopnea and increase dead space, or not sense them and decrease dead space.

Another particular embodiment of a logic diagram or flow chart illustrating the actions of the microcontroller executing the software is shown in Fig. 20. As can be seen, a preset apnea threshold is set and the hardware of the sleep apnea therapy device 100 is initialized (Block 400). Then, when breath presents, patient breathing volume is measured for a period of time (e.g., 30 sec) in order to calculate the normal one (1) breathing cycle volume, and the preset apnea threshold is reset to a normal breathing volume threshold (Block 402). The apnea detection algorithm then is applied to execute the instructions of the microcontroller. Namely, the total volume for a period of time (e.g., every 8 sec) is calculated and recorded (Block 404). This may be recorded as the average breathing volume. This average breathing volume is queried (Block 406). At Block 408 if the volume is greater than (or not less than) the normal breathing volume

threshold, and no apneic events have occurred for a period of time (e.g., greater than or equal to 20 min), in other words normal breathing volume threshold occurred for the period of time and current position of the dead space volume is at a predetermined position (e.g., at least 2 steps from the beginning position), then dead space volume may be decreased by one (1) step (Block 410). The total volume for a period of time is again calculated and recorded. Likewise, during the foregoing process steps, the total volume for a period of time may be continually calculated and recorded (Block 404). If the calculated average breathing volume (from Block 406) is less than the normal breathing volume threshold, then an apneic event counter is queried (Block 412). If the events equal one (1) event, then the increment apneic event counter adds one (1) event (Block 414) and returns to calculating and recording the total volume for a period of time (Block 404). If the apneic event counter does not equal one (1) event, then it is queried (at Block 416) whether the apneic event counter equals two (2) events. If the events equal two (2) events, then the dead space volume is increased by two (2) steps (Block 418), and the system returns to calculating and recording the total volume for a period of time (Block 404). If the apneic event counter equals two (2), the system queries whether the dead space volume has or has not reached its maximum (Block 420) – if not reached then the dead space volume is increased by one (1) step (Block 422), and the system returns to calculating and recording the total volume for a period of time (Block 404). Alternatively, if the dead space volume has reached its maximum, then the system stops increasing the dead space (Block 424), and returns to Block 408 and continues through the process. Note, in one or more preferred examples of embodiments, two (2) apneic events may be needed to begin dead space adjustment.

Continuing with Fig. 20, if at Block 402 hypopnea is detected, and then the system proceeds to Block 426. At Block 426, the system initializes and buffers breathing cycle tracking. Then the

system records and tracks the inhalation pattern for one (1) breathing cycle (Block 428). The system then queries whether the inhaling time cycle is greater than or equal to a predetermined period of time (e.g., 0.5 sec) (Block 430). If no, then the system returns to Block 426 and repeats the process. If yes, the system begins tracking an exhalation pattern (Block 432). The system then queries whether the exhale time is greater than a period of time (e.g., 0.5 seconds) (Block 434). If no, the system returns to Block 426 and repeats the process. If yes, then the system calculates the total volume of one (1) breath cycle (Block 436). The system then queries whether the total volume of one breath cycle is lower than a percentage (e.g., 60%) of the normal breathing volume threshold (Block 438). If no, then the system sets the hypopnea counter to zero (0) (Block 440) returns to Block 426 and repeats the process. If yes, then the hypopnea counter equals one (1) (Block 442) and the system returns to Block 426 and repeats the process. In one or more preferred examples of embodiments, the system requires three (3) hypopnea events in a row to increase the dead space volume. Accordingly, the system also queries whether the hypopnea counter is greater than or equal to three (3) (Block 444). If no, the system returns to Block 426 and repeats the process. If the hypopnea counter is greater than or equal to three (3), the system increases the dead space volume one (1) step (Block 446). The hypopnea counter is then returned to zero (0) (Block 448), the system returns to Block 426 and repeats the process. According to the foregoing algorithms, the system automatically adjusts the dead space volume in response to detected events in the patient.

Accordingly, the sleep apnea therapy devices described herein use algorithms based on measurements of airflow in order to identify and execute necessary changes in dead space volume during sleep. The device automatically changes the length of dead space, or blends exhaled gas and fresh air in order to alter the hypercapnic conditions, and prevent apneas from

occurring. The device also stores data within a memory device; these data may be used for follow up care or in clinical settings. Data could also be sent directly to personal computers or smart phones for immediate personal accessibility. Accordingly the sleep apnea therapy device may utilize a self-regulated detecting system to provide treatment to patients.

The embodiments described herein is implemented by a lightweight plastic construction. The device is made of material that is not CO_2 permeable and does not react with high concentrations of CO_2. The device is also small enough not to be cumbersome or uncomfortable during sleep, and all attachments may be portable. A loose-fitting harness around the body may be provided, formed out of a suitable material, to hold the device over the sternum while permitting body movement while sleeping.

Generally, the method includes providing a sleep apnea therapy device as described, identifying an apneic event with the sleep apnea therapy device, and adjusting the dead space volume of such device so as to reduce apnea in a patient.

One or more specific examples of a method of using a sleep apnea therapy device , for example, the device shown in Fig. 7 controls CO_2 concentrations by moving the threaded disc, and thereby changes the dead space volume within the reservoir. By varying the volume of the dead space, exhaled CO_2 builds up in the dead space and does not get recycled in the ambient surroundings. The exhaled CO_2 mixes with ambient air in the dead space to raise the CO_2 concentrations in the rebreathed dead space. Once the user inhales, the excess CO_2 from the dead space raises the CO_2 concentration in the user. CO_2 levels in the user are fluctuated by adjusting the amount of dead space present for inhalation. The larger the dead space, the more CO_2 that can accumulate without being ejected from the device during exhalation.

When the sleep apnea therapy device of Fig. 7 records a hypopnea from the patient/user with the device's sensors, it actuates the motor shown in Fig. 7 and drives the worm gear to incrementally advance the threaded disc for expansion of the dead space. As more hypopneas occur, the device may keep incrementing, or incrementally moving, the threaded disc until apneas discontinue. If a hyperpnoea occurs, then the device may retract the threaded disc and reduce the volume of dead space the user rebreathes. This retraction continues until no hypo-/hyperpnoea occur, at which point the device maintains the current dead space volume.

In Fig. 7, exhaled breath from the wearer/user/patient comes into the device through the inlet on the top left side of the device shown in Fig. 7 and enters the dead space. The dead space in Fig. 7 is defined as the volume of the container from the plate (threaded disc) that connects to the open air to the plate (wall) that connects to the flexible breathing tube. The threaded disc contains an outlet for airflow and a threaded hole that interfaces with the worm gear center shaft. The motor, located below the inlet in Fig. 7, drives the worm gear hat results in a translation of the threaded disc to either expand or contract the dead space (expansion of the dead space is the movement of the threaded disc). The dead space is contained within a larger cylindrical casing that contains holes or apertures for the air exchange and prevents interference from external objects to the moving parts.

7.4 Results

It has been shown increases in end tidal carbon dioxide concentration ($P_{ET}CO_2$) of as little as 1–2 mmHg (achieved via rebreathing) to be highly effective in removing and preventing central apneas and periodic breathing induced by either high altitude hypoxia in health [207] or via CHF [214]. Research at the University of Wisconsin, Madison [7] concluded that increasing

respiratory motor output using moderate hypercapnia conditions eliminated obstructive sleep apneic events in patients with moderate to highly collapsible airways and a wide range of CO_2 chemosensitivity. This was achieved through exposing the apnea patient to inhaled gas from a CO_2 reservoir; a process that increased $P_{ET}CO_2$ during normal breathing by 4.2 ± 1 mmHg (range +2 to 5 mmHg). The main focus of Xie et al's research was on the Apnea-Hypopnea Index (AHI), a measure of the number of apneic episodes per hour. In 21 patients with moderate-to-severe obstructive and central apneas, all but 4 of those who received inhaled gas from a CO_2 reservoir showed a reduction in the AHI in excess of 30% below control. 17 of the 21 patients displayed extremely successful results, with a reduction of AHI by 94 ± 3% of control with no significant impact on sleep state stability. Even OSA patients with extremely collapsible airways responded positively to the CO_2 treatment. Most of these results were obtained during periods of 4 to 6 h of CO_2 therapy during the night – but the findings were consistent with those obtained in a smaller number of patients studied throughout the night. Xie et al also utilized a system which sensed the transient overventilation phase which often precedes apnea and then switched the patient into a CO_2 reservoir system. This added small amounts of CO_2 thereby preventing transient hypocapnia and resulted in no change in the normal (normocapnic) $P_{ET}CO_2$.

This selective inhalation of gas from a CO2 reservoir, i.e., an "isocapnic" system, reduced obstructive sleep apneas by 30 to 70% in 60% of the OSA patients. The results of these isocapnic treatments, and especially the modestly hypercapnic treatments in the OSA patients to date, suggest that a carefully regulated increase of 1–3 mmHg $P_{ET}CO_2$ would be effective and safe over long durations of time each night and over many nights in most patients with multiple obstructive, central and/or mixed apneas.

The rationale for using CO_2 manipulation as a treatment of OSA is based on two premises: a) preventing transient reductions in $PaCO_2$ will prevent the patient from reaching their apneic threshold; and b) raising $PaCO_2$ even a minimal amount provides a strong recruitment of upper airway dilator muscles [2, 274], thereby preventing airway obstruction. In addition, a study conducted at John Rankin James Skatrud Sleep lab in Madison, Wisconsin's Veteran's Administration hospital showed that continuous dead space rebreathing (an increase in anywhere from 2 to 5 mmHg of CO_2) led to the stabilization of the central respiratory output and prevented airway obstruction in a significant percentage of patients with mild to severe obstructive sleep apnea. This increase in CO_2 effectively stopped apneas from occurring during sleep.

Referring to the Figures, experimental data are shown illustrating different dead space rebreathing conditions. External dead space is defined as the volume of space contained within the user's mask, connecting tube, and reservoir ending at the outlet hole of the reservoir. Fig. 21 illustrates experimental data under "control" conditions with repeated obstructive apneas. That is, under "control" conditions, periodic breathing with recurrent stagnation and no airflow (obstructive apneas), as well as, frequent and dramatic dips in oxygen saturation occur. During the experiment, airway obstruction was confirmed through the paradoxical movements of the chest versus abdomen. When the chest expanded, the abdomen contracted, and as a result, no airflow between the upper airway and the lungs was seen and obstructive apneas occurred.

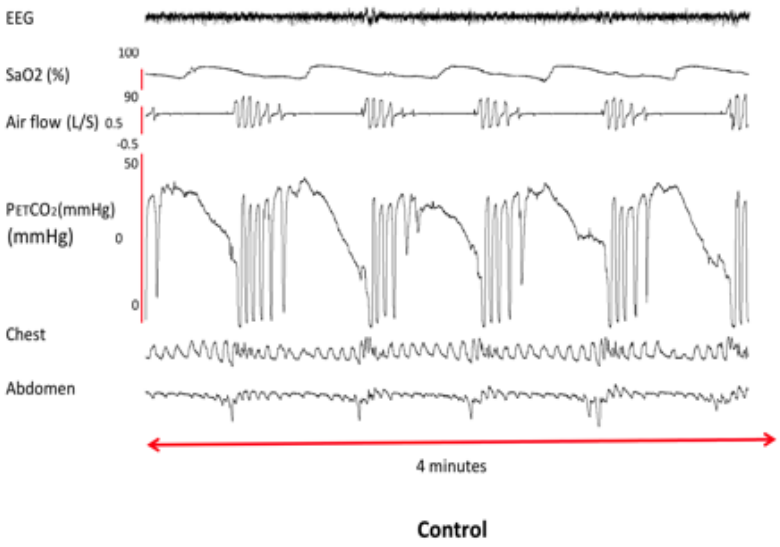

Figure 21 shows observed experimental data under "control" conditions with repeated obstructive apneas.

Figure. 22 illustrates experimental data under "low" dead space conditions (450 ml). In "low" dead space conditions, apneas and hypopneas are reduced below the control (Fig. 1), but many of the shorter duration events still exist. Fig. 22 shows under "low" dead space conditions, that respiration still demonstrated paradoxical chest versus abdomen movements, few apneic episodes, and several short hypopneas (decreases in O_2 saturation levels). It is also important to note that under "low" dead space conditions the post-hypopnea airflow increased significantly due to extra chemical stimulation.

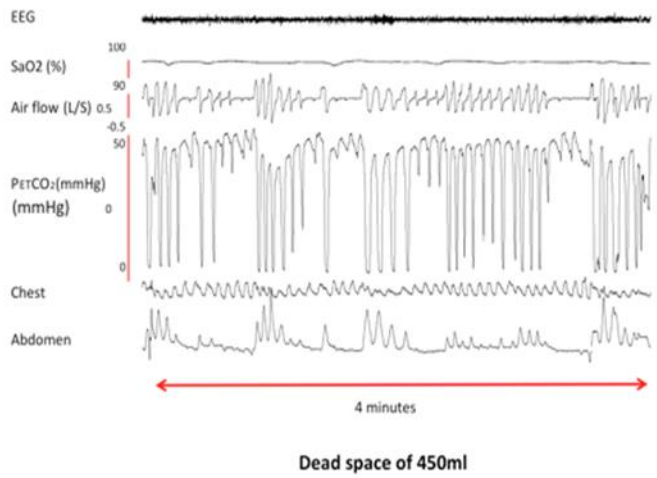

Figure 22 is a chart illustrating experimental data under "low" dead space conditions (450 ml).

Fig. 23 illustrates observed experimental data under "high" dead space concentrations (570 ml). In "high" dead space conditions, no apneas (i.e. time of zero flow) are present, and only a few hypopneas remain. Fig. 23 illustrates that under "high" dead space conditions no apneas were observed. Additionally, no fluctuations in O_2 saturation were observed, indicating stable, steady breathing patterns. Airflow also remained relatively unchanged (compared to the previous two conditions), due to the lack of hypopneas and related chemical-mechanical stimulations.

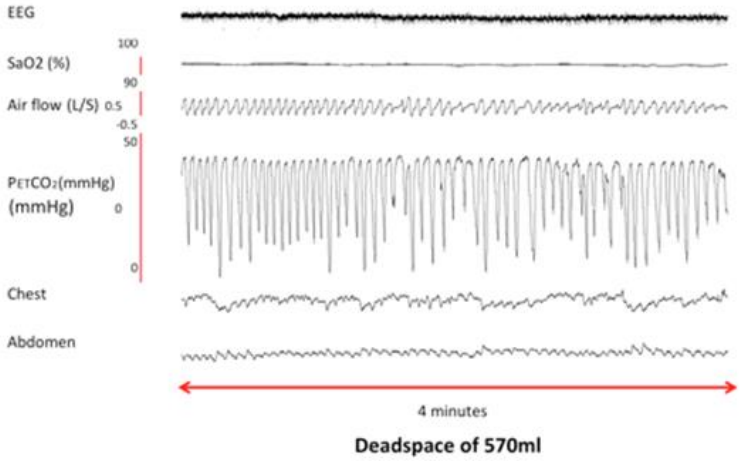

Figure 23 is a chart illustrating observed experimental data under "high" dead space concentrations (570 ml).

7.5 Conclusion

A comfortable device for treating sleep apnea incorporates a mask, a flexible hose and a chamber for collecting expired air containing CO_2. A sensor detects apnea and a control system automatically adjusts the amount of rebreathed CO_2 to minimize apnea and also minimize arousal.

8 Chapter 9 Conclusion and Recommendations

8.1 Conclusions

This dissertation presents a body of work that establishes the feasibility of using "Smart CO_2" to gain insight into the effects of using supplemental inspired CO_2 via rebreathing on treating obstructive, central, and mixed sleep apneas. In summary, to date we have proof of principle evidence that added CO_2 will markedly reduce obstructive and central apneas in most OSA patients—at least at fixed levels of rebreathe dead space and increased $P_{ET}CO_2$ (+1-5 mmHg) over 1-6 h of sleep. In this thesis a custom-made variable CO_2 rebreathe device was used which capable of automatically detecting SAS and changing rebreathe volume and $P_{ET}CO_2$ to relieve SAS in simulated voluntary disordered breathing experiments in healthy subjects. We are proposing the use of supplemental inspired CO_2 via rebreathing as a means of treating obstructive, central, and mixed sleep apneas. Supplemental CO_2 via a fixed rebreathe volume has previously been used successfully by us and others to effectively treat central sleep apnea and in conjunction with CPAP to treat residual sleep apnea i.e. "complex sleep apnea". So the use of added CO_2 per se is not innovative. Rather, our innovation includes the following: a) using added CO_2 by itself without any positive airway pressure (based on our proposed device)—to treat obstructive and central sleep apnea; b) provide breath-by-breath monitoring of ventilation in order to increase/decrease rebreathe dead space volume automatically, thereby changing the level of hypercapnia; and c) to determine over multiple nights of sleep the effects of our "Smart CO_2" device on diverse potential side effects such as sleep state disruption.

8.2 Recommendation

Projects presented in this dissertation are part of the ongoing research in the The John Rankin Laboratory at the Department of Population Health Sciences, Department of Medicine, and Webster's group at the Department of Biomedical Engineering at University of Wisconsin-Madison. A limitation of the presented work was the small number of patients recruited for the project. In future studies, recruiting more patients should be a priority since it would enable stronger conclusions to be drawn. Also, a larger and more diverse study population would allow investigation of differences as a function of age, sex, therapy, disease subtype, etc.

(Sleep Study): is to assess fit and tolerance of the Smart CO_2 rebreathing device for each individual patient. First, the subject will be familiarized with the apparatus, determine mask type and absence of substantial leakage between the rebreathe device and the subject. Then, four trials of 30-60 min each, by switching the patient in and out of the rebreathing device during sleep will be conducted. These will determine the transitional effects on and off the rebreathe device on breathing and on sleep state. Specifically, if there is no sleep disordered breathing detected, the subject breathes with no rebreathing, i.e. inspired gases are room air. Once apnea or significant reductions in tidal volume (to <60% of steady-state VT during quiet resting pre-sleep wakefulness) are detectable over a minimum of 10–30 s periods, the device automatically switches to a "rebreathe" mode which elevates the CO_2 in the inspired air. If the sleep disordered breathing is eliminated, the subject continues to rebreathe at the minimum level of dead space rebreathing. If measureable sleep disordered breathing persists, the rebreathe volume and therefore the inspired CO_2 are increased to the point where the alveolar PCO_2 (measured breath by breath) reaches 4 mmHg above baseline air breathing (control), or if the subject arouses and is

unable to return to sleep, at which time the dead space rebreathing will be stopped by the investigators. Monitoring will include electroencephalogram (EEG), electrooculogram (EOG), electromyogram (EMG), O_2 saturation, rib cage and chest wall movement, air flow, and alveolar PCO_2.

9 Appendices

These chapters are partially based on the following publications [293, 294]:

Mehdi Shokoueinejad , Rayan Alkashgari, Hisham A. Mosli, Nazeeh Alothmany, John G. Webster,"Video Voiding Device For Diagnosing Lower Urinary Tract Dysfunction". (Accepted for publication, Journal of Medical and Biological Engineering, June 2016)

Nazeeh Alothmany, Hisham Mosli, John G. Webster, **Mehdi Shokoueinejad**, Rayan Alkashgari1, "Critical Review of Uroflowmetry Methods". (Submitted, Journal of Medical Device 2016)

A. Review of Uroflowmetry Methods

A.1 Abstract

Greater than 60% of men (age 40+) are affected by lower urinary tract symptoms, and NIH has estimated that at least 10 million US men and women suffer from urinary incontinence. However, it is thought that these statistics grossly underestimate the actual prevalence of these types of illnesses. This can be partially attributed to inhibition of a patients' voiding process if someone is watching them, which often leads to inaccurate results as well as sometimes avoidance of medical help altogether.

There are a number of different urodynamic tests that are used to assess how well the bladder and urethra store and release the urine. These tests include measuring the urine flow rate, volume, pressure, leakage, frequency, urge to urinate, urine stream, pain level while urinating, and urinary tract infections. There are a variety of techniques to conduct these tests. Some techniques are simple and noninvasive where physicians listen to a patient while urinating to understand the pattern of urination. Other techniques are invasive and involve inserting a catheter into the urinary tract to measure the volume of the urine. To preserve the integrity of the results, it is beneficial to shift toward more private methods of urodynamic testing. Uroflowmetry is one of the common urodynamic tests to diagnose urinary incontinence, and it allows for privacy during the voiding process.

This section briefly explains the types of tests involved in urodynamics and then provides a review of the different techniques used in uroflowmetry. This review will help research teams to design new noninvasive systems to measure urine flow rate and voiding volume.

A.2 Introduction to Urodynamics

Micturition involves two processes: 1) Bladder filling and urine storage, 2) Bladder emptying. Bladder filling requires:

1) Ability to store an increasing volume of urine at a low intracervical pressure and sensation;

2) A bladder outlet that is able to remain closed while the intracervical pressure increases;

3) Absence of involuntary contractions of the bladder.

Bladder emptying requires:

1) Smooth contraction for the muscles of the bladder;

2) Low resistance at the outlet of the bladder (sphincter);

3) Absence of obstruction [295, 296].

The aim of Urodynamic studies is to evaluate the ability of the ureter, urinary tract, bladder and sphincter to store and release the urine. These studies range from simple observation of the voiding process to inserting catheters with pressure sensors to measure the intra-ureter pressure. There are several type of Urodynamic studies [297]:

- Uroflowmetry: Aims to measure voiding volume, time, average and maximum urine flow rates. These tests involve having the patient urinating privately into a funnel that collects the urine and directs it to a measuring system to calculate the required parameters.

- Residual Volume Measurement: Aims to measure the volume of the urine left in the bladder after the voiding process is completed. Clinicians use ultrasound to measure this volume.
- Cystometric Test: Aims to measure how much urine the bladder holds and the pressure build up inside the bladder. These tests involve inserting a catheter with pressure sensors into the bladder and measuring the parameters while emptying the bladder.
- Electromyography tests involve measuring the electrical activities from the muscles and nerves around the bladder and sphincter.
- Video urodynamic tests involve taking ultrasonic or X-ray images of the bladder while filling up or emptying. If X-ray fluoroscopy is used, a contrast media is injected into the bladder through a catheter.

The first part of the paper introduces the concept of urodynamic techniques other than uroflowmetry without providing a review. The second part of the paper provides a review of the different techniques used in uroflowmetry for the purpose of explaining the work for the research team in developing a new technique for measuring urine flow rate and voiding volume.

Drinnan and Griffiths present a comprehensive description of urine flow and voided volume, uroflow signal conditioning conditioning and processing, flowmeter calibration and frequency response, uroflowmetry, recording, interpretation and display of flow and volume, bladder pressure, and video urodynamics [298].

A.3 Cystometry and Fluoroscopy Techniques

The flow rate is a function of the internal pressure in the bladder and hydraulic resistance of the urinary tract. Since uroflowmetry focuses on external measurement, it can only be considered as a good diagnostic tool to determine abnormal flow patterns. It gives very little information on the causes of abnormalities.

Cystometry is a technique that measures the storage abilities of the bladder and determines the relation between the pressure in the bladder, resistance of the urinary tract, and the voiding process. It uses internal pressure sensors to measure both the abdominal P_{abd} and bladder pressures P_{blad}. The difference between these two pressures together with the flow rate can be used to calculate the resistance of the urinary track as well as many other parameters that can be used in diagnosing problems in the urinary system [299].

Fluoroscopy techniques utilizing X-ray technology are also used to diagnose the micturition process (filling and emptying the bladder). Images of the urinary tract can be made while coughing, sneezing, at rest, while voiding and filling are taken and used to diagnose the patient problem [295] but since X ray and invasive pressure and flow sensors are involved, this procedure is used with patients with severe complications. Nuclear Medicine based methods were also used in which patients were orally given a liquid isotope and after 40–60 min, a scintillation detector measured the amount of the collected urine in the bladder. But since the method involves using isotopes, it is not a commonly used technique. Furthermore, this technique does not give the flow rate or the voiding volume and requires a long time [300].

Electromyography was also used to measure the contraction of several muscles in the urinary system using invasive electrodes placed on the bladder and sphincter of the subject [295, 296].

A.4 Uroflowmetry

In Uroflowmetry, a patient is asked to privately urinate in a funnel that collects the urine into a container that has a device to measure different parameters related to the voiding process. These parameters help in evaluating the urination function of the bladder. Clinicians used to observe patients while voiding which caused embarrassment for the patients [301]. There are several parameters used to describe the urine flow.

- Flow rate: volume of urine per unit time and usually referred to in milliliters per second (ml/s)
- Maximum flow rate Q_{max}
- Voiding volume
- Flow time
- Time to reach Q_{max}

Figure 24 shows sketches of the parameters that describe continuous urinary flow rate. Some patients have intermittent flow that has breaks in the flow. The total flow time is the sum of the voiding times and the break times in between. The normal flow patterns have a bell shape with maximum flow reached in the first 5 s of the voiding time and the rest of the shape varies depending on the voiding volume and time. Figure 25 shows sketches of abnormal flow curves.

Different flow patterns indicate different voiding abnormalities [302]. Five flow curve patterns have been defined Normal, Prostatic, Fluctuating, Fractionated, and Plateau flow curves and each type indicates a different diagnosis [303]. Q_{max} greater than 15 ml/s is normal for men where Q_{max} less than 10 ml/s is considered abnormal. For women, Q_{max} may be between 20–36 ml/s [303, 304].

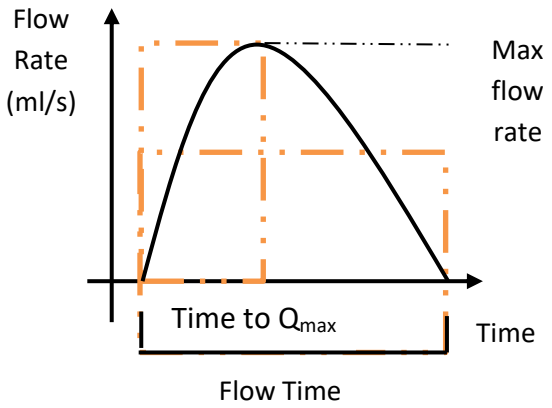

Figure 24 Sketch of parameters describing urinary flow

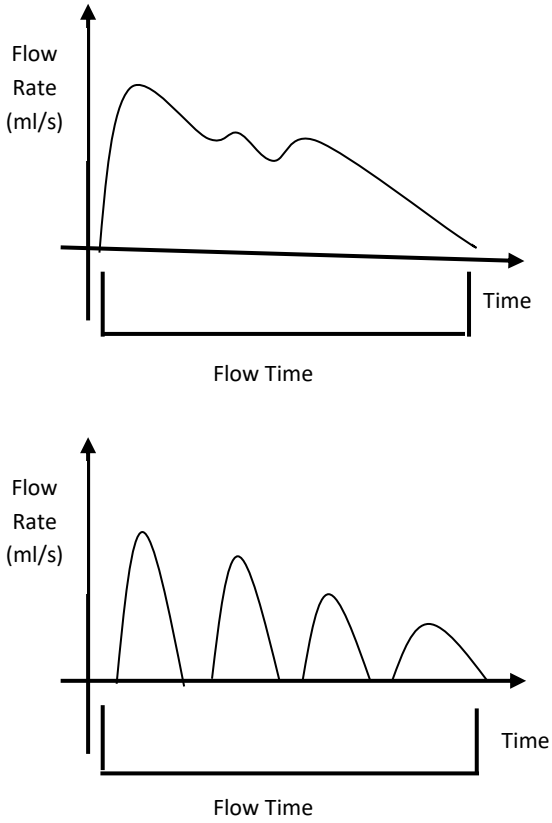

Figure 25 Abnormal flow curve sketches

The shape of uroflowmetry curve may indicate abnormality in the urinary tract, however, further diagnosis is required to identify the cause of abnormality. Several factors affect the urine flow, the contractability of the Detrusor muscle, Bladder flow resistance, Bladder volume, and the measurement technique itself [299]. The recorded shapes can be fed to an Artificial Neural

Network to automatically classify the shape of the curve as "healthy", "possible pathologic" and "pathologic" [305].

Urbonavičius and Kaškonas review lower urinary tract symptoms (LUTS), which affect the quality of life of older age people. One of the most widely used LUTS diagnostic methods is uroflowmetry. This diagnostic test offers simplicity and a wide array of diagnostic information. Many variations of equipment allow performing the uroflowmetric measurements. Studies show the psychological stress and awkwardness, experienced by patients affect the results of the test. Some methods are aimed at clinical use only, but there is a prominent trend of developing and producing devices that can be used by a patient in the comfort of his/her home. Different uroflowmetry techniques are discussed, including gravimetric, volumetric, image processing, acoustic, etc. Possibilities to apply these methods for men and women, as well as children are overviewed [306].

Chou et al studied the effect of urinating in women while standing instead of sitting [307]. Their study included 21 women and concluded that there is no change between Q_{max} and Q_{ave} if women urinate while standing. Amjadi et al showed that statistically, there is no significant difference in flow rate parameters if men change their positions while urinating from standing, sitting or squatting [308]. However, this was not the case with men urinating while laying down [309].

The first attempt made to measure urine flow rate was in 1897 by Rehfish. He used the air displaced by the urine filling an apparatus to move a pen writing on a moving paper. This system could not capture the flowrate, voiding volume and time [300]. Rehfish's method was improved by including a transducer in the system. The air displaced by the urine went over a hot wire and the energy required to maintain the wire's temperature at 300 °C was proportional to the urine

flow rate [310]. Key limitations for these techniques were the need for maintaining an air tight system and constant temperature. However, the measurements of these systems were adequately accurate and satisfactory [310].

Schwarz and Brenner in 1922 approximated the velocity of the urine stream from the parabolic stream resulting from males voiding horizontally [311]. They used several containers arranged in a line in front of the patient to collect the urine. The volume of the urine collected in these successive vessels and the overall voiding time enabled them to approximate the flow rate and the voiding volume. In 1925, Grownwell proposed the first uroflowmeter. A pen floating on a graph paper on a moving drum was used. The pen was attached to a receptacle that rose as urine fell on it and the pen drew the flow against time on the paper [312], [313].

Cardus et al designed an electromagnetic based flowmeter to measure the urine flow [314]. They used a sensor with rubber made adaptors connected to a funnel in which both male and female patients could urinate. They calibrated the flow meter using a normal saline fluid and managed to obtain the bell shaped curve for the voiding process. The total voiding volume was obtained by integrating the curve. This work proved that instantaneous flow rate could be measured using such sensors.

Flow clinics were used since the early 1950s [315]. Patients were asked to drink plenty of water and then enter into the flow room. The door was then closed and patients were left to urinate in privacy. The clinic consisted of a flow meter installed near a bed, and an ultrasound machine to assess the residual urine in the bladder after the urination was completed. Patients were usually asked to urinate three times and the data from the flow meters together with the ultrasound analysis were combined to generate the flow rate nomograms [316-320].

Many types of flowmeters were used in these studies; some of these types are explained below [301, 321, 322]:

- A weight transducer flowmeter weighs the voided urine. The volume can be calculated by using the weight and density. In addition, the flow rate can be determined by differentiating the volume with respect to time.
- A spinning disc flow meter causes the urine to fall onto a disc that is driven by a servo motor. As the urine falls on the disc, the motor torque increases due to the weight of the urine. The power needed to rotate the disc is proportional to the flow rate and can be used to generate the flow diagram.
- A capacitance based flowmeter uses a metal strip capacitor attached to a plastic dipstick vertically dipped into the urine container. The urine conducts electricity across the capacitance and changes the overall capacitance as it fills the container. The change in the capacitance is proportional to the flow rate.

Developments in microprocessors and controllers lead to designing home-based and battery operated flowmeters that use microcontrollers. Patients use these devices to record the voiding process and bring the device to the hospital to download the voiding data on a computer [322].

Viarani et al designed a resistive based microsystem flow sensor. The device utilized the hot wire anemometer principle [323]. The resistive micromachined sensor was covered with a thin film of gold that was heated while the fluid under test flowed above it. The flow rate was sensed by measuring the temperature differences between four temperature sensors placed on the membrane. Data were fed into a computer that calculated the flow rate and displayed the results

on a digital screen. The system was only tested through simulations. Dejhan and Yimman designed a rotating disk based flow meter that calculated the urine flow rate and displayed the results on smart phones used by the patient or the physician [324]. Otero et al reported satisfactory accuracy for the device [325].

Carter and Vaughn introduced a toilet mounted urine flow meter [326]. The urine was collected through a funnel and a tubing system that was connected to a pressure sensor. When the urine was collected through the funnel, the pressure on the sensor changed as the urine flowed through the toilet seat. The sensor generated an electrical signal that was fed into a computer to generate a flow rate diagram. The patent didn't provide information on the accuracy of the device, but such a system would involve time delay between the actual and measured urine flow. In addition, it required calibrating the pressure sensor for different flow rates. Furthermore, one of the advantages of this system was that the sensor was not in contact with the urine. Suryawanshi and Joshi used a closed air tube located above the urine flowing into a funnel [327]. A pressure sensor connected to a computer was placed in the air tube to measure changes in pressure in the tube that were due to the changes in the urine flow rate. Their system could calculate the maximum and average flow rate, the voiding volume and other important parameters needed in uroflowmetry.

Wurster developed a urine flow meter that used an apparatus that measured the volume of the collected urine at any time [328]. Then by differentiating the volume with respect to time it provided the flow rate at any time. A capacitance was used to measure the volume of the urine by designing it in a way that made the capacitance value change as the amount of urine collected changed. The electrical signal resulting from the changing capacitance was fed into a computer that was used to calculate the flow rate.

Home based urine flow measurement techniques can be as simple as dividing the volume of the voided urine measured in a collection vessel by the voiding time calculated by a stopwatch and obtaining the average flow rate i.e. finding Q_{ave} rather than Q_{max}. Handheld funnel based devices can also be used at home. Users void into a funnel. The urine flows out of the funnel into a restricted aperture into a measuring container; the aperture contains a flow sensor calibrated for several ranges of flow rates [322]. The accuracy of these devices can be measured by dropping a fluid in them at a controlled and known flow rate and then comparing the recorded flow rate with the actual known one. These flowmeters have clinically accepted results if the volume error is 1–8% and flow rate errors 4–15% [303, 321]. Drach and Binard used a portable flowmeter made of plastic consisting of two chambers opened on each other [329]. A strip that changed colors in steps of 2 ml/s was used to calculate the Q_{max}. The reported accuracy of the system was ±1.5 ml/s of the maximum flow rate. The device was disposable, easy to use and could be used to calculate the Q_{ave} if the voiding time was calculated.

Caffarel et al showed that calculating the average value for the maximum flow Q_{max} measured multiple times at home improves that accuracy of the measurement and brings it closer to the value measured using uroflowmeters within clinics [330]. They asked 22 patients to record their Max flow rate twice a day for 12 consecutive days. In addition, they used a rotating disk

based urine flow meter in the clinic to measure the flow rate at the start and end of the 12 days. The mean values for home base uroflowmeters and rotating disk flowmeter showed good agreement.

The Streamtest cup is a simple device to evaluate urine flow at home or in a Urology clinic [331]. It is basically a plastic disposable cup with an exit tube in the bottom center of the cup. The exit tube was designed to allow a maximum flow rate of 12 ml/s. A marker was placed near the bottom of the cup representing a 200 ml of urine filling the cup while exiting from the bottom of the cup at the same time with a rate of 12 ml/s. If a patient urinating in the cup at a flowrate less than 12 ml/s, then the urine never reaches the marker in the cup indicating a problem in the urinary tract. If the urine reaches the marker and begins to over flow the cup, then the urine flow rate is higher than 12 ml/s and the urinary tract is normal. The system was tested on 50 patients and all patients with flow rate higher than 12 ml/s overflowed the cup and those with flow rate less than 12 ml/s didn't manage to reach the marker. The system provides an insight on the flow rate but cannot measure the instantaneous flow rate. Severely obese and visually impaired patients may not be able to observe the marker on the cup while urinating.

De La Rosette et al designed a home based portable uroflowmeter and compared its performance with another system based in a urology clinic [332]. The portable flowmeter consisted of four calibrated volume sensors printed on paper-like disposable material. The paper was shaped like a cone placed in a beaker to collect the urine. The electrical properties for the volume sensors varied as the fluid volume increased in the beaker. The system was connected to a microcontroller that calculated the flow rate and stored it in its memory. The performance of this portable system was compared with an invasive catheter based uroflowmeter system with 67

patients. Comparison results showed that home based uroflowmeters can provide reliable measurements for the voiding process.

Another disposable home-based uroflowmeter to calculate Q_{max} and voiding volume comprised a collecting funnel with a spout divided into three chambers. The device was pre-calibrated such that filling of the chambers corresponded to Q_{max} values of 10, 10–15 and 15 ml/s. The performance of this device was compared with a standard flowmeter [333]. The study involved 46 men who were asked to use the funnel at home twice a day for seven days. Results showed that the device has sufficient accuracy and reliability to give an initial assessment for Lower Urinary Tract Diseases.

Lyon and Smith used sound-based techniques to measure the flowrate [333]. A microphone was placed at the edge of the toilet seat to record the sound of the voiding process and a vessel was used to collect the urine to measure the overall volume. When the voiding process was completed, the recorded sound was played and a stopwatch was used to measure the voiding time based on the sound. This enabled the calculation of the average flow rate and voiding volume. Hitt et al attempted to correlate the sound of the urine hitting a liquid free surface with the flow rate [334]. They designed a system that used a syringe pump with fixed flow rate to simulate the urine. The system included a digital microphone with a sampling rate of 44 kbps that records the splashing sound of the urine hitting a clear surface. The sound recordings were spectrally analyzed in MATLAB to evaluate the time-frequency and wavelet transform contents. This work was just experimental and did not materialize to be tested on patients. In addition, they stated that they can only make general statements about the correlation between the acoustical signature and flow parameters.

Sonouroflowmetry (SUF) captures the sound generated by a stream of urine striking the water in a toilet bowl. Krhut et al validated SUF using simultaneous uroflowmetry [335]. A dedicated cell phone recorded the sound visualization showed sound intensity over time. Simultaneous sets of UF and SUF were analyzed. Correlations were for flow time (0.87), voided volume (0.68), and maximal flow rate (Q_{max}) (0.38).

The international continent society (ICS) developed comprehensive guidelines for Good urodynamic practice in both clinical and research investigation. The guidelines covered three main elements (the measurement practice, the quality control, and documentation). The guidelines stated that urodynamic practices cannot be fully automated except for uroflowmetry. The accuracy for flow rate measurement needs to be ±1 ml/s, with a flow rate range between 0 and 50 ml/s and a total voiding volume of 1000 ml with many other documentation and safety requirements. One of the techniques used in uroflowmetry is the flow curve shown in Figure 24. Some flow curves may show abnormality, however, the guidelines state that a diagnosis can't be made using flow curves alone. Further invasive measurements for the pressure in the bladder are needed to have an accurate diagnosis for any abnormality appearing on the flow curve.

Note that the flowrate measurement and the flow curve are affected by the signal processing involved and the method used to calculate them. A collecting funnel, or tubing used to direct the urine, or the flow sensor will eventually cause modification to the actual flowrate. Therefore, the guidelines stated that an electronic measurement of Q_{max} requires smoothing the flow curve by averaging over 2 s to remove the spikes in the signal. In addition, a minimum rate of 10 Hz is required for the analog to digital conversion. ICS also required that the maximum flow rate should be rounded to the nearest whole number while the voiding and residual volumes should be rounded to the nearest 10 ml [299].

The guidelines developed by ICS in 2002 went further to provide information on quality measures required for invasive pressure-flow measurements. It stated that typical information such as voiding volume and maximum flowrate should be obtained from noninvasive techniques before moving towards invasive ones.

In 2014, the ICS published more updated guidelines to serve as a benchmark for the performance of urodynamic devices [313]. The guidelines aimed to provide a summary for the performance requirements, technical specifications, and comparison of different technologies used in urodynamics. Furthermore, the guidelines proposed a set of tests for assessing of different systems.

The guidelines suggested that any urodynamic system should be able to measure the difference between the intravesical and abdominal pressures together with the voiding volume and flowrate. Clinicians may require additional measurements such as urethral pressure and the electromyography signal (EMG) of urethral muscle. The updated guidelines didn't change the clinical values introduced in the previous version as shown below:

- Accuracy of flow measurement should be ±1 ml/s.
- The resolution of the voided volume should be at most 2 ml with a ±3% error in the value
- The range of flow measurement necessary is 0–50 ml/s, with a volume range of 0–1,000 ml
- Sample rate of volume measurement ≥ 2 Hz
- Bandwidth between 0–5 Hz is recommended to record flow measurement with a sampling rate of at least 0.2 Hz.
- A low pass filter with a cutoff frequency of 1 Hz needs to be used to smooth and average the flow curve.

The guidelines added desirable features for uroflowmetry equipment that included the need to state the minimum recordable volume or flowrate change. In addition, documentation should indicate the signal processing method used in the measurement.

Flowmeters need to be able to measure low flowrates that have clinical significance. Obstructed bladder may lead to very low flowrate and it is important to be able to capture that measurement. A device should be able to measure down to its accuracy of 1 ml/s and this number should be mentioned in the documentation associated with the device.

Requirements on some of the common technologies used in uroflowmetry were included in the guidelines.

The load cell flowmeter (gravimetric) flow meters rely on fluid weight measurement during voiding. Volume of urine can be calculated by multiplying it with its density and flow is change in the volume with time. The guidelines required the scale to remain horizontal for reliable measurement. A set zero volume function should be available to overcome the difficulty of emptying the flowmeter between voids.

The spinning disk flowmeter or momentum-flux flowmeter is also used in uroflowmetery. Urine falling on a spinning disk slows it down, therefore, more power would be needed to keep the disk rotating at the same speed. The flowrate will be proportional to the power needed to keep the disk rotating at a constant speed. This method enables calculating the mass flow directly without the need for using the density of the urine as it is the case with load cell method. The volume can be calculated by integrating the flow.

To enable male patients to undergo uroflowmetry in a private condition without medical supervision, Terai et al devised an automatic switching and patient guidance system for the spinning disk uroflowmeter Urodyn 1000, using two commercial electronic devices [336]. To

avoid mechanical wear of the spinning disk, an infrared motion sensor tap RPC-03 (Logic Pack, Iwata, Japan) turns on its two AC taps when a pyroelectric infrared sensor detects human motion within 5 m. A vacuum fluorescent display (VFD) module SCK256 × 64F-3101-A (Noritake Itron, Ise, Japan) displays a series of messages consisting of 'In preparation. Please wait for X seconds.' with X counting down from 10 to 1, and 'Ready. Now you can start urination.' The voided urine is directly drained into a wall urinal. The devices are automatically turned off 5 min after the patient leaves the room. With the use of our system, men already acquainted with uroflowmetry could perform self-administered uroflowmetry any time in private. The system was considered useful for improving the quality of patient service.

Dipstick methods for measuring flow use a capacitive stick dipped into a container that is filled with urine. The change in the capacitance is proportional to the flowrate. The guidelines stated that the method was proven reliable but no clinical publications were associated with it. Drop spectrometry is another method mentioned in ICS guidelines, however, it was technically demanding and unreliable.

The ICS guidelines required a calibration method for uroflowmeters. After 10 voiding measurements, a volume of 300 ml of water is to be poured into the device at a constant flow rate to verify its operation. Another method can be to empty the urine collected from a device into a measuring beaker to verify the value of the collected volume. If the flow sensor requires calibration frequently, then it might be better to replace it.

Many possible sources of errors were mentioned in the ICS guidelines, designs of device should account for them and adjust performance to compensate for them:

- Load Cell method: The density of the urine used is 1 g/ml which might not be the case with patients using contrast medium or having dehydration. Allowing the user to modify the density in accordance with patient conditions may reduce its effect.
- The momentum of urine falling on the spinning desk may cause artifact in the volume calculated.
- Time delay between the change in ureter pressure and urine flowrate, in addition, low pass filtering techniques used in signal processing will cause further delays. ICS estimated the delay to be 0.4–0.6 s.

Further guidelines related to other Urodynamic techniques were developed by ICS as well [313].

Gomes et al note that in the elderly, an adequate uroflow measurement may be difficult to obtain for the following reasons [337]: (1) geriatric patients commonly void small volumes; (2) the bladder may be empty at the moment of the study, and the patient may have urgency or urge-incontinence; (3) mental status may be limiting and (4) some patients have difficulty voiding in an unfriendly/unfamiliar place. Despite its limitations in diagnosing, uroflowmetry is a sensitive indicator of voiding dysfunction and can be used to distinguish patients who will promptly need further investigation from those who can be started on a treatment regimen and avoid extensive urodynamic testing. It can also be used in patients with a known bladder outlet restriction as a measure of progression of the disease or to determine the efficacy of treatment modalities that are expected to improve bladder emptying.

Sand notes that measurement of the maximum flow rate is more useful in men than in women because of its ability to detect physical obstruction of the urethra, a condition that is rare in women [338]. Uroflowmetry is primarily a measure of voiding velocity and is measured in ml/s. Because there is little concern of physical urethral obstruction in women, the pattern of the

uroflow curve is more important than the quantitative measurement of voiding velocity. A normal bell-shaped uninterrupted uroflowmetry curve is readily identified as a normal study. An abnormal uroflowmetry study shows an interrupted intermittent flow pattern, which may suggest voiding dysfunction.

Jørgensen et al tested the Da Capo™ home flowmeter versus the Urodyn 1000™ flowmeter. The two flowmeters are based on different principles [339]. The Da Capo is a portable, battery powered flowmeter designed to record all voidings during a period of time (e.g. 24 h) for a single patient. The flowmeters were tested with regard to accuracy of measurement of the voided volume and maximum flow (Q_{max}). The Da Capo was tested by 10 healthy male volunteers, median age 47 years, range 21–57. Both flowmeters were very accurate measuring Q_{max} and voided volume. A few artifacts arose, i.e. extremely high Q_{max} values were recorded. All test persons found the flowmeter easy to handle. The weight transducer based Da Capo home flowmeter proved as accurate as the stationary flowmeters. It is easy to handle and it provides all-day monitoring of uroflow and voided volume.

Guan et al designed a new portable home electronic uroflowmeter and compared it with traditional methods. The system consisted of collectors, urine conducting apparatus, intelligent cell phone, wireless network communication technology, computer analysis and drawing, and data storage technology, etc., and can automatically collect voiding information from patients with lower urinary tract symptoms (LUTS) [340]. Through Bluetooth, the voiding information was sent to the patient's cell phone from the collector, then stored directly by cell phone and wirelessly transmitted to the workstation in hospital. The system was primarily tested with regard to accuracy of measurement of the voided volume. Multiple doses with known volume were introduced in the system and Laborie uroflowmeter. 38 outpatients who had LUTS were tested

simultaneously with the system and Laborie uroflowmeter. Among the subjects, there were 22 male patients and 16 female patients, with a total of 57 tests. The system accurately collected and analyzed voiding time, uroflowmetry, voided volume, and automatically provided uroflowmetry parameters. The measurement error at 100, 200, 300, 500 and 800 ml was less than 5%. 12.28%, 5.26% and 3.51% of the Q_{max}, Qave and voided volume points were beyond the 95% limits of agreement. The maximum absolute values of the Q_{max}, Q_{ave} and voided volume differences were 0.38 ml/s, 0.70 ml/s and 2.90 ml, respectively. They agreed with the recommendation of Standardization International Continence Society. The new portable home electronic uroflowmeter had good agreement with Laborie uroflowmeter, and is a new LUTS monitoring system integrated with correct, reliable, real-time, convenient and easy-managing advantages. It is as noninvasive and reliable as traditional methods, and its portable feature facilitates application out of hospitals. It can also record voiding diaries.

Chan et al found electronic uroflowmetry reasonably predicts the likelihood of bladder outlet obstruction (BOO) and risk of acute urinary retention (AUR) [341]. This low-cost device, Uflowmeter(™) , allows men to perform uroflowmetry at home with ease and the results are compatible with that of electronic uroflowmetry. It can also estimate risk of AUR and the need for transurethral resection of the prostate (TURP) to relieve lower urinary tract symptoms (LUTS).

To show the clinical value of a simple flowmeter, which has been devised to measure uroflow on an ordinal scale (<10, 10–15, 15–19 and >19 ml/s) at home, for the management of male (LUTS) a total of 186 men with LUTS were enrolled in the study. The mean follow-up was 220 days. The men's mean age was 65.5 years, mean (range) maximum urinary flow rate (Q_{max}) 12.8 (4.3–39.5) ml/s, mean (range) voided volume 294.8 (151–686) ml; mean (range) postvoid residual

urine volume (PVR) 50 (0–303) ml and mean (range) International Prostate Symptom Score (IPSS) 13.5 (1–31). The men underwent electronic uroflowmetry ('clinic uroflowmetry') and completed an International Prostate Symptom Score (IPSS) questionnaire in the clinic. They then conducted 10 measurements with the device at home ('home uroflowetry').

The uroflowmetry and IPSS questionnaire were repeated 2 weeks later. The sensitivity and specificity of the home uroflowmetry values corresponded to the mean Q_{max} of clinic uroflowmetry. Similar analyses were performed for the IPSS.

Home uroflowmetry was most sensitive in identifying a mean Q_{max} of >19 ml/s and most specific in identifying a mean Q_{max} of <10 ml/s. The home uroflowmetry works best in ruling out a mean Q_{max} of <19 ml/s followed by a mean Q_{max} of <15 ml/s and a mean Q_{max} of <10 ml/s. Men with a home uroflowmetry value ≤10 ml/s were more likely than those with a home uroflowmetry value >10 ml/s to develop AUR or require TURP. The IPSS failed to display the same discriminative capability.

Home uroflowmetry using this simple device is a satisfactory estimation of clinic uroflowmetry using an electronic flowmeter and can predict the significant progression of male LUTS.

Boci et al studied home uroflowmetry and compared this method to free or "traditional" uroflowmetry in the evaluation of patients with symptomatic benign prostatic hyperplasia (BPH), and the relationship between the values of home uroflowmetry parameters and bladder outlet obstruction (BOO) [342]. Twenty-five patients (mean age, 67 years) with symptomatic BPH were examined with home uroflowmetry, free uroflowmetry, and pressure-flow measurement. The patients were assessed using the International Prostate Symptom score (IPSS); digital rectal examination; routine blood chemistry, including serum prostate-specific

antigen level; urinanalysis; transrectal ultrasonography; and post-void residual urine. The 24 h were divided into "active time" (AT) and "sleep time" (ST). AT home uroflowmetry parameters were compared to ST ones. The home uroflowmetry parameters were compared to respective ones of the free uroflowmetry as well and those obtained by pressure-flow measurement. The patients were asked about their opinion of home uroflowmetry. Home uroflowmetry was found to be a simpler and more acceptable method than free uroflowmetry. The mean Q_{max} of AT was significantly greater than the mean Q_{max} of ST, but the mean voided volume and mean voiding time of ST were significantly larger than those of AT. There was a close relationship between the mean Q_{max} at home and the Q_{max} in hospital, but the voided volume and voiding time measured in hospital were significantly larger than those at home. Home uroflowmetry provided an estimation of BOO for 46% of the patients as low if the home mean Q_{max} was >14 ml/s, and as high if the home mean Q_{max} was <10 ml/s. Home uroflowmetry was well accepted by the patients and gave more information than free uroflowmetry. In 46% of the cases, an estimation of BOO was obtained with home uroflowmetry.

Mombelli et al investigated the possibility that patients could carry out a urine flow assessment at home by themselves, in comfort, without expense and without the use of equipment [343]. They compared this strategy of "Do-It-Yourself" (DIY) uroflowmetry with traditional, hospital uroflowmetry.

One hundred and twenty patients were enrolled. The patients underwent conventional, free uroflowmetry in hospital. Subsequently, the patients were asked to carry out the following procedure at home: urinate into a graduated container to quantify the total voided volume and determine the flow time by measuring the duration of micturition with a stopwatch or simply

with the second hand of a clock. This procedure had to be performed three times without preparation.

One hundred patients completed the study. The mean age of the patients analyzed was 64.12 years. Their free uroflowmetry values were as follows: the mean voiding time was 44.28 s, the mean voided volume was 290.92 ml, the mean Q_{max} was 15.17 ml/s, the mean Q_{mean} was 7.87 ml/s, and the mean post-void residual volume was 78.44 ml. The mean Q_{mean} measured by the "DIY-uroflowmetry" was 8.33 ml/s, which was not statistically significantly different ($P = 0.12$). Assuming that pathological hospital uroflowmetry values are equivalent to a DIY-$Q_{mean} \leq 10$ ml/s and that normal hospital values are equivalent to a DIY-$Q_{mean} > 10$ ml/s, the concordance was 100%.

The proposed DIY evaluation of urine flow, together with the International Prostatic Symptom Score (IPSS), provides a good estimate of the results of free uroflowmetry, enabling unnecessary hospital investigations to be avoided.

Reynard et al explored the relationship between uroflow variables and lower urinary tract symptoms (LUTS): to define performance statistics (sensitivity, specificity, positive and negative predictive values) for maximum urinary flow rate (Q_{max}) with respect to bladder outlet obstruction (BOO) at various threshold values; and to investigate the diagnostic value of low-volume voids [344].

The study comprised 1271 men aged between 45 and 88 years recruited from 12 centers in Europe, Australia, Canada, Taiwan and Japan over a 2-year period. Symptom questionnaires, voiding diaries, uroflowmetry and pressure-flow data were recorded. The relationship between uroflow variables and symptoms, Q_{max} and BOO, and the diagnostic performance of low volume voids were analyzed.

The relationship between symptoms and uroflow variables was poor. The mean difference between home-recorded and clinic-recorded voided volumes was –48 ml. Q_{max} was significantly lower in those with BOO (9.7 ml/s for void 1) than in those with no obstruction (12.6 ml/s; $P<0.001$) and Q_{max} was negatively correlated with obstruction grade, even when controlling for the negative correlation between age and Q_{max}. A threshold value of Q_{max} of 10 ml/s had a specificity of 70%, a positive predictive value (PPV) of 70% and a sensitivity of 47% for BOO. The specificity using a threshold Q_{max} of 15 ml/s was 38%, the PPV 67% and the sensitivity 82%. Those voiding <150 ml had a 72% chance of BOO (overall prevalence of BOO 60%). In those voiding >150 ml the likelihood of BOO was 56%. The addition of a specific threshold of 10 ml/s to these higher volume voiders improved the PPV for BOO to 69%.

While uroflowmetry cannot replace pressure-flow studies in the diagnosis of BOO, it can provide a valuable improvement over symptoms alone in the diagnosis of the cause of lower urinary tract dysfunction in men presenting with LUTS. This study provides performance statistics for Q_{max} with respect to BOO: such statistics may be used to define more accurately the presence or absence of BOO in men presenting with LUTS, so avoiding the need for formal pressure-flow studies in everyday clinical practice, while improving the likelihood of a successful outcome from prostatectomy. This study also shows that low-volume uroflowmetry can provide useful diagnostic information and that, as such, the data from such voids should not be discarded.

Unsal and Cimentepe investigated the effect of voiding position using uroflowmetry and post-void residual (PVR) urine volume assessment in healthy men and women [345].

The study population comprised 72 healthy volunteers. The mean (range) ages of the male (n = 36) and female (n = 36) subjects were 30 (18–40) years and 32 (21–44) years, respectively. The uroflowmetric studies were repeated in the standing, sitting and crouching positions for men and

in the sitting and crouching positions for women. At least three measurements were obtained for all voiding positions for each volunteer. PVR volumes were measured using trans-abdominal ultrasound after each voiding. Maximum flow rate (Q_{max}), average flow rate (Q_{ave}), voided volume (VV) and PVR values obtained in each voiding position were compared with those obtained in the other positions.

The mean Q_{max} and Q_{ave} values obtained in the sitting, crouching and standing positions in men were 24.29 ± 0.73 and 15.67 ± 0.37, 23.28 ± 0.64 and 15.56 ± 0.33, and 23.58 ± 0.63 and 15.81 ± 0.34 ml/s, respectively. The mean VV and PVR values obtained in the sitting, crouching and standing positions in men were 297.5 ± 12.71 and 13.52 ± 1.02, 306.3 ± 13.46 and 14.02 ± 1.08, and 309.9 ± 13.14 and 12.92 ± 0.95 ml, respectively. In women, the mean Q_{max} and Q_{ave} values obtained in the sitting and crouching positions were 28.09 ± 0.66 and 18.26 ± 0.36, and 27.98 ± 0.59 and 17.31 ± 0.35 ml/s, respectively. The mean VV and PVR values obtained in the sitting and crouching positions in women were 331.8 ± 13.28 and 11.82 ± 0.99, and 326.9 ± 12.87 and 12.79 ± 1.07 ml, respectively. There were no significant differences in any of the parameters between voiding positions in either group.

Urinary flow rates and PVR urine volume do not seem to be affected by voiding position in healthy men and women.

Wiens et al tested an optical uroflowmeter that consisted of a camera, a filling container and lighting source contained within an enclosure [346]. A funnel directed the urine stream into the filing container, which had a vertical channel, perforated at the bottom to minimize horizontal surface disturbances. A JVC GZ-HM440AU camera imaged the volume of urine within the container as it filled. Volume data were differentiated to yield flow rate. The lighting source was a 5 × 6 array of white LEDs. The first frame of the video file was assigned as a background

frame. Subsequent frames were subtracted from the background frame and thresholded to yield a black and white image which showed the urine surface height. When urine was clear, detection was difficult. Thus they viewed a refracted image of lines drawn on the side of the container and this image changed when urine surface height increased. They found comparable accuracy between traces resulting from the optical uroflowmeter and a Labore Urocap III uroflowmeter when a pump supplied simulated normal, abdominally strained, and obstructed flows.

Shokoueinejad et al designed and tested a novel noninvasive video voiding device (VVD) that can be used to diagnose lower urinary tract dysfunction [293]. The VVD has three positioned cameras. A side camera views the urine stream from a 90^{o} horizontal angle on a black background. A top camera views the urine stream from a 90^{o} vertical angle on a black background. A lower back camera (the cylinder camera) monitors the accumulation of urine into a 1000 ml cylinder. Three G-LUX series 8 W LED Spot Lights illuminate the stream to provide best contrast. Two LEDs are mounted on the wall facing the patient (above and below the urine stream line of action). One LED is mounted at the top of the right side wall, shedding light from a steep downward orientation/trajectory towards the funnel. The combination of these three LED placements shedding light from three different angles results in complete illumination of the urine stream, ensuring high contrast and visibility.

To use the VVD, the patient stands in front of the device and urinates. The urine is guided by a large 53 cm diameter funnel leading it to the cylinder. The urination is captured from two angles using two cameras (top and side). The cylinder camera captures the filling process of the cylinder in order to compute the instantaneous flow rate, max flow rate, total voiding time, and total voided volume. Software was developed using MATLAB to analyze the video recording of

the urine accumulating in the cylinder and calculate the instantaneous flow rate, max flow rate, total voiding time, and total voided volume.

The device was clinically tested on patients. It allowed patients to urinate privately and gave urologists the advantage of observing the video of the voiding stream giving them the ability to determine any abnormalities or obstructions in the urinary tract. The accuracy of the measurement was tested by integrating a mass flowmeter into the setup and simultaneously measuring the instantaneous flow rate of a predetermined voided volume in order to verify the accuracy of the device compared to the mass flowmeter. The accuracy recorded was ±2% and ±3% relative to full scale. The device performance satisfied the ICS guidelines previously described in this review.

A.5 Conclusion

Uroflowmetry is a noninvasive method used in Urodynamic techniques for the purpose of evaluating the urinary function. Table 7 summarizes these techniques.

A variety of uroflowmetry techniques were reviewed. The techniques were both home based and those that were more sophisticated involving electronic sensors and microprocessors. Uroflowmetry results assist in identifying the existence of a problem and which urodynamic techniques are required to identify the exact problem. The review showed that sensors used in Uroflowmetry have not changed much, the development is currently in interfacing these sensors with microcomputers for utilization of digital technology. Shokoueinejad et al introduced a novel device that used video cameras to recording the voiding process and then calculate some of the important parameters for diagnosing lower urinary tract dysfunction [53].

Guidelines of International Continence Society for designing new uroflowmetry devices were also reviewed. The guidelines were discussed to aid interested researchers in inventing new methods and techniques for measuring urine flow rate and voiding volume.

Table 7: Summary of uroflometry methods

Invasive	Catheter	Pressure sensor	Internal and external pressure, path resistance
		Flow sensor	Flow rate
	Fluoroscopy	Camera with contrast	Ureter function (X ray)
	Myography	Electrodes	Internal muscles and sphincter contraction activity
Noninvasive and can be integrated with a microprocessor	Ultrasound	Residual urine volume in ureter	
	Hotwire Temperature	Flow rate	
	Floating pen on a moving drum	Flow graph, Max flow, voiding time	
	Electromagnetic sensor	Instantaneous flow rate	
	Weight based sensor	Average flow rate, voiding volume, flow diagram	
	Spinning disk	Average flow rate, voiding volume, flow diagram	
	Capacitive sensor	Average flow rate	
	Resistive thermistors	Average flow rate	
	Pressure sensor with tubing and funnel	Average flow rate	
	Handheld funnel calibrated to a certain flow rate	Determine if flow exceeds certain values or not	
	Microphone sensing voiding sound	Flow rate (not proven clinically)	
	Video camera	Flow rate, voiding volume, instantaneous flow rate, voiding time, Q_{max}, Q_{min}, Q_{ave}	

A.6 Acknowledgements

This study was funded by the Deanship of Scientific Research (DSR), King Abdulaziz University, under grant (HiCi/1432-4-8). The team acknowledges the deanship technical and administrative support

B. Video Voiding Device For Diagnosing Lower Urinary Tract Dysfunction in Men

B.1 Abstract

We introduce a novel diagnostic Visual Voiding Device (VVD), which has the ability to visually document urinary voiding events and calculate key voiding parameters such as instantaneous flow rate. The observation of the urinary voiding process along with the instantaneous flow rate can be used to diagnose symptoms of Lower Urinary Tract Dysfunction (LUTD) and improve evaluation of LUTD treatments by providing subsequent follow-up documentations of voiding events after treatments. The VVD enables a patient to have a urinary voiding event in privacy while a urologist monitors, processes, and documents the event from a distance. The VVD consists of two orthogonal cameras which are used to visualize urine leakage from the urethral meatus, urine stream trajectory, and its break-up into droplets. A third, lower back camera monitors a funnel topped cylinder where urine accumulates that contains a floater for accurate readings regardless of the urine color. Software then processes the change in level of accumulating urine in the cylinder and the visual flow properties to calculate urological parameters. Video playback allows for reexamination of the voiding process. The proposed device was tested by integrating a mass flowmeter into the setup and simultaneously measuring the instantaneous flow rate of a predetermined voided volume in order to verify the accuracy of VVD compared to the mass flowmeter. The VVD and mass flowmeter were found to have an accuracy of ±2% and ±3% relative to full scale, respectively. A VVD clinical trial was conducted on 16 healthy male volunteers ages 23–65.

B.2 Introduction

In human physiology there are two phases of the micturition cycle: the storage phase and the voiding phase. However, a third post-voiding phase appears with pathological disorders such as Benign Prostatic Hyperplasia (BPH). Thus disturbances of the storage phase are described as storage symptoms and those of the voiding phase are described as voiding symptoms. Voiding symptoms involve abnormalities of the urinary stream such as weakness, loss of force, diminished caliber, intermittency, spraying and deviation of the stream to one side, and straining to void. Post-voiding symptoms are described as post-voiding dribbling and sensation of incomplete bladder emptying.

During the assessment of Lower urinary symptoms (LUTS), the clinician obtains a full voiding history, details of the patient's complaints, and depends heavily on the patient's narrative description of his voiding disturbances. While storage symptoms are usually due to bladder dysfunction, voiding symptoms are thought to be due to obstruction of the urinary passage by lesions such as BPH, urethral stricture, meatal stenosis and other urethral disorders such as stones, malignancy or traumatic lesions. A major and essential step in the medical evaluation of LUTS is physical examination of the patient. This usually focuses on the examination of the urinary bladder and the prostate gland. However, there have never been any published documents on the actual observation of terminal or post-void dribbling and no direct examination of elements of voiding symptoms by watching the urinary stream during voiding and observation of the patient's facial expression during straining. Therefore, the clinician judges the severity of these voiding symptoms depending only the description given by the patient without actual verification or documentation.

This paper describes a novel method to examine the voiding and post-voiding phases of micturition for voiding symptoms. The method enables a physician to verify a patient's

description, and evaluate any voiding and post-voiding symptoms by visually documenting the whole voiding process and measuring any urological parameters, such as flow rate, simultaneously. Therefore it is an improvement to the existing diagnostic tools, and would help greatly in the follow-up assessment of patients.

Video and image processing are essential parts of modern medical image analysis and computer vision-aided healthcare services. Urinary voiding visual inspection plays a useful role in the diagnosis of a number of urological disorders. When an expert eye is allowed to visualize and examine a disorder, a solid conclusion can be made and a therapeutic decision is based on clear evidence, the power of vision. Traditional testing of voiding such as uroflowmetry, urethrography and urethral calibration do not include an actual visual examination of voiding by the clinician's eye [347]. They produce graphic traces, radiological images and impressions that are less helpful than watching the act itself [348]. Furthermore, the confirmation of clinical diagnosis of some voiding disorders such as stress urinary incontinence depends solely on visual inspection. For instance, visualization of the urine leakage from the urethral meatus with a cough is a diagnosis of stress urinary incontinence [349].

Most patients are willing to allow their urologists to observe them during voiding or at times of urinary incontinence in order for the treating urologist to make a judgment of the condition that would help in finding the correct solution for the problem. Patients lack the expertise to estimate and describe the subjective impression of the force and caliber of their urine flow since they do not have a means to compare with others; some of them just don't observe their urine flow by nature such as men who are not able to make this observation because of their shape, weight, age, or illness [350]. Documentation and post-processing of the video footage of the urination provide useful information for the urologist to diagnose the urinary problems.

Lower urinary tract dysfunction (LUTD) is common in both men and women, and the incidence and prevalence increase with advancing age [351]. Symptoms of LUTD encompass all urinary symptoms including storage, voiding, incontinence, and post-micturition symptoms [352]. “Symptoms of LUTD are highly prevalent and occur in both genders to a similar extent, with 51% of men and 59% of women exhibiting storage symptoms; 26% of men and 20% of women exhibiting voiding symptoms; and 17% of men and 14% of women exhibiting post-micturition symptoms. The impact and burden of symptoms of LUTD to individuals and to the nation are enormous. Those patients with symptoms of LUTD suffer considerable morbidity resulting in a significant decrease in quality of life for both the patient and his/her partner.” [353].

The VVD visually documents urinary voiding events remotely. In addition, it also has the ability to measure the instantaneous flow rate at any given moment in time during urinary voiding. The VVD should improve the initial diagnosis of LUTD, and also improve the evaluation of LUTD treatments by providing subsequent follow-up documentations of voiding events after treatments. The VVD enables a patient to have a urinary voiding event in privacy while a urologist monitors, processes, and documents the event from a distance. By helping to make the correct diagnosis and evaluating the degree of LUTD severity, the VVD should be of clinical importance, especially in the documentation and further monitoring of the progress of the LUTD condition.

The following should be the clinical application of the use of this device that reflects its importance in the diagnosis and management of LUTD, therefore helping to improve this condition:

1. In the initial confirmation of the presence of Lower Urinary Tract Symptoms (LUTS), as claimed by the patient (diagnosis).
2. Documentation of the type and degree of urinary incontinence (UI): such as urine leakage during physical stress. The degree of stress urinary incontinence (SUI) is determined by direct measuring of the actual amount of urine leaked.
3. In the follow-up monitoring of the various types of treatment such as:
    a. Physiotherapy and pelvic floor exercises: the VVD should help in monitoring the progress of UI following this type of therapy.
    b. Medical treatment of UI: the VVD should help in monitoring the effectiveness of medical treatment of diseases such as Benign Prostatic Hyperplasia (BPH) and bladder neck obstruction.
    c. Surgical treatment of UI: the VVD should help in monitoring the success or failure of surgical management, the degree of improvement of UI can be assessed and documented following this type of therapy.

This study has two primary objectives. The first is to document the urine voiding process by video recording the urine stream from two angles (top and side). Observing the shape of the urine stream can be a practical diagnostic tool for medical practitioners since it provides a noninvasive method of estimating subjective impression of the force and urethral dilation. The second objective is to extract parameters that would benefit the urologist in making better diagnoses and decisions, such as the Maximum (Peak) Flow Rate, Average Flow Rate, Instantaneous Flow Rate, Total Voiding Time, and Total Voided Volume. We have analyzed and

measured the important urological parameters with VVD using the proposed video processing algorithm.

The rest of the paper is organized as follows. Section 2 examines the related work and the background. Section 3 describes the overall methodology. Results and methodology validations are discussed in section 4 and its different subsections. Finally, discussion, conclusion and future directions of the present work are discussed in sections 5 and 6 respectively.

B.3 Background

The devices currently used to study urinary voiding actually measure urine-flow or volume per unit time (also called uro-flow-rate), time of voiding, average flow rate over the total voiding time etc. [344]. Among those, the most important parameter is the maximum flow rate (*Q*-max.) or the peak flow rate defined as the highest point on the curve the flow reaches during the period of voiding [299]. This is purely physics and recorded by a device that depends only on the physical properties of the voided urine, that is weight and the speed of its accumulation [354]. It records the measurement at the end of the urine stream or column at a point the stream may have already been slowed, branched, bifurcated or turned into a spray rather than one solid stream. Therefore, other important clinical characteristics of the act of voiding and the nature of the voided urine are not observed. Clearly, to the urologist, learning about the subjective impression of the urine force during its natural flow as visually observed and noting its direction and caliber is equally important especially in certain medical circumstances such as obstructed flow of urine, deviated stream [355], stress urinary incontinence and conditions associated with interrupted stream such as detrusor sphincter dyssenergia [309].

Researchers have suggested simple devices that can measure flow in the home or office [331, 356-358]. Today's technology allows us to use miniature devices to provide a clear view

for the treating urologist to make the needed diagnosis. This device can be used for men, women and children of different age groups. It is more convenient for both the patient and the urologist to observe the act of voiding remotely using a monitor while the patient is standing or seated comfortably in separated privacy.

One of the simple approaches, namely visual examination of the urinary stream without taking any measurements has also been recommended for assessing voiding ability in children [359]. This approach provides an estimation of the strength of the stream; it can scarcely be viewed as quantitative.

Another method to assess voiding ability used 8 mm film to measure velocity of the urinary stream [360]. This method experienced some of the more common drawbacks inherent in other routines.

Photography of the urinary stream was later utilized and showed that patients' urinary stream breaks into drops when it leaves the external meatus [361]. By using light-beam interruption methods they measured the volume, and velocity patterns of the drops. Nonetheless this creative technique was used as a tool for urological research and it was used to obtain voiding patterns of normal and obstructed males but it had drawbacks that the rendered result was unsuitable for routine clinical and office use [362]. It did not provide quick outcome, cost and complexity were high, and expertise was required for the translation of the results.

A picture taken in 1906 showed a boy urinating following surgical correction of a congenital urethral anomaly [355]. At that time no urodynamic machine was developed yet and the visual inspection of the still picture served the purpose of demonstrating the good urinary stream just fine.

Researchers advocated a “new” way to help patients to describe their symptoms and encompass a picture (silhouette) of a urinating man with different flow magnitudes in order for the patient to compare his own stream with one of them [191]. Video recording of the patient’s stream live and inspecting it by the urologist is much more realistic, practical and convenient especially if it can be sent by e-mail over the internet to the urologist in his office.

Therefore, the need is evident to find a better way to examine the urine flow during the act of voiding to note its subjective impression direction, force and caliber. By studying previous work, the VVD is capable of monitoring the urine stream with three cameras, which helps the urologist to learn about the force and direction of the urine during its natural flow.

The VVD and its method can be used alone or in conjunction with the traditional urodynamic study devices. This should be an optimal combination to study the act of voiding from all its aspects. VVD can improve evaluation of LUTD treatments by providing subsequent follow-up.

B.4 Materials and Methods

This section describes the overall design and the proposed video processing algorithm and software [363].

Description of the overall experimental set up

The VVD consists of a lightweight plastic booth with LED lights, and video cameras on the left, top, and lower back sides. The left and top cameras are used to visualize urine leakage from the urethral meatus, urine stream trajectory, its break-up into droplets, etc. The lower back camera monitors a cylinder where urine accumulates. Software then processes the change in level of accumulating urine in the cylinder and calculates parameters like the Maximum (Peak) Flow

Rate, Average Flow Rate, and Instantaneous Flow Rate. Figure. 26 shows an overview map of the VVD components divided into hardware and software.

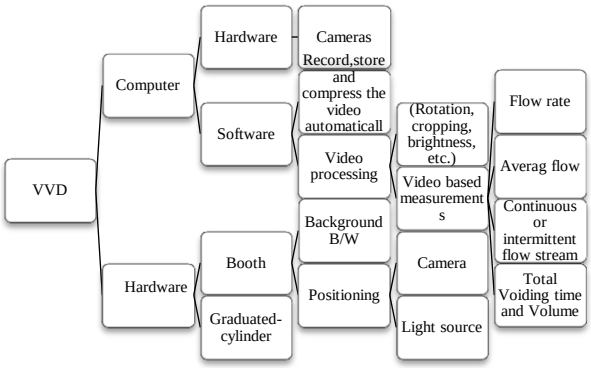

Figure 26, VVD development requires (top) computer hardware and software, cameras, video processing, storage and transmission and (bottom) hardware for the booth, toilet, and graduated cylinder (The part where the patient actually voids (urinates) into)

The VVD has three positioned cameras. The side camera views the urine stream from a 90° horizontal angle on a black background. The top camera views the urine stream from a 90° vertical angle on a black background. The cameras used here were a Logitech c920, which is a digital full HD 1080p pro Webcam, with 20-step autofocus lens. The lower back camera (the cylinder camera) monitors the accumulation of urine into a 1000 ml cylinder. Three G-LUX series 8 W LED Spot Lights illuminate the stream to provide best contrast.

Two LEDs are mounted on the wall facing the patient (above and below the urine stream line of action). One LED is mounted at the top of the right side wall, shedding light from a steep downward orientation/trajectory towards the funnel. The combination of these three LED placements shedding light from three different angles results in complete illumination of the urine stream, ensuring high contrast and visibility.

To use the VVD, the patient stands in front of the device and urinates. The urine is guided by the large 53 cm diameter funnel leading it to the cylinder. The urination is captured

from two angles using two cameras (top and side). The cylinder camera captures the filling process of the cylinder in order to compute the instantaneous flow rate, max flow rate, total voiding time, and total voided volume. (See Fig. 27)

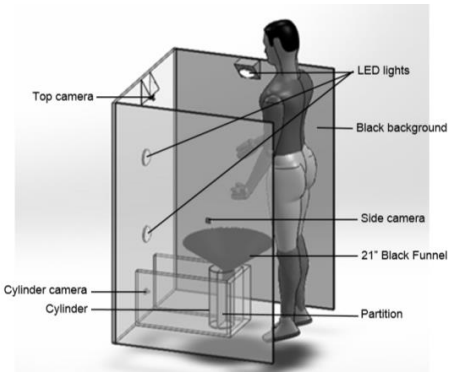

Figure 27. A perspective view of one VVD booth setup illustrating a male patient standing ready to urinate with three cameras monitoring from the side, top, and back (cylinder view).

Description of the developed software

Software was developed using MATLAB to analyze the video recording of the urine accumulating in the cylinder and calculate the instantaneous flow rate, max flow rate, total voiding time, and total voided volume. However, urine can sometimes be clear in color, which makes it very challenging to be traced using a camera. So a blue hollow piece of plastic (floater), which can be recognized by our software, is added at the bottom of the cylinder prior to the voiding process. As urine flows in, the floater floats on the urine surface and rises to keep track of urine level in the cylinder. To help avoid water start-up artifact and any errors in measurement that may arise due to nonuniform graduate cylinder bottoms, the graduate cylinder is prefilled with a predetermined amount of water enough to float the floater [298].

Figure 28 shows the software starts by acquiring the video frames and isolating the cylinder from its surroundings. Each frame is then cropped to only show the middle part of the cylinder. Contrast is enhanced by binarizing the image. After that an algorithm tracks the level of urine in the cylinder and measures the volume at each frame. A series of moving average filters (ranging from 21-term to 3-term moving average) are applied on the graph of volume versus time to smooth it as much as possible without deforming it. As a result, differentiating the volume versus time gives a smooth and precise flow graph without any noisy fluctuations. Both the flow graph and instant flow at each frame are embedded within the video to provide a deeper insight by allowing the urologist to track the flow instantaneously as the patient urinates.

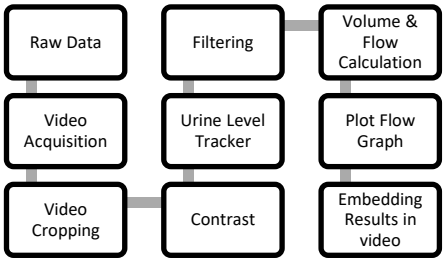

Figure 28. The software acquires the video, processes it, and displays images and flow versus time.

B.5 Results

Performance of the proposed VVD was evaluated by recording and processing 21 bench-testing videos of simulated voiding at the instrumentation laboratory of University of Wisconsin-Madison (described in section 4.1) and 3 clinical-testing videos on volunteer patients at department of urology of King Abdulaziz University, (described in section 4.3).

Method Validation (bench testing)

Method validation is the process that we used to confirm that the analytical and computational procedure employed for our video processing is suitable. Results from method validation were used to judge the quality, reliability and consistency of analytical results.

In order to validate the precision and accuracy of the flow rate measurements based on the video processing approach VVD, a scale was used as a mass flowmeter in an experiment to compare its flow rate measurements to that of the VVD. The experiment was designed so that it simulates human urinary voiding. A water filled balloon was used to simulate the function of a human bladder. As the balloon wall puts pressure on the water inside it, it squeezes out the water through a tube that simulates the urethra. The tube directs the water toward a funnel resting on top of a graduated cylinder and a scale. Data from the VVD camera and mass flowmeter scale are acquired simultaneously (Fig. 29).

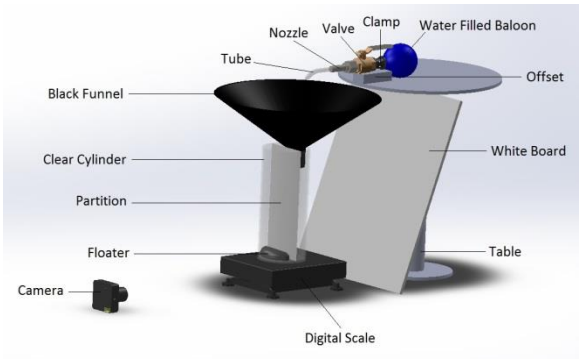

Figure 29. Bench testing setup - A balloon squeezes out a water stream directed by a tube toward a black funnel that guides the stream into a graduated cylinder sitting on a digital scale. The camera monitors the graduated cylinder and records volume versus time, which is used to derive flow versus time. The digital scale (iWeigh-002M-6D-DI100-LV1000 model by Loadstar Sensors) records weight versus time, which is used to derive flow versus time.

The validation experiment was done using 3 accurately measured predetermined volumes of water as a gold standard (100 ml, 300 ml, and 500 ml). To give a reasonable assessment of accuracy and repeatability, for each volume, the validation experiment was repeated 7 times. A method of data plotting, Bland-Altman plot, was used in analyzing the agreement between two

different assays for VVD vs. predetermined volumes and mass flowmeter vs. predetermined volumes, respectively (see Fig. 30&31) [364]. Figure 30.a-c show the mean differences between the predetermined total voided volumes (100 ml, 300 ml, and 500 ml) and the total voided volumes measured by the VVD, a new technique, are 0%, 0.07%, and 0.12%, respectively. A positive mean difference indicates that the VVD tends to give a little bit higher reading of the 95% confidence interval. Figure. 30.d–f show the mean differences between the predetermined total voided volumes (100 ml, 300 ml, and 500 ml).The total voided volumes measured by the mass flowmeter for these three instances are –1.05%, –0.89%, and –1.03%, respectively. A negative mean difference indicates that the mass flowmeter tends to give a little bit lower reading of the 95% confidence interval. However, the fact that at least 95% of the differences, for the VVD and mass flowmeter, are less than two standard deviations and the mean differences are close to zero indicates both systems are repeatable and accurate [364]. Table 8 shows the VVD and mass flowmeter both produce accurate repeatable results.

Table 8 Comparison between VVD and mass flowmeter measurements of predetermined voided volume - 100*(mean ± SD)/ predetermined volume (%)

Predetermined Voided Volumes (ml)	Voided Volume Accuracy - VVD	Voided Volume Accuracy – mass flowmeter
100	100 ± 1.6	99 ± 0.9
300	100.1 ± 0.9	99.1 ± 0.8
500	100.1 ± 0.8	99 ± 0.5

Figure. 31compares flow rate versus time as measured by the VVD and mass flowmeter. It shows that the VVD is comparable to the mass flowmeter, and is able to detect the start and ending points of the voiding period. The maximum flow rate and the overall shape of the voiding periods are relatively close together. As the urine stream descends through the funnel and

graduated cylinder, a delay occurs between the start of voiding and the start of flow rate measurements. However, this delay presents itself as a shift in time of the whole voiding flow graph and so it can be shifted in time to synchronize with the start of voiding.

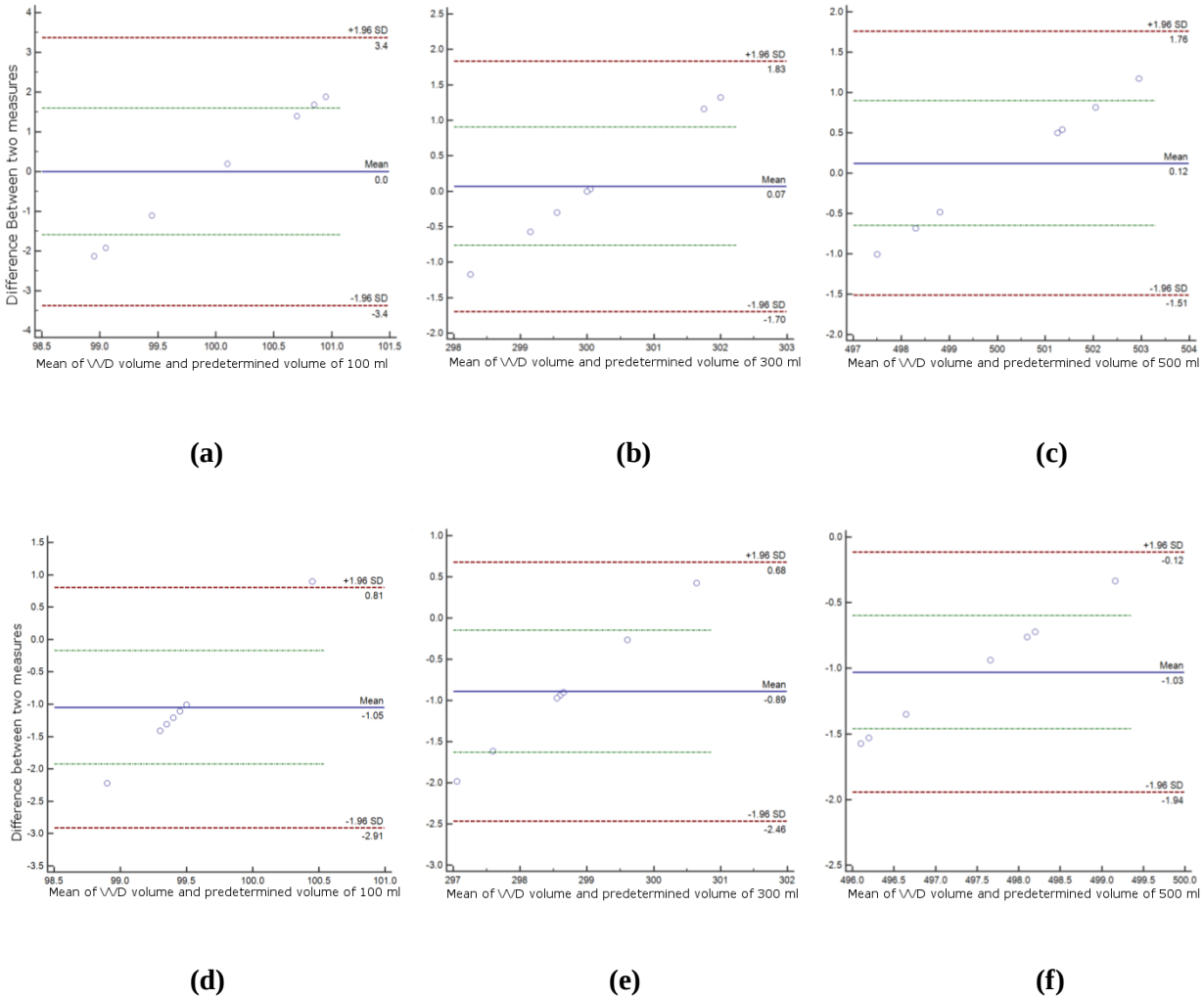

Figure 30. (a)–(c) A Bland-Altman plot showing the difference between the total voided volume measured by the VVD and the true total voided volume of a) 100 ml b) 300 ml c) 500 ml. (d)–(f) A Bland-Altman plot showing the difference between the total voided volume measured by the mass flowmeter and the true total voided volume of d) 100 ml. e) 300 ml f) 500 ml. The green lines represent the 95% confidence interval.

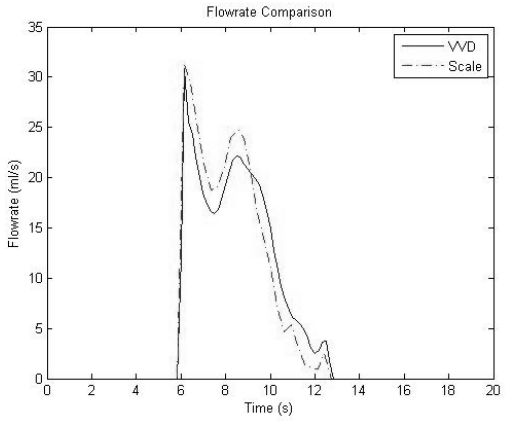

Figure 31. Flow rate versus time as measured by the VVD and scale mass flowmeter.

Measuring VVD Frequency Response

The step response test is used to determine the frequency response of an uroflowmeter. A steady flow using the bottle described in Griffiths *et al* paper was used to measure the frequency response of the first-order system [331]. Due to assumption of a first order system with one time constant τ the measured flow will drop to 37% of its starting value [358]. By using the logarithmic method given in (1) and (2) the calculated cut off frequency of the VVD is equal to 5.5 Hz.

$$\tau = \frac{\Delta t}{\Delta \log_e Q} \qquad (1)$$

$$f_c = \frac{1}{2\pi\tau} \qquad (2)$$

where Q is the flow rate, t is time, and f_c is cut off frequency.

Clinical Testing

Clinical testing was done on 3 male subjects (age 46–65). The feedback from human testing helped significantly in further development and fine tuning of the VVD software. Table 2 shows the results obtained by the VVD software from three recording sessions of three healthy volunteers. The average flow rate was found to be 12.7 ml/s. Similarly, the US National Library

of Medicine (2014) states that the average flow rate in males between the ages of 46 to 65 is 12 ml/s [365]. Figure. 32 shows the VVD software displaying all three cameras plus a live flow graph mid-voiding and post-voiding, respectively. The software also displays the patients name, sex, age, case notes, instantaneous flow rate, max flow rate, average flow rate, voiding time, and voided volume.

Figure 32 Screenshot of the VVD software mid-voiding displaying all three cameras, patient information, uroflowmetry results, and a live flow graph.

Table 9 Clinical testing measurements of 3 healthy volunteers.

Volunteer No.	Max. Flow Rate (ml/s)	Average Flow Rate (ml/s)	Voiding Time (s)	Voided Volume (ml)
1	24.4	16.1	21.9	352.6
2	16.2	7.2	64.6	465.6
3	20.0	14.9	44.8	667.5

B.6 Discussion

The International Continence Society (ICS) technical report recommends the following standards: a range of 0–50 ml/s for Q_{max}, a range of 0–1000 ml for voided volume, maximum time constant of 0.75 s, and an accuracy of ±5% relative to full scale [299]. The VVD is capable

of measuring a range of 0–50 ml/s for Q_{max}, has the capacity to accommodate 1000 ml of voided volume, has a maximum time constant of 0.18 s, and an accuracy of ±2% relative to full scale, thus, satisfying the ICS technical report standards.

The mass flowmeter is capable of measuring a range of 0–50 ml/s for Q_{max}, has the capacity to accommodate 1000 ml of voided volume, has a maximum time constant of 0.21 s, and an accuracy of ±3% relative to full scale. However, for most mass flowmeters, the fluid content and concentration can induce variations in the fluid specific gravity, which directly influence the measured flow rate. For example, urine of high concentration may increase apparent flow rate by 3% [299]. This would lead to an accuracy of 6% relative to full scale, which does not meet the ICS technical report standards. The VVD is not a mass flowmeter, thus, it is not affected by the fluid specific gravity, which makes it a more accurate source of diagnostic information than existing commercial mass flowmeters.

A urologist has tested the VVD and found the following. The main function of the device is unique, has several important clinical values that have not been described before in any other currently available devices. The Video-based Visual Voiding Device (VVD) is expected to simultaneously perform the following:

1. Defining the subjective impression *direction* of the urine flow in relation to the vertical axis of the human body i.e. deviation to the right or left and in relation to the direction of the flaccid penis i.e. upwards and downwards and determination of the degree of the angle of deviation i.e. 15, 20, 30 up to 90° deviation.
2. Recognition of fluid spraying, splitting and *branching* (bifurcation/trifurcation) of the urine stream.

3. Measure/calculate the *total voiding time* in seconds accurately. The voided urine is collected and its volume is measured. The maximum voiding flow rate and the *average voiding flow rate* (total urine volume divided by total voiding time in seconds) are calculated [366].
4. Video recording, documentation and playback of the whole urinary voiding event from two distinct angles.
5. Video recording, documentation and playback of momentarily loss (leak) of urine during coughing, sneezing and laughing, a condition known as *stress urinary incontinence* in males.

Most of the available household and clinical uroflowmeters do not have the ability to record the video of the voiding process for further diagnosis and analysis, which means the voiding test result of these types of devices is only available in the form of charts and graphs. Also, simple visual examination by an expert can give important qualitative information during patient voiding but this process is not recorded for another colleague's review and it is hard for them to note the direction, caliber, etc. of the urine stream. The VVD represents a paradigm shift by integrating quantitative urological parameters with recorded qualitative visual examination, and displays all information in real time on one screen for the expert. (See Table 9)

Table 10 shows the primary differentiation factors of VVD with the previous devices, compares the difference between commercial uroflowmeters, simple visual examination, and the VVD. Commercially available flowmeters, which have generally acceptable accuracy, include the following: 1) Weight transducer flowmeter which weighs the urine voided—measuring the volume of urine voided and hence measuring the urine flow rate by differentiation with respect to time. 2) Ordinary pressure sensor in which the hydrostatic pressure exerted by a column of urine also can be applied to measure the weight of the urine voided, and 3) Rotating disc

flowmeter which has a spinning disc on which urine falls. Although all these available uroflowmeters can measure some urologic parameters accurately, they cannot record other important clinical characteristics of the act of voiding, such as noting the direction of the urine, the urine leakage, and caliber of the urine. Obviously, in certain medical conditions such as obstructed flow of urine and deviated stream, visually observing and studying aforementioned parameters can provide important information for medical diagnosis[355].

Table 10 Comparison of the Uroflowmeters, simple visual examination, and VVD's features

	Commercial Uroflowmeters	**Visual Examination**	**VVD**
Observations	Not accessible	Visual, seen by expert eyes one time	Visual, seen by expert eyes, recorded video footage for further analysis
Accuracy	Generally accurate but varies based on device	Estimation only	Accurate (±2%)
Volume and Stream caliber	Volume is measured in ml; stream caliber cannot be observed	Volume cannot be measured; Caliber is observed by urologist (one time)	Volume is measured in ml; Caliber is observed and recorded
Flow rate and direction	Flow is measured in ml per second; direction cannot be measured	Flow cannot be measured; direction can be observed (one time)	Flow is measured as ml per second; direction is observed and recorded
Urine stream continuity	Charted on graph	Observed by urologist (one time)	Charted on graph while being observed by urologist
Observation angle	Not accessible	Observed by urologist from one angle (one time)	Observed by urologist on the screen from two angles and recorded by VVD for future examination

B.7 Conclusions

The VVD uses lower cost components than existing commercial flowmeters. The estimated total parts cost of the VVD in 2015 is $300 which mainly consists of the 3 cameras and hardware structure. The future cost could be easily reduced based on the new cameras introduced in the market. The new proposed device can couple measuring the instantaneous urological parameters and voiding visual inspection.

We speculate that there is an added value in a video record of the voiding process, especially in urinary incontinence. VVD is a more dignified way of assessing incontinence. In

addition, many voiding behaviors and artefacts would be obvious on a video record. It's not easy to assess this added value of video record, however being able to accurately measure and record urine volumes less than 50 ml, an objective method of quantifying the amount leaked urine during coughing or straining in cases of stress urinary incontinence will be available at hand, no matter how small the leaked volume of urine was. Obviously this will be of value in both the initial diagnosis and assessment of severity of the condition, in order to select a suitable treatment modality as well as in follow-up to assess treatment outcome.

B.8 Acknowledgements

This paper was funded by the Deanship of Scientific Research (DSR), King Abdulaziz University, under grant (HiCi/1433-4-8). World Health Organization (2012) (WHO) states that access of patients to medical devices would increase if third world countries invest in local manufacturing of medical devices [367]. Rise of unemployment rates in Saudi lead policy makers to initiate and support entrepreneurship programs to transfer job seekers to job makers [368]. This strategic goal for Saudi Arabia, lead King Abdulaziz City for Science and Technology (KACST) to launch BADIR, a technical incubation program that supports the establishment of local technical entrepreneurs [191]. In addition, several universities in Saudi Arabia established technical valleys and pushed for patenting the scientific work being done locally within those universities in an effort to push the country's move towards a knowledge based society. In addition, the ministry of higher education encouraged collaboration with international experts to help in technology transfer and localization of technology and this project is one result for collaboration between researchers from King Abdulaziz University, Jeddah, Saudi Arabia and researchers from the University of Wisconsin, Madison USA.

B.9 Ethical approval

"All procedures performed in studies involving human participants were in accordance with the ethical standards of the institutional and/or national research committee and with the 1964 Helsinki declaration and its later amendments or comparable ethical standards."

B.10 Informed consent

"Informed consent was obtained from all individual participants included in the study."

References

[1] A. Xie, M. Teodorescu, D. F. Pegelow, M. C. Teodorescu, Y. Gong, J. E. Fedie*, et al.*, "Effects of stabilizing or increasing respiratory motor outputs on obstructive sleep apnea," *J Appl Physiol (1985),* vol. 115, pp. 22-33, Jul 2013.

[2] J. A. Dempsey, A. Xie, D. S. Patz, and D. Wang, "Physiology in medicine: obstructive sleep apnea pathogenesis and treatment--considerations beyond airway anatomy," *J Appl Physiol (1985),* vol. 116, pp. 3-12, Jan 2014.

[3] R. N. Aurora, S. Chowdhuri, K. Ramar, S. R. Bista, K. R. Casey, C. I. Lamm*, et al.*, "The treatment of central sleep apnea syndromes in adults: practice parameters with an evidence-based literature review and meta-analyses," *Sleep,* vol. 35, pp. 17-40, Jan 2012.

[4] R. N. Aurora, S. R. Bista, K. R. Casey, S. Chowdhuri, D. A. Kristo, J. M. Mallea*, et al.*, "Updated Adaptive Servo-Ventilation Recommendations for the 2012 AASM Guideline: "The Treatment of Central Sleep Apnea Syndromes in Adults: Practice Parameters with an Evidence-Based Literature Review and Meta-Analyses"," *J Clin Sleep Med,* vol. 12, pp. 757-61, 2016.

[5] T. D. Bradley, A. G. Logan, R. J. Kimoff, F. Sériès, D. Morrison, K. Ferguson*, et al.*, "Continuous positive airway pressure for central sleep apnea and heart failure," *N Engl J Med,* vol. 353, pp. 2025-33, Nov 2005.

[6] T. E. Weaver and R. R. Grunstein, "Adherence to continuous positive airway pressure therapy: the challenge to effective treatment," *Proc Am Thorac Soc,* vol. 5, pp. 173-8, Feb 2008.

[7] A. Xie, M. Teodorescu, D. F. Pegelow, M. C. Teodorescu, Y. Gong, J. E. Fedie*, et al.*, "Effects of stabilizing or increasing respiratory motor outputs on obstructive sleep apnea," *Journal of Applied Physiology,* vol. 115, pp. 22-33, 2013.

[8] A. Xie, J. B. Skatrud, and J. A. Dempsey, "Effect of hypoxia on the hypopnoeic and apnoeic threshold for CO2 in sleeping humans," *The Journal of Physiology,* vol. 535, pp. 269-278, 2001.

[9] J. A. Dempsey, S. C. Veasey, B. J. Morgan, and C. P. O'Donnell, "Pathophysiology of sleep apnea," *Physiol Rev,* vol. 90, pp. 47-112, Jan 2010.

[10] E. Kaczmarek, J. P. Bakker, D. N. Clarke, E. Csizmadia, O. Kocher, A. Veves*, et al.*, "Molecular biomarkers of vascular dysfunction in obstructive sleep apnea," *PLoS One,* vol. 8, p. e70559, 2013.

[11] C. Guilleminault and V. C. Abad, "Obstructive Sleep Apnea," *Curr Treat Options Neurol,* vol. 6, pp. 309-317, Jul 2004.

[12] B. A. Edwards, S. A. Sands, D. J. Eckert, D. P. White, J. P. Butler, R. L. Owens*, et al.*, "Acetazolamide improves loop gain but not the other physiological traits causing obstructive sleep apnoea," *J Physiol,* vol. 590, pp. 1199-211, Mar 2012.

[13] A. Wellman, A. Malhotra, A. S. Jordan, K. E. Stevenson, S. Gautam, and D. P. White, "Effect of oxygen in obstructive sleep apnea: role of loop gain," *Respir Physiol Neurobiol,* vol. 162, pp. 144-51, Jul 2008.

[14] D. J. Eckert, D. P. White, A. S. Jordan, A. Malhotra, and A. Wellman, "Defining phenotypic causes of obstructive sleep apnea. Identification of novel therapeutic targets," *Am J Respir Crit Care Med,* vol. 188, pp. 996-1004, Oct 2013.

[15] J. B. Skatrud and J. A. Dempsey, "Interaction of sleep state and chemical stimuli in sustaining rhythmic ventilation," *J Appl Physiol Respir Environ Exerc Physiol,* vol. 55, pp. 813-22, Sep 1983.

[16] C. Iber, S. F. Davies, R. C. Chapman, and M. M. Mahowald, "A possible mechanism for mixed apnea in obstructive sleep apnea," *Chest,* vol. 89, pp. 800-5, Jun 1986.

[17] A. Berssenbrugge, J. Dempsey, C. Iber, J. Skatrud, and P. Wilson, "Mechanisms of hypoxia-induced periodic breathing during sleep in humans," *J Physiol,* vol. 343, pp. 507-24, Oct 1983.

[18] A. Sankari, A. T. Bascom, S. Chowdhuri, and M. S. Badr, "Tetraplegia is a risk factor for central sleep apnea," *J Appl Physiol (1985),* vol. 116, pp. 345-53, Feb 2014.

[19] R. N. Khayat, A. Xie, A. K. Patel, A. Kaminski, and J. B. Skatrud, "Cardiorespiratory effects of added dead space in patients with heart failure and central sleep apnea," *Chest,* vol. 123, pp. 1551-60, May 2003.

[20] A. Xie, F. Rankin, R. Rutherford, and T. D. Bradley, "Effects of inhaled CO2 and added dead space on idiopathic central sleep apnea," *J Appl Physiol (1985),* vol. 82, pp. 918-26, Mar 1997.

[21] G. Lorenzi-Filho, F. Rankin, I. Bies, and T. Douglas Bradley, "Effects of inhaled carbon dioxide and oxygen on cheyne-stokes respiration in patients with heart failure," *Am J Respir Crit Care Med,* vol. 159, pp. 1490-8, May 1999.

[22] M. A. Haxhiu, E. van Lunteren, J. Mitra, and N. S. Cherniack, "Comparison of the response of diaphragm and upper airway dilating muscle activity in sleeping cats," *Respir Physiol,* vol. 70, pp. 183-93, Nov 1987.

[23] R. L. Horner, X. Liu, H. Gill, P. Nolan, H. Liu, and S. Sood, "Effects of sleep-wake state on the genioglossus vs.diaphragm muscle response to CO(2) in rats," *J Appl Physiol (1985),* vol. 92, pp. 878-87, Feb 2002.

[24] G. Warner, J. B. Skatrud, and J. A. Dempsey, "Effect of hypoxia-induced periodic breathing on upper airway obstruction during sleep," *J Appl Physiol (1985),* vol. 62, pp. 2201-11, Jun 1987.

[25] M. S. Badr, J. B. Skatrud, and J. A. Dempsey, "Effect of chemoreceptor stimulation and inhibition on total pulmonary resistance in humans during NREM sleep," *J Appl Physiol (1985),* vol. 76, pp. 1682-92, Apr 1994.

[26] G. S. Gilmartin, R. W. Daly, and R. J. Thomas, "Recognition and management of complex sleep-disordered breathing," *Curr Opin Pulm Med,* vol. 11, pp. 485-93, Nov 2005.

[27] R. J. Thomas, "Effect of added dead space to positive airway pressure for treatment of complex sleep-disordered breathing," *Sleep Med,* vol. 6, pp. 177-8, Mar 2005.

[28] S. Kuna, J. Gillen, and S. Levine, "Effects of respiratory gases on the frequency and duration of obstructive apneic episodes in a patient with the sleep apnea-hypersomnolence syndrome," *Respiration,* vol. 43, pp. 108-13, 1982.

[29] Y. Fukuda, A. Sato, A. Suzuki, and A. Trzebski, "Autonomic nerve and cardiovascular responses to changing blood oxygen and carbon dioxide levels in the rat," *J Auton Nerv Syst,* vol. 28, pp. 61-74, Oct 1989.

[30] M. Tanaka, S. Takaishi, and Y. Honda, "Carbon dioxide-heart rate responses during hyperoxia, euoxia, and hypoxia," *Jpn J Physiol,* vol. 39, pp. 703-12, 1989.

[31] T. Suutarinen, "Cardiovascular response to changes in arterial carbon dioxide tension. An experimental study on thoractomized dogs," *Acta Physiol Scand Suppl,* vol. 266, pp. 1-76, 1966.

[32] K. Gleeson, C. W. Zwillich, and D. P. White, "The influence of increasing ventilatory effort on arousal from sleep," *Am Rev Respir Dis,* vol. 142, pp. 295-300, Aug 1990.

[33] J. B. Dean, "Hypercapnia causes cellular oxidation and nitrosation in addition to acidosis: implications for CO2 chemoreceptor function and dysfunction," *J Appl Physiol (1985),* vol. 108, pp. 1786-95, Jun 2010.

[34] K. J. Reichmuth, J. M. Dopp, S. R. Barczi, J. B. Skatrud, P. Wojdyla, D. Hayes*, et al.*, "Impaired vascular regulation in patients with obstructive sleep apnea: effects of continuous positive airway pressure treatment," *Am J Respir Crit Care Med,* vol. 180, pp. 1143-50, Dec 2009.

[35] B. J. Morgan, K. J. Reichmuth, P. E. Peppard, L. Finn, S. R. Barczi, T. Young*, et al.*, "Effects of sleep-disordered breathing on cerebrovascular regulation: A population-based study," *Am J Respir Crit Care Med,* vol. 182, pp. 1445-52, Dec 2010.

[36] M. T. Naughton, "Cheyne-Stokes respiration: friend or foe?," *Thorax,* vol. 67, pp. 357-60, Apr 2012.

[37] I. Szollosi, M. Jones, M. J. Morrell, K. Helfet, A. J. Coats, and A. K. Simonds, "Effect of CO2 inhalation on central sleep apnea and arousals from sleep," *Respiration,* vol. 71, pp. 493-8, Sep-Oct 2004.

[38] R. D. Steens, T. W. Millar, X. Su, D. Biberdorf, P. Buckle, M. Ahmed*, et al.*, "Effect of inhaled 3% CO2 on Cheyne-Stokes respiration in congestive heart failure," *Sleep,* vol. 17, pp. 61-8, Feb 1994.

[39] P. E. Peppard, T. Young, J. H. Barnet, M. Palta, E. W. Hagen, and K. M. Hla, "Increased prevalence of sleep-disordered breathing in adults," *American journal of epidemiology,* p. kws342, 2013.

[40] T. Young, P. E. Peppard, and D. J. Gottlieb, "Epidemiology of obstructive sleep apnea: a population health perspective," *American journal of respiratory and critical care medicine,* vol. 165, pp. 1217-1239, 2002.

[41] T. I. Morgenthaler, V. Kagramanov, V. Hanak, and P. A. Decker, "Complex sleep apnea syndrome: is it a unique clinical syndrome?," *SLEEP-NEW YORK THEN WESTCHESTER-,* vol. 29, p. 1203, 2006.

[42] D. J. Gottlieb, G. Yenokyan, A. B. Newman, G. T. O'Connor, N. M. Punjabi, S. F. Quan*, et al.*, "Prospective study of obstructive sleep apnea and incident coronary heart disease and heart failure the sleep heart health study," *Circulation,* vol. 122, pp. 352-360, 2010.

[43] S. J. Durning, V. F. Capaldi II, A. R. Artino Jr, J. Graner, C. van der Vleuten, T. J. Beckman*, et al.*, "A pilot study exploring the relationship between internists' self-reported sleepiness, performance on multiple-choice exam items and prefrontal cortex activity," *Medical teacher,* vol. 36, pp. 434-440, 2014.

[44] J. L. Hossain and C. M. Shapiro, "The prevalence, cost implications, and management of sleep disorders: an overview," *Sleep and Breathing,* vol. 6, pp. 85-102, 2002.

[45] H. J. Cho, H. Lavretsky, R. Olmstead, M. J. Levin, M. N. Oxman, and M. R. Irwin, "Sleep disturbance and depression recurrence in community-dwelling older adults: a prospective study," *American Journal of Psychiatry,* 2008.

[46] K. Wulff, D.-J. Dijk, B. Middleton, R. G. Foster, and E. M. Joyce, "Sleep and circadian rhythm disruption in schizophrenia," *The British Journal of Psychiatry,* vol. 200, pp. 308-316, 2012.

[47] M. Bruyneel, C. Sanida, G. Art, W. Libert, L. Cuvelier, M. Paesmans*, et al.*, "Sleep efficiency during sleep studies: results of a prospective study comparing home-based and in-hospital polysomnography," *Journal of sleep research,* vol. 20, pp. 201-206, 2011.

[48] J. F. Masa, J. Corral, R. Pereira, J. Duran-Cantolla, M. Cabello, L. Hernández-Blasco*, et al.*, "Effectiveness of home respiratory polygraphy for the diagnosis of sleep apnoea and hypopnoea syndrome," *Thorax,* p. thx. 2010.152272, 2011.

[49] D. Leger, V. Bayon, J. P. Laaban, and P. Philip, "Impact of sleep apnea on economics," *Sleep medicine reviews,* vol. 16, pp. 455-462, 2012.

[50] A. Mulchrone, M. Shokoueinejad, and J. Webster, "A review of preventing central sleep apnea by inspired CO 2," *Physiological Measurement,* vol. 37, p. R36, 2016.

[51] A. Sassani, L. J. Findley, M. Kryger, E. Goldlust, C. George, and T. M. Davidson, "Reducing motor-vehicle collisions, costs, and fatalities by treating obstructive sleep apnea syndrome," *SLEEP-NEW YORK THEN WESTCHESTER-,* vol. 27, pp. 453-458, 2004.

[52] W. K. Wohlgemuth, D. A. Chirinos, S. Domingo, and D. M. Wallace, "Attempters, adherers, and non-adherers: Latent profile analysis of CPAP use with correlates," *Sleep medicine,* vol. 16, pp. 336-342, 2015.

[53] T. Penzel and R. Conradt, "Computer based sleep recording and analysis," *Sleep Medicine Reviews,* vol. 4, pp. 131-148, 4// 2000.

[54] R. Ferber, R. Millman, M. Coppola, J. Fleetham, C. F. Murray, C. Iber*, et al.*, "Portable recording in the assessment of obstructive sleep apnea. ASDA standards of practice," *Sleep,* vol. 17, pp. 378-392, 1994.

[55] R. Peslin and C. Duvivier, "Partitioning of airway and respiratory tissue mechanical impedances by body plethysmography," *Journal of Applied Physiology,* vol. 84, pp. 553-561, 1998.
[56] J. Webster, *Medical instrumentation: application and design*: John Wiley & Sons, 2014.
[57] J. Ehrenwerth, J. B. Eisenkraft, and J. M. Berry, *Anesthesia equipment, principles and applications (expert consult: online and print), 2: anesthesia equipment*: Elsevier Health Sciences, 2013.
[58] M. Ardekani and M. M. Motlagh, "Ordinary hot-wire/hot-film method for spirography application," *Measurement,* vol. 43, pp. 31-38, 2010.
[59] M. Shokoueinejad, C. Fernandez, E. Carroll, F. Wang, J. Levin, S. Rusk*, et al.*, "Sleep apnea: a review of diagnostic sensors, algorithms, and therapies " *Physiological measurement,* 2017.
[60] R. G. Norman, M. M. Ahmed, J. A. Walsleben, and D. M. Rapoport, "Detection of respiratory events during NPSG: nasal cannula/pressure sensor versus thermistor," *Sleep,* vol. 20, pp. 1175-1184, 1997.
[61] H. Teichtahl, D. Cunnington, G. Cherry, and D. Wang, "Scoring polysomnography respiratory events: the utility of nasal pressure and oro-nasal thermal sensor recordings," *Sleep medicine,* vol. 4, pp. 419-425, 2003.
[62] J. M. Montserrat, R. Farré, E. Ballester, M. A. Felez, M. Pastó, and D. Navajas, "Evaluation of nasal prongs for estimating nasal flow," *American journal of respiratory and critical care medicine,* vol. 155, pp. 211-215, 1997.
[63] R. B. Berry, G. L. Koch, S. Trautz, and M. H. Wagner, "Comparison of respiratory event detection by a polyvinylidene fluoride film airflow sensor and a pneumotachograph in sleep apnea patients," *CHEST Journal,* vol. 128, pp. 1331-1338, 2005.
[64] S. Berg, J. Haight, V. Yap, V. Hoffstein, and P. Cole, "Comparison of direct and indirect measurements of respiratory airflow: implications for hypopneas," *Sleep,* vol. 20, pp. 60-64, 1997.
[65] R. Farre, J. Rigau, J. M. Montserrat, E. Ballester, and D. Navajas, "Relevance of linearizing nasal prongs for assessing hypopneas and flow limitation during sleep," *American journal of respiratory and critical care medicine,* vol. 163, pp. 494-497, 2001.
[66] P. A. Bradley, I. L. Mortimore, and N. J. Douglas, "Comparison of polysomnography with ResCare Autoset in the diagnosis of the sleep apnoea/hypopnoea syndrome," *Thorax,* vol. 50, pp. 1201-1203, 1995.
[67] J. Kiely, C. Delahunty, S. Matthews, and W. McNicholas, "Comparison of a limited computerized diagnostic system (ResCare Autoset) with polysomnography in the diagnosis of obstructive sleep apnoea syndrome," *European Respiratory Journal,* vol. 9, pp. 2360-2364, 1996.
[68] K. Rees, P. Wraith, M. Berthon-Jones, and N. Douglas, "Detection of apnoeas, hypopnoeas and arousals by the AutoSet in the sleep apnoea/hypopnoea syndrome," *European Respiratory Journal,* vol. 12, pp. 764-769, 1998.
[69] L. Hernández, E. Ballester, R. Farré, J. R. Badia, R. Lobelo, D. Navajas*, et al.*, "Performance of nasal prongs in sleep studies: spectrum of flow-related events," *Chest,* vol. 119, pp. 442-450, 2001.
[70] P. Mayer, J. Meurice, F. Philip-Joet, A. Cornette, D. Rakotonanahary, N. Meslier*, et al.*, "Simultaneous laboratory-based comparison of ResMed Autoset with polysomnography in the diagnosis of sleep apnoea/hypopnoea syndrome," *European Respiratory Journal,* vol. 12, pp. 770-775, 1998.
[71] B. Fleury, D. Rakotonanahary, C. Hausser-Hauw, B. Lebeau, and C. Guilleminault, "A laboratory validation study of the diagnostic mode of the Autoset system for sleep-related respiratory disorders," *Sleep,* vol. 19, pp. 502-505, 1996.

[72] R. Thurnheer, X. Xie, and K. E. Bloch, "Accuracy of nasal cannula pressure recordings for assessment of ventilation during sleep," *American journal of respiratory and critical care medicine,* vol. 164, pp. 1914-1919, 2001.

[73] M. Kryger, T. Eiken, and L. Qin, "The use of combined thermal/pressure polyvinylidene fluoride film airflow sensor in polysomnography," *Sleep and Breathing,* vol. 17, pp. 1267-1273, 2013.

[74] H. L. Watson, D. A. Poole, and M. A. Sackner, "Accuracy of respiratory inductive plethysmographic cross-sectional areas," *Journal of Applied Physiology,* vol. 65, pp. 306-308, 1988.

[75] Z. Zhang, J. Zheng, H. Wu, W. Wang, B. Wang, and H. Liu, "Development of a respiratory inductive plethysmography module supporting multiple sensors for wearable systems," *Sensors,* vol. 12, pp. 13167-13184, 2012.

[76] H. Gonzalez, B. Haller, H. L. Watson, and M. A. Sackner, "Accuracy of Respiratory Inductive Plethysmograph over Wide Range of Rib Cage and Abdominal Compartmental Contributions to Tidal Volume in Normal Subjects and in Patients with Chronic Obstructive Pulmonary Disease 1–3," *American Review of Respiratory Disease,* vol. 130, pp. 171-174, 1984.

[77] W. Grimm and U. Koehler, "Cardiac arrhythmias and sleep-disordered breathing in patients with heart failure," *International journal of molecular sciences,* vol. 15, pp. 18693-18705, 2014.

[78] M. Vegfors, H. Ugnell, B. Hok, P. Oberg, and C. Lennmarken, "Experimental evaluation of two new sensors for respiratory rate monitoring," *Physiological measurement,* vol. 14, p. 171, 1993.

[79] T. Gordh, N. Rawal, S. Ström, and B. Hök, "Respiratory monitoring during postoperative analgesia," *Journal of clinical monitoring,* vol. 11, pp. 365-372, 1995.

[80] A. Roebuck, V. Monasterio, E. Gederi, M. Osipov, J. Behar, A. Malhotra*, et al.*, "A review of signals used in sleep analysisThis review article is dedicated to the memory of Joe Mietus, who spent his life in the service of cardiorespiratory analysis, often with a focus in the field of sleep. His friendship, hard work, persistence and exceptional skills will be sadly missed," *Physiological measurement,* vol. 35, p. R1, 2013.

[81] C. M. Rembold and P. M. Suratt, "Children with obstructive sleep-disordered breathing generate high-frequency inspiratory sounds during sleep," *SLEEP-NEW YORK THEN WESTCHESTER-,* vol. 27, pp. 1154-1162, 2004.

[82] C. M. Rembold and P. M. Suratt, "Airway turbulence and changes in upper airway hydraulic diameter can be estimated from the intensity of high frequency inspiratory sounds in sleeping adults," *The Journal of physiology,* vol. 592, pp. 3831-3839, 2014.

[83] M. A. Ramsay, M. Usman, E. Lagow, M. Mendoza, E. Untalan, and E. De Vol, "The accuracy, precision and reliability of measuring ventilatory rate and detecting ventilatory pause by rainbow acoustic monitoring and capnometry," *Anesthesia & Analgesia,* vol. 117, pp. 69-75, 2013.

[84] Y. Takemura, J.-y. Sato, and M. Nakajima, "A respiratory movement monitoring system using fiber-grating vision sensor for diagnosing sleep apnea syndrome," *Optical review,* vol. 12, pp. 46-53, 2005.

[85] R. Nandakumar, S. Gollakota, and N. Watson, "Contactless sleep apnea detection on smartphones," in *Proceedings of the 13th Annual International Conference on Mobile Systems, Applications, and Services*, 2015, pp. 45-57.

[86] A. Magnan, F. Philip-Joet, M. Rey, M. Reynaud, F. Porri, and A. Arnaud, "End-tidal CO 2 Analysis in Sleep Apnea Syndrome: Conditions for Use," *Chest,* vol. 103, pp. 129-131, 1993.

[87] R. B. Berry, R. Brooks, C. E. Gamaldo, S. Hardling, C. Marcus, and B. Vaughn, "The AASM Manual for the Scoring of Sleep and Associated Events," *Rules, Terminology and Technical Specifications, Darien, Illinois, American Academy of Sleep Medicine,* 2012.

[88] P. Eberhard, "The design, use, and results of transcutaneous carbon dioxide analysis: current and future directions," *Anesthesia & Analgesia,* vol. 105, pp. S48-S52, 2007.

[89] W. W. Flemons, M. R. Littner, J. A. Rowley, P. Gay, W. M. Anderson, D. W. Hudgel*, et al.*, "Home diagnosis of sleep apnea: a systematic review of the literature: an evidence review cosponsored by the American Academy of Sleep Medicine, the American College of Chest Physicians, and the American Thoracic Society," *CHEST Journal,* vol. 124, pp. 1543-1579, 2003.

[90] T. Hayakawa, M. Terashima, Y. Kayukawa, T. Ohta, and T. Okada, "Changes in cerebral oxygenation and hemodynamics during obstructive sleep apneas," *CHEST Journal,* vol. 109, pp. 916-921, 1996.

[91] J. D. Tobias, "Cerebral oximetry monitoring with near infrared spectroscopy detects alterations in oxygenation before pulse oximetry," *Journal of intensive care medicine,* 2008.

[92] A. Keikhosravi, E. Zahedi, H. M. Attar, and H. Aghajani, "Experimental investigation of the roles of blood volume and density in finger photoplethysmography," *IEEE Sensors Journal,* vol. 13, pp. 1397-1398, 2013.

[93] M. Ghamari, C. Aguilar, C. Soltanpur, and H. Nazeran, "Rapid Prototyping of a Smart Device-Based Wireless Reflectance Photoplethysmograph," in *2016 32nd Southern Biomedical Engineering Conference (SBEC)*, 2016, pp. 175-176.

[94] U. A. Leuenberger, J. C. Hardy, M. D. Herr, K. S. Gray, and L. I. Sinoway, "Hypoxia augments apnea-induced peripheral vasoconstriction in humans," *Journal of Applied Physiology,* vol. 90, pp. 1516-1522, 2001.

[95] V. K. Somers, M. E. Dyken, M. P. Clary, and F. M. Abboud, "Sympathetic neural mechanisms in obstructive sleep apnea," *Journal of Clinical Investigation,* vol. 96, p. 1897, 1995.

[96] M. Nitzan, A. Babchenko, B. Khanokh, and D. Landau, "The variability of the photoplethysmographic signal-a potential method for the evaluation of the autonomic nervous system," *Physiological measurement,* vol. 19, p. 93, 1998.

[97] F. Roche, J.-M. Gaspoz, P. Minini, V. Pichot, D. Duverney, F. Costes*, et al.*, "Screening of obstructive sleep apnea syndrome by heart rate variability analysis," *Circulation,* vol. 100, pp. 1411-1415, 1999.

[98] T. Shiomi, C. Guilleminault, R. Sasanabe, I. Hirota, M. Maekawa, and T. Kobayashi, "Augmented very low frequency component of heart rate variability during obstructive sleep apnea," *Sleep,* vol. 19, pp. 370-377, 1996.

[99] N. Meziane, S. Yang, M. Shokoueinejad, J. Webster, M. Attari, and H. Eren, "Simultaneous comparison of 1 gel with 4 dry electrode types for electrocardiography," *Physiological measurement,* vol. 36, p. 513, 2015.

[100] H. Al-Angari, "Evaluation of chin EMG activity at sleep onset and termination in obstructive sleep apnea syndrome," in *2008 Computers in Cardiology*, 2008, pp. 677-679.

[101] W. S. Mezzanotte, D. J. Tangel, and D. P. White, "Waking genioglossal electromyogram in sleep apnea patients versus normal controls (a neuromuscular compensatory mechanism)," *Journal of Clinical Investigation,* vol. 89, p. 1571, 1992.

[102] M. G. Terzano, L. Parrino, M. Boselli, M. C. Spaggiari, and G. Di Giovanni, "Polysomnographic analysis of arousal responses in obstructive sleep apnea syndrome by means of the cyclic alternating pattern," *Journal of clinical neurophysiology,* vol. 13, pp. 145-155, 1996.

[103] E. Svanborg and C. Guilleminault, "EEG frequency changes during sleep apneas," *Sleep,* vol. 19, pp. 248-254, 1996.

[104] W. R. Ruehland, F. J. O'Donoghue, R. J. Pierce, A. T. Thornton, P. Singh, J. M. Copland*, et al.*, "The 2007 AASM recommendations for EEG electrode placement in polysomnography: impact on sleep and cortical arousal scoring," *Sleep,* vol. 34, pp. 73-81, 2011.

[105] C. Iber, *The AASM manual for the scoring of sleep and associated events: rules, terminology and technical specifications*: American Academy of Sleep Medicine, 2007.
[106] D. J. Eckert and A. Malhotra, "Pathophysiology of Adult Obstructive Sleep Apnea," *Proceedings of the American Thoracic Society,* vol. 5, pp. 144-153, 07/31/received

08/22/accepted 2008.
[107] C. Griffiths, B. Cooper, and G. Gibson, "A video system for investigating breathing disorders during sleep," *Thorax,* vol. 46, pp. 136-140, 1991.
[108] Y. Sivan, A. Kornecki, and T. Schonfeld, "Screening obstructive sleep apnoea syndrome by home videotape recording in children," *European Respiratory Journal,* vol. 9, pp. 2127-2131, 1996.
[109] T. F. Anders and A. M. Sostek, "The Use of Time Lapse Video Recording of Sleep-Wake Behavior in Human Infants," *Psychophysiology,* vol. 13, pp. 155-158, 1976.
[110] R. Silvestri, A. Gagliano, I. Aricò, T. Calarese, C. Cedro, O. Bruni*, et al.*, "Sleep disorders in children with Attention-Deficit/Hyperactivity Disorder (ADHD) recorded overnight by video-polysomnography," *Sleep medicine,* vol. 10, pp. 1132-1138, 2009.
[111] R. B. Berry, R. Budhiraja, D. J. Gottlieb, D. Gozal, C. Iber, V. K. Kapur*, et al.*, "Rules for scoring respiratory events in sleep: update of the 2007 AASM manual for the scoring of sleep and associated events," *J Clin Sleep Med,* vol. 8, pp. 597-619, 2012.
[112] R. M. Benca, *Sleep Disorders: The Clinician's Guide to Diagnosis and Management*: Oxford University Press, 2012.
[113] R. S. Rosenberg and S. Van Hout, "The American Academy of Sleep Medicine inter-scorer reliability program: sleep stage scoring," *J Clin Sleep Med,* vol. 9, pp. 81-87, 2013.
[114] R. S. Rosenberg and S. Van Hout, "The American Academy of Sleep Medicine inter-scorer reliability program: respiratory events," *Journal of clinical sleep medicine: JCSM: official publication of the American Academy of Sleep Medicine,* vol. 10, p. 447, 2014.
[115] M. Cabrero-Canosa, E. Hernandez-Pereira, and V. Moret-Bonillo, "Intelligent diagnosis of sleep apnea syndrome," *Engineering in Medicine and Biology Magazine, IEEE,* vol. 23, pp. 72-81, 2004.
[116] A. Malhotra, M. Younes, S. T. Kuna, R. Benca, C. A. Kushida, J. Walsh*, et al.*, "Performance of an automated polysomnography scoring system versus computer-assisted manual scoring," *Sleep,* vol. 36, pp. 573-582, 2013.
[117] S. T. Kuna, R. Benca, C. A. Kushida, J. Walsh, M. Younes, B. Staley*, et al.*, "Agreement in computer-assisted manual scoring of polysomnograms across sleep centers," *Sleep,* vol. 36, pp. 583-589, 2013.
[118] P. Anderer, G. Gruber, S. Parapatics, M. Woertz, T. Miazhynskaia, G. Klösch*, et al.*, "An E-health solution for automatic sleep classification according to Rechtschaffen and Kales: validation study of the Somnolyzer 24× 7 utilizing the Siesta database," *Neuropsychobiology,* vol. 51, pp. 115-133, 2005.
[119] P. Anderer, A. Moreau, M. Woertz, M. Ross, G. Gruber, S. Parapatics*, et al.*, "Computer-assisted sleep classification according to the standard of the American Academy of Sleep Medicine: validation study of the AASM version of the Somnolyzer 24× 7," *Neuropsychobiology,* vol. 62, pp. 250-264, 2010.
[120] D. Alvarez-Estevez and V. Moret-Bonillo, "Computer-Assisted Diagnosis of the Sleep Apnea-Hypopnea Syndrome: A Review," *Sleep disorders,* vol. 2015, 2015.
[121] B. Şen, M. Peker, A. Çavuşoğlu, and F. V. Çelebi, "A Comparative Study on Classification of Sleep Stage Based on EEG Signals Using Feature Selection and Classification Algorithms," *Journal of Medical Systems,* vol. 38, pp. 1-21, 2014.
[122] M. Ronzhina, O. Janoušek, J. Kolářová, M. Nováková, P. Honzík, and I. Provazník, "Sleep scoring using artificial neural networks," *Sleep medicine reviews,* vol. 16, pp. 251-263, 2012.

[123] O. Kocak, A. Erdamar, L. Ozparlak, O. Erogul, T. Bayrak, and Z. Telatar, *Automated detection and classification of sleep apnea types using electrocardiogram (ECG) and electroencephalogram (EEG) features*: INTECH Open Access Publisher, 2012.

[124] A. H. Khandoker, J. Gubbi, and M. Palaniswami, "Automated scoring of obstructive sleep apnea and hypopnea events using short-term electrocardiogram recordings," *Information Technology in Biomedicine, IEEE Transactions on,* vol. 13, pp. 1057-1067, 2009.

[125] A. Krakovská and K. Mezeiová, "Automatic sleep scoring: A search for an optimal combination of measures," *Artificial intelligence in medicine,* vol. 53, pp. 25-33, 2011.

[126] S.-F. Liang, C.-E. Kuo, Y.-H. Hu, Y.-H. Pan, and Y.-H. Wang, "Automatic stage scoring of single-channel sleep EEG by using multiscale entropy and autoregressive models," *Instrumentation and Measurement, IEEE Transactions on,* vol. 61, pp. 1649-1657, 2012.

[127] K. T. Sweeney, E. Mitchell, J. Gaughran, T. Kane, R. Costello, S. Coyle*, et al.*, "Identification of sleep apnea events using discrete wavelet transform of respiration, ecg and accelerometer signals," in *2013 IEEE International Conference on Body Sensor Networks*, 2013, pp. 1-6.

[128] G. Garg, V. Singh, J. Gupta, A. Mittal, and S. Chandra, "Computer assisted automatic sleep scoring system using relative wavelet energy based neuro fuzzy model," *WSEAS Transactions on Biology and Biomedicine,* vol. 8, pp. 12-24, 2011.

[129] L. Fraiwan, K. Lweesy, N. Khasawneh, H. Wenz, and H. Dickhaus, "Automated sleep stage identification system based on time–frequency analysis of a single EEG channel and random forest classifier," *Computer methods and programs in biomedicine,* vol. 108, pp. 10-19, 2012.

[130] E. Kaimakamis, C. Bratsas, L. Sichletidis, C. Karvounis, and N. Maglaveras, "Screening of patients with Obstructive Sleep Apnea Syndrome using C4. 5 algorithm based on non linear analysis of respiratory signals during sleep," in *Engineering in Medicine and Biology Society, 2009. EMBC 2009. Annual International Conference of the IEEE*, 2009, pp. 3465-3469.

[131] K. Karandikar, T. Q. Le, A. Sa-ngasoongsong, W. Wongdhamma, and S. T. Bukkapatnam, "Detection of sleep apnea events via tracking nonlinear dynamic cardio-respiratory coupling from electrocardiogram signals," in *Neural Engineering (NER), 2013 6th International IEEE/EMBS Conference on*, 2013, pp. 1358-1361.

[132] P. Dagum and A. Galper, "Forecasting sleep apnea with dynamic network models," in *Proceedings of the Ninth international conference on Uncertainty in artificial intelligence*, 1993, pp. 64-71.

[133] U. R. Acharya, E. C.-P. Chua, K. C. Chua, L. C. Min, and T. Tamura, "Analysis and automatic identification of sleep stages using higher order spectra," *International journal of neural systems,* vol. 20, pp. 509-521, 2010.

[134] L.-F. Chen, C.-T. Su, K.-H. Chen, and P.-C. Wang, "Particle swarm optimization for feature selection with application in obstructive sleep apnea diagnosis," *Neural Computing and Applications,* vol. 21, pp. 2087-2096, 2012.

[135] S. Reisch, J. Daniuk, H. Steltner, K.-H. Rühle, J. Timmer, and J. Guttmann, "Detection of sleep apnea with the forced oscillation technique compared to three standard polysomnographic signals," *Respiration,* vol. 67, pp. 518-525, 2000.

[136] B. Taha, J. Dempsey, S. Weber, M. Badr, J. Skatrud, T. Young*, et al.*, "Automated detection and classification of sleep-disordered breathing from conventional polysomnography data," *Sleep,* vol. 20, pp. 991-1001, 1997.

[137] H. Steltner, R. Staats, J. Timmer, M. Vogel, J. Guttmann, H. Matthys*, et al.*, "Diagnosis of sleep apnea by automatic analysis of nasal pressure and forced oscillation impedance," *American journal of respiratory and critical care medicine,* vol. 165, pp. 940-944, 2002.

[138] T. Ning and J. Bronzino, "Autoregressive and bispectral analysis techniques: EEG applications," *Engineering in Medicine and Biology Magazine, IEEE,* vol. 9, pp. 47-50, 1990.

[139] S.-F. Liang, C.-E. Kuo, Y.-H. Hu, Y.-H. Pan, and Y.-H. Wang, "Automatic stage scoring of single-channel sleep EEG by using multiscale entropy and autoregressive models," *IEEE Transactions on Instrumentation and Measurement,* vol. 61, pp. 1649-1657, 2012.

[140] V. Vapnik, *The nature of statistical learning theory*: Springer Science & Business Media, 2013.

[141] H. M. Al-Angari and A. V. Sahakian, "Automated recognition of obstructive sleep apnea syndrome using support vector machine classifier," *Information Technology in Biomedicine, IEEE Transactions on,* vol. 16, pp. 463-468, 2012.

[142] F. Chapotot and G. Becq, "Automated sleep–wake staging combining robust feature extraction, artificial neural network classification, and flexible decision rules," *International Journal of Adaptive Control and Signal Processing,* vol. 24, pp. 409-423, 2010.

[143] L. Fraiwan, N. Khaswaneh, and K. Lweesy, "Automatic sleep stage scoring with wavelet packets based on single EEG recording," *Proceedings World Academy of Science, Engineering and Technology, Paris,* vol. 54, pp. 385-488, 2009.

[144] A. A. EI-Solh, M. J. Mador, E. Ten—Brock, D. W. Shucard, M. Abul-Khoudoud, and B. J. Grant, "Validity of neural network in sleep apnea," *Sleep,* vol. 22, p. 1, 1999.

[145] A. Flexer, G. Gruber, and G. Dorffner, "A reliable probabilistic sleep stager based on a single EEG signal," *Artificial Intelligence in Medicine,* vol. 33, pp. 199-207, 2005.

[146] R. A. Teferra, B. J. Grant, J. W. Mindel, T. A. Siddiqi, I. H. Iftikhar, F. Ajaz*, et al.*, "Cost minimization using an artificial neural network sleep apnea prediction tool for sleep studies," *Annals of the American Thoracic Society,* vol. 11, pp. 1064-1074, 2014.

[147] P. Várady, T. Micsik, S. Benedek, and Z. Benyó, "A novel method for the detection of apnea and hypopnea events in respiration signals," *Biomedical Engineering, IEEE Transactions on,* vol. 49, pp. 936-942, 2002.

[148] D. Álvarez-Estévez and V. Moret-Bonillo, "Fuzzy reasoning used to detect apneic events in the sleep apnea-hypopnea syndrome," *Expert Systems with Applications,* vol. 36, pp. 7778-7785, 2009.

[149] L. AZadeh, "Fuzzy sets" information and Control, vol. 8," 1965.

[150] H. Nazeran, A. Almas, K. Behbehani, J. Burk, and E. Lucas, "A fuzzy inference system for detection of obstructive sleep apnea," in *Engineering in Medicine and Biology Society, 2001. Proceedings of the 23rd Annual International Conference of the IEEE*, 2001, pp. 1645-1648 vol.2.

[151] K. M. Al-Ashmouny, A. A. Morsy, and S. F. Loza, "Sleep apnea detection and classification using fuzzy logic: clinical evaluation," in *Engineering in Medicine and Biology Society, 2005. IEEE-EMBS 2005. 27th Annual International Conference of the*, 2006, pp. 6132-6135.

[152] M. Längkvist, L. Karlsson, and A. Loutfi, "Sleep stage classification using unsupervised feature learning," *Advances in Artificial Neural Systems,* vol. 2012, p. 5, 2012.

[153] J. Zhang, Y. Wu, J. Bai, and F. Chen, "Automatic sleep stage classification based on sparse deep belief net and combination of multiple classifiers," *Transactions of the Institute of Measurement and Control,* p. 0142331215587568, 2015.

[154] M. Najafian and J. Hansen, "Speaker independent diarization for child language environment analysis using Deep Neural Networks," in *Speech and Language Technology (SLT)*, 2016.

[155] M. Senoussaoui, P. Kenny, N. Dehak, and P. Dumouchel, "An i-vector Extractor Suitable for Speaker Recognition with both Microphone and Telephone Speech," in *Odyssey*, 2010, p. 6.

[156] M. Najafian, D. Irvin, Y. Luo, B. S. Rous, and J. H. Hansen, "Automatic measurement and analysis of the child verbal communication using classroom acoustics within a child care center," in *Workshop on Child Computer Interaction (WOCCI)*, 2016, pp. 56-61.

[157] A. Kaguara, K. M. Nam, and S. Reddy, "A deep neural network classifier for diagnosing sleep apnea from ECG data on smartphones and small embedded systems," 2015.

[158] M. Ciolek, M. Niedźwiecki, S. Sieklicki, J. Drozdowski, and J. Siebert, "Automated detection of sleep apnea and hypopnea events based on robust airflow envelope tracking," in *2014 22nd European Signal Processing Conference (EUSIPCO)*, 2014, pp. 2090-2094.

[159] E. Estrada, H. Nazeran, P. Nava, K. Behbehani, J. Burk, and E. Lucas, "EEG feature extraction for classification of sleep stages," in *Engineering in Medicine and Biology Society, 2004. IEMBS'04. 26th Annual International Conference of the IEEE*, 2004, pp. 196-199.

[160] T. Ning and J. Bronzino, "Autoregressive and bispectral analysis techniques: EEG applications," *IEEE Engineering in Medicine and Biology Magazine,* vol. 9, pp. 47-50, 1990.

[161] V. Acharya, "Improving common-mode rejection using the right-leg drive amplifier," *Texas Instruments,* pp. 1-11, 2011.

[162] J. Shi, X. Liu, Y. Li, Q. Zhang, Y. Li, and S. Ying, "Multi-channel EEG-based sleep stage classification with joint collaborative representation and multiple kernel learning," *Journal of neuroscience methods,* vol. 254, pp. 94-101, 2015.

[163] S.-F. Liang, C.-E. Kuo, Y.-H. Hu, and Y.-S. Cheng, "A rule-based automatic sleep staging method," *Journal of neuroscience methods,* vol. 205, pp. 169-176, 2012.

[164] C. Fernandez, S. Rusk, N. Glattard, and M. Shokoueinejad, "Computational phenotyping in polysomnography: using interpretable physiology-based machine learning models to predict health outcomes," *J Sleep Res,* vol. 40, p. A26, 2017.

[165] M. A. Levitt, "A prospective, randomized trial of BiPAP in severe acute congestive heart failure," *The Journal of emergency medicine,* vol. 21, pp. 363-369, 2001.

[166] S. Essouri, F. Nicot, A. Clément, E.-N. Garabedian, G. Roger, F. Lofaso*, et al.*, "Noninvasive positive pressure ventilation in infants with upper airway obstruction: comparison of continuous and bilevel positive pressure," *Intensive care medicine,* vol. 31, pp. 574-580, 2005.

[167] C. Philippe, M. Stoica-Herman, X. Drouot, B. Raffestin, P. Escourrou, L. Hittinger*, et al.*, "Compliance with and effectiveness of adaptive servoventilation versus continuous positive airway pressure in the treatment of Cheyne-Stokes respiration in heart failure over a six month period," *Heart,* vol. 92, pp. 337-342, 2006.

[168] K. M. Ho and K. Wong, "A comparison of continuous and bi-level positive airway pressure non-invasive ventilation in patients with acute cardiogenic pulmonary oedema: a meta-analysis," *Critical care,* vol. 10, p. R49, 2006.

[169] C. Hukins, "Comparative study of autotitrating and fixed-pressure CPAP in the home: a randomized, single-blind crossover trial," *Sleep,* vol. 27, pp. 1512-1517, 2004.

[170] W. J. Randerath, O. SCHRAEDER, W. GALETKE, F. FELDMEYER, and K.-H. RÜHLE, "Autoadjusting CPAP therapy based on impedance efficacy, compliance and acceptance," *American journal of respiratory and critical care medicine,* vol. 163, pp. 652-657, 2001.

[171] N. T. Ayas, S. R. Patel, A. Malhotra, M. Schulzer, M. Malhotra, D. Jung*, et al.*, "Auto-titrating versus standard continuous positive airway pressure for the treatment of obstructive sleep apnea: results of a meta-analysis," *SLEEP-NEW YORK THEN WESTCHESTER-,* vol. 27, pp. 249-253, 2004.

[172] C. Sullivan, M. Berthon-Jones, F. Issa, and L. Eves, "Reversal of obstructive sleep apnoea by continuous positive airway pressure applied through the nares," *The Lancet,* vol. 317, pp. 862-865, 1981.

[173] N. B. Kribbs, A. I. Pack, L. R. Kline, J. E. Getsy, J. S. Schuett, J. N. Henry*, et al.*, "Effects of one night without nasal CPAP treatment on sleep and sleepiness in patients with obstructive sleep apnea," *American Review of Respiratory Disease,* vol. 147, pp. 1162-1168, 1993.

[174] T. E. Weaver, C. Mancini, G. Maislin, J. Cater, B. Staley, J. R. Landis*, et al.*, "Continuous positive airway pressure treatment of sleepy patients with milder obstructive sleep apnea: Results of the

CPAP Apnea Trial North American Program (CATNAP) randomized clinical trial," *American Journal of Respiratory and Critical Care Medicine,* vol. 186, pp. 677-683, 2012.
[175] H. F. Becker, A. Jerrentrup, T. Ploch, L. Grote, T. Penzel, C. E. Sullivan*, et al.*, "Effect of nasal continuous positive airway pressure treatment on blood pressure in patients with obstructive sleep apnea," *circulation,* vol. 107, pp. 68-73, 2003.
[176] T. E. Weaver and R. R. Grunstein, "Adherence to continuous positive airway pressure therapy: the challenge to effective treatment," *Proceedings of the American Thoracic Society,* vol. 5, pp. 173-178, 2008.
[177] H. M. Engleman and M. R. Wild, "Improving CPAP use by patients with the sleep apnoea/hypopnoea syndrome (SAHS)," *Sleep medicine reviews,* vol. 7, pp. 81-99, 2003.
[178] M. Arzt, J. S. Floras, A. G. Logan, R. J. Kimoff, F. Series, D. Morrison*, et al.*, "Suppression of Central Sleep Apnea by Continuous Positive Airway Pressure and Transplant-Free Survival in Heart Failure A Post Hoc Analysis of the Canadian Continuous Positive Airway Pressure for Patients With Central Sleep Apnea and Heart Failure Trial (CANPAP)," *Circulation,* vol. 115, pp. 3173-3180, 2007.
[179] R. J. Zdrojkowski and M. Estes, "Breathing gas delivery method and apparatus," ed: Google Patents, 2000.
[180] S. F. Hussain, L. Love, H. Burt, and J. A. Fleetham, "A randomized trial of auto-titrating CPAP and fixed CPAP in the treatment of obstructive sleep apnea–hypopnea," *Respiratory medicine,* vol. 98, pp. 330-333, 2004.
[181] M. R. Cowie, H. Woehrle, K. Wegscheider, C. Angermann, M.-P. d'Ortho, E. Erdmann*, et al.*, "Adaptive Servo-Ventilation for Central Sleep Apnea in Systolic Heart Failure," *New England Journal of Medicine,* vol. 373, pp. 1095-1105, 2015.
[182] M. Berthon-Jones, "Ventilatory assistance for treatment of cardiac failure and cheyne-stokes breathing," ed: Google Patents, 2014.
[183] P. D. Hill, "Method and apparatus for providing variable positive airway pressure," ed: Google Patents, 2004.
[184] G. Matthews, M. T. Kane, W. K. Duff, R. Eisert, and D. Martin, "Auto-titration pressure support system and method of using same," ed: Google Patents, 2007.
[185] G. Matthews, W. K. Duff, D. Martin, U. S. Shankar, and H. Ressler, "Auto-titration bi-level pressure support system and method of using same," ed: Google Patents, 2012.
[186] M. Berthon-Jones, "Ventilatory assistance for treatment of cardiac failure and cheyne-stokes breathing," 6,532,959

2003.
[187] M. J. Morrell, M. S. Badr, C. A. Harms, and J. A. Dempsey, "The assessment of upper airway patency during apnea using cardiogenic oscillations in the airflow signal," *Sleep,* vol. 18, pp. 651-658, 1995/10// 1995.
[188] M. Berthon-Jones, "Determination of patency of the airway," ed: Google Patents, 2010.
[189] D. C. C. Martin and J. D. Oates, "Systems, methods, and/or apparatuses for non-invasive monitoring of respiratory parameters in sleep disordered breathing," ed: Google Patents, 2014.
[190] I. Ayappa, R. G. Norman, and D. M. Rapoport, "Cardiogenic oscillations on the airflow signal during continuous positive airway pressure as a marker of central apnea," *CHEST Journal,* vol. 116, pp. 660-666, 1999.
[191] M. S. Khorsheed and M. A. Al-Fawzan, "Fostering university–industry collaboration in Saudi Arabia through technology innovation centers," *Innovation,* vol. 16, pp. 224-237, 2014.

[192] C. A. Massie, R. W. Hart, K. Peralez, and G. N. Richards, "Effects of humidification on nasal symptoms and compliance in sleep apnea patients using continuous positive airway pressure," *CHEST Journal,* vol. 116, pp. 403-408, 1999.

[193] D. R. Ogden, "Start-up ramp system for CPAP system with multiple ramp shape selection," ed: Google Patents, 1997.

[194] V. Hoffstein, "Review of oral appliances for treatment of sleep-disordered breathing," *Sleep and Breathing,* vol. 11, pp. 1-22, 2007.

[195] C. A. Kushida, T. I. Morgenthaler, M. R. Littner, C. A. Alessi, D. Bailey, J. Coleman*, et al.*, "Practice parameters for the treatment of snoring and obstructive sleep apnea with oral appliances: an update for 2005," *SLEEP-NEW YORK THEN WESTCHESTER-,* vol. 29, p. 240, 2006.

[196] W. Schmidt-Nowara, A. Lowe, L. Wiegand, R. Cartwright, F. Perez-Guerra, and S. Menn, "Oral appliances for the treatment of snoring and obstructive sleep apnea: a review," *Sleep-Lawrence,* vol. 18, pp. 501-510, 1995.

[197] M. Marklund, H. Stenlund, and K. A. Franklin, "Mandibular advancement devices in 630 men and women with obstructive sleep apnea and snoring: tolerability and predictors of treatment success," *CHEST Journal,* vol. 125, pp. 1270-1278, 2004.

[198] A. Mehta, J. Qian, P. Petocz, M. A. Darendeliler, and P. A. Cistulli, "A randomized, controlled study of a mandibular advancement splint for obstructive sleep apnea," *American journal of respiratory and critical care medicine,* vol. 163, pp. 1457-1461, 2001.

[199] E. Rose, R. Staats, C. Virchow, and I. E. Jonas, "A comparative study of two mandibular advancement appliances for the treatment of obstructive sleep apnoea," *The European Journal of Orthodontics,* vol. 24, pp. 191-198, 2002.

[200] W. H. Tsai, J.-C. Vazquez, T. Oshima, L. Dort, B. Roycroft, A. A. Lowe*, et al.*, "Remotely controlled mandibular positioner predicts efficacy of oral appliances in sleep apnea," *American journal of respiratory and critical care medicine,* vol. 170, pp. 366-370, 2004.

[201] S. A. Deane, P. A. Cistulli, A. T. Ng, B. Zeng, P. Petocz, and M. A. Darendeliler, "Comparison of mandibular advancement splint and tongue stabilizing device in obstructive sleep apnea: a randomized controlled trial," *Sleep,* vol. 32, p. 648, 2009.

[202] R. J. Schwab, C. Kim, L. Siegel, B. Keenan, J. Black, M. Farid-Moayer*, et al.*, "Examining the mechanism of action of a new device using oral pressure therapy for the treatment of obstructive sleep apnea," *Sleep,* vol. 37, p. 1237, 2014.

[203] G. M. Barthlen, L. K. Brown, M. R. Wiland, J. S. Sadeh, J. Patwari, and M. Zimmerman, "Comparison of three oral appliances for treatment of severe obstructive sleep apnea syndrome," *Sleep medicine,* vol. 1, pp. 299-305, 2000.

[204] M. Farid-Moayer, L. C. Siegel, and J. Black, "A feasibility evaluation of oral pressure therapy for the treatment of obstructive sleep apnea," *Therapeutic advances in respiratory disease,* vol. 7, pp. 3-12, 2013.

[205] L. J. Epstein, D. Kristo, P. J. Strollo Jr, N. Friedman, A. Malhotra, S. P. Patil*, et al.*, "Clinical guideline for the evaluation, management and long-term care of obstructive sleep apnea in adults," *J Clin Sleep Med,* vol. 5, pp. 263-276, 2009.

[206] I. M. Colrain, J. Black, L. C. Siegel, R. K. Bogan, P. M. Becker, M. Farid-Moayer*, et al.*, "A multicenter evaluation of oral pressure therapy for the treatment of obstructive sleep apnea," *Sleep Medicine,* vol. 14, pp. 830-837.

[207] A. Berssenbrugge, J. Dempsey, C. Iber, J. Skatrud, and P. Wilson, "Mechanisms of hypoxia-induced periodic breathing during sleep in humans," *The Journal of Physiology,* vol. 343, p. 507, 1983.

[208] G. Lorenzi-Filho, F. Rankin, I. BIES, and T. D. Bradley, "Effects of inhaled carbon dioxide and oxygen on Cheyne-Stokes respiration in patients with heart failure," *American Journal of Respiratory and Critical Care Medicine,* vol. 159, pp. 1490-1498, 1999.

[209] A. Xie, F. Rankin, R. Rutherford, and T. D. Bradley, "Effects of inhaled CO2 and added dead space on idiopathic central sleep apnea," *Journal of Applied Physiology,* vol. 82, pp. 918-926, 1997.

[210] R. D. Steens, T. W. Millar, X. Su, D. Biberdorf, P. Buckle, M. Ahmed*, et al.*, "Effect of inhaled 3% CO2 on Cheyne-Stokes respiration in congestive heart failure," *Sleep,* vol. 17, pp. 61-68, 1994.

[211] M. S. Badr, J. E. Grossman, and S. A. Weber, "Treatment of refractory sleep apnea with supplemental carbon dioxide," *American journal of respiratory and critical care medicine,* vol. 150, pp. 561-564, 1994.

[212] I. Szollosi, M. Jones, M. Morrell, K. Helfet, A. Coats, and A. Simonds, "Effect of CO2 inhalation on central sleep apnea and arousals from sleep," *Respiration,* vol. 71, pp. 493-498, 2004.

[213] S. Andreas, K. Weidel, G. Hagenah, and S. Heindl, "Treatment of Cheyne-Stokes respiration with nasal oxygen and carbon dioxide," *European Respiratory Journal,* vol. 12, pp. 414-419, 1998.

[214] R. N. Khayat, A. Xie, A. K. Patel, A. Kaminski, and J. B. Skatrud, "Cardiorespiratory effects of added dead space in patients with heart failure and central sleep apnea," *CHEST Journal,* vol. 123, pp. 1551-1560, 2003.

[215] G. S. Gilmartin, R. W. Daly, and R. J. Thomas, "Recognition and management of complex sleep-disordered breathing," *Current opinion in pulmonary medicine,* vol. 11, pp. 485-493, 2005.

[216] R. J. Thomas, "Effect of added dead space to positive airway pressure for treatment of complex sleep-disordered breathing," *Sleep medicine,* vol. 6, pp. 177-178, 2005.

[217] A. Tarasiuk and H. Reuveni, "The economic impact of obstructive sleep apnea," *Current opinion in pulmonary medicine,* vol. 19, pp. 639-644, 2013.

[218] AASM, *The International Classification of Sleep Disorders: Diagnostic and Coding Manual 2nd edn,* 2005.

[219] M. Thorpy, *The International Classification of Sleep Disorders: Diagnostic and Coding Manual* 1990.

[220] L. A. Panossian and A. Y. Avidan, "Review of sleep disorders," *Med Clin North Am,* vol. 93, pp. 407-25, ix, Mar 2009.

[221] J. F. Pagel, "Excessive daytime sleepiness," *Am Fam Physician,* vol. 79, pp. 391-6, Mar 1 2009.

[222] T. Young, P. E. Peppard, and D. J. Gottlieb, "Epidemiology of obstructive sleep apnea: a population health perspective," *Am J Respir Crit Care Med,* vol. 165, pp. 1217-39, May 1 2002.

[223] J. L. Hossain and C. M. Shapiro, "The prevalence, cost implications, and management of sleep disorders: an overview," *Sleep Breath,* vol. 6, pp. 85-102, Jun 2002.

[224] M. E. Dyken, V. K. Somers, T. Yamada, Z. Y. Ren, and M. B. Zimmerman, "Investigating the relationship between stroke and obstructive sleep apnea," *Stroke,* vol. 27, pp. 401-7, Mar 1996.

[225] L. J. Findley, M. E. Unverzagt, and P. M. Suratt, "Automobile accidents involving patients with obstructive sleep apnea," *Am Rev Respir Dis,* vol. 138, pp. 337-40, Aug 1988.

[226] J. M. Marin, S. J. Carrizo, E. Vicente, and A. G. Agusti, "Long-term cardiovascular outcomes in men with obstructive sleep apnoea-hypopnoea with or without treatment with continuous positive airway pressure: an observational study," *Lancet,* vol. 365, pp. 1046-53, Mar 19-25 2005.

[227] N. A. Antic, C. Buchan, A. Esterman, M. Hensley, M. T. Naughton, S. Rowland*, et al.*, "A randomized controlled trial of nurse-led care for symptomatic moderate-severe obstructive sleep apnea," *Am J Respir Crit Care Med,* vol. 179, pp. 501-8, Mar 15 2009.

[228] N. Collop, "The effect of obstructive sleep apnea on chronic medical disorders," *Cleve Clin J Med,* vol. 74, pp. 72-8, Jan 2007.

[229] D. Leger, V. Bayon, J. P. Laaban, and P. Philip, "Impact of sleep apnea on economics," *Sleep Med Rev,* vol. 16, pp. 455-62, Oct 2012.
[230] S. J. Durning, V. F. Capaldi, 2nd, A. R. Artino, Jr., J. Graner, C. van der Vleuten, T. J. Beckman*, et al.*, "A pilot study exploring the relationship between internists' self-reported sleepiness, performance on multiple-choice exam items and prefrontal cortex activity," *Med Teach,* vol. 36, pp. 434-40, May 2014.
[231] H. J. Cho, H. Lavretsky, R. Olmstead, M. J. Levin, M. N. Oxman, and M. R. Irwin, "Sleep disturbance and depression recurrence in community-dwelling older adults: a prospective study," *Am J Psychiatry,* vol. 165, pp. 1543-50, Dec 2008.
[232] K. Wulff, D. J. Dijk, B. Middleton, R. G. Foster, and E. M. Joyce, "Sleep and circadian rhythm disruption in schizophrenia," *Br J Psychiatry,* vol. 200, pp. 308-16, Apr 2012.
[233] J. Behar, A. Roebuck, J. S. Domingos, E. Gederi, and G. D. Clifford, "A review of current sleep screening applications for smartphones," *Physiol Meas,* vol. 34, pp. R29-46, Jul 2013.
[234] A. Roebuck, V. Monasterio, E. Gederi, M. Osipov, J. Behar, A. Malhotra*, et al.*, "A review of signals used in sleep analysis," *Physiol Meas,* vol. 35, pp. R1-57, Jan 2014.
[235] P. A. Deutsch, M. S. Simmons, and J. M. Wallace, "Cost-effectiveness of split-night polysomnography and home studies in the evaluation of obstructive sleep apnea syndrome," *J Clin Sleep Med,* vol. 2, pp. 145-53, Apr 15 2006.
[236] M. Bruyneel, C. Sanida, G. Art, W. Libert, L. Cuvelier, M. Paesmans*, et al.*, "Sleep efficiency during sleep studies: results of a prospective study comparing home-based and in-hospital polysomnography," *J Sleep Res,* vol. 20, pp. 201-6, Mar 2011.
[237] J. F. Masa, J. Corral, R. Pereira, J. Duran-Cantolla, M. Cabello, L. Hernandez-Blasco*, et al.*, "Effectiveness of home respiratory polygraphy for the diagnosis of sleep apnoea and hypopnoea syndrome," *Thorax,* vol. 66, pp. 567-73, Jul 2011.
[238] S. Hesselbacher, A. Mattewal, M. Hirshkowitz, and A. Sharafkhaneh, "Classification, technical specification, and types of home sleep testing devices for sleep-disordered breathing," *Sleep Med Clin,* vol. 6, pp. 261-82, 2011.
[239] M. Schweitzer, A. Mohammad, R. Binder, R. Steinberg, W. Schreiber, and H. Weeb, "Biosomnia-validity of a mobile system to detect sleep and sleep quality," *Somnologie,* vol. 8, pp. 131-8

2004.
[240] W. W. Flemons, N. J. Douglas, S. T. Kuna, D. O. Rodenstein, and J. Wheatley, "Access to diagnosis and treatment of patients with suspected sleep apnea," *Am J Respir Crit Care Med,* vol. 169, pp. 668-72, Mar 15 2004.
[241] H. Reuven, E. Schweitzer, and A. Tarasiuk, "A cost-effectiveness analysis of alternative at-home or in-laboratory technologies for the diagnosis of obstructive sleep apnea syndrome," *Med Decis Making,* vol. 21, pp. 451-8, Nov-Dec 2001.
[242] T. H. Inge, W. C. King, T. M. Jenkins, A. P. Courcoulas, M. Mitsnefes, D. R. Flum*, et al.*, "The effect of obesity in adolescence on adult health status," *Pediatrics,* vol. 132, pp. 1098-104, Dec 2013.
[243] P. E. Peppard, T. Young, J. H. Barnet, M. Palta, E. W. Hagen, and K. M. Hla, "Increased prevalence of sleep-disordered breathing in adults," *Am J Epidemiol,* vol. 177, pp. 1006-14, May 1 2013.
[244] S. F. Quan, R. Budhiraja, S. Batool-Anwar, D. J. Gottlieb, P. Eichling, S. Patel*, et al.*, "Lack of Impact of Mild Obstructive Sleep Apnea on Sleepiness, Mood and Quality of Life," *Southwest J Pulm Crit Care,* vol. 9, pp. 44-56, 2014.
[245] T. Young, L. Evans, L. Finn, and M. Palta, "Estimation of the clinically diagnosed proportion of sleep apnea syndrome in middle-aged men and women," *Sleep,* vol. 20, pp. 705-6, Sep 1997.
[246] W. W. Flemons, M. R. Littner, J. A. Rowley, P. Gay, W. M. Anderson, D. W. Hudgel*, et al.*, "Home diagnosis of sleep apnea: a systematic review of the literature. An evidence review cosponsored

by the American Academy of Sleep Medicine, the American College of Chest Physicians, and the American Thoracic Society," *Chest,* vol. 124, pp. 1543-79, Oct 2003.

[247] C. L. Marcus, K. J. Omlin, D. J. Basinki, S. L. Bailey, A. B. Rachal, W. S. Von Pechmann*, et al.*, "Normal polysomnographic values for children and adolescents," *Am Rev Respir Dis,* vol. 146, pp. 1235-9, Nov 1992.

[248] A. Qureshi and R. D. Ballard, "Obstructive sleep apnea," *J Allergy Clin Immunol,* vol. 112, pp. 643-51; quiz 652, Oct 2003.

[249] D. J. Eckert, A. S. Jordan, P. Merchia, and A. Malhotra, "Central sleep apnea: Pathophysiology and treatment," *Chest,* vol. 131, pp. 595-607, Feb 2007.

[250] S. Javaheri, T. J. Parker, J. D. Liming, W. S. Corbett, H. Nishiyama, L. Wexler*, et al.*, "Sleep apnea in 81 ambulatory male patients with stable heart failure. Types and their prevalences, consequences, and presentations," *Circulation,* vol. 97, pp. 2154-9, Jun 2 1998.

[251] S. R. Houser, K. B. Margulies, A. M. Murphy, F. G. Spinale, G. S. Francis, S. D. Prabhu*, et al.*, "Animal models of heart failure: a scientific statement from the American Heart Association," *Circ Res,* vol. 111, pp. 131-50, Jun 22 2012.

[252] G. C. Sieck and M. E. Wylam, "Paradoxical use of tumor necrosis factor in treating pulmonary edema," *Am J Respir Crit Care Med,* vol. 190, pp. 595-6, Sep 15 2014.

[253] D. Mansfield, D. M. Kaye, H. Brunner La Rocca, P. Solin, M. D. Esler, and M. T. Naughton, "Raised sympathetic nerve activity in heart failure and central sleep apnea is due to heart failure severity," *Circulation,* vol. 107, pp. 1396-400, Mar 18 2003.

[254] T. P. Olson, R. P. Frantz, E. M. Snyder, K. A. O'Malley, K. C. Beck, and B. D. Johnson, "Effects of acute changes in pulmonary wedge pressure on periodic breathing at rest in heart failure patients," *Am Heart J,* vol. 153, pp. 104 e1-7, Jan 2007.

[255] P. Solin, P. Bergin, M. Richardson, D. M. Kaye, E. H. Walters, and M. T. Naughton, "Influence of pulmonary capillary wedge pressure on central apnea in heart failure," *Circulation,* vol. 99, pp. 1574-9, Mar 30 1999.

[256] D. Lloyd-Jones, R. J. Adams, T. M. Brown, M. Carnethon, S. Dai, G. De Simone*, et al.*, "Executive summary: heart disease and stroke statistics--2010 update: a report from the American Heart Association," *Circulation,* vol. 121, pp. 948-54, Feb 23 2010.

[257] A. S. Go, D. Mozaffarian, V. L. Roger, E. J. Benjamin, J. D. Berry, M. J. Blaha*, et al.*, "Heart disease and stroke statistics--2014 update: a report from the American Heart Association," *Circulation,* vol. 129, pp. e28-e292, Jan 21 2014.

[258] A. D. Calvin, V. K. Somers, B. D. Johnson, C. G. Scott, and L. J. Olson, "Left atrial size, chemosensitivity, and central sleep apnea in heart failure," *Chest,* vol. 146, pp. 96-103, Jul 2014.

[259] S. Javaheri, T. J. Parker, L. Wexler, S. E. Michaels, E. Stanberry, H. Nishyama*, et al.*, "Occult sleep-disordered breathing in stable congestive heart failure," *Ann Intern Med,* vol. 122, pp. 487-92, Apr 1 1995.

[260] O. Oldenburg, B. Lamp, L. Faber, H. Teschler, D. Horstkotte, and V. Topfer, "Sleep-disordered breathing in patients with symptomatic heart failure: a contemporary study of prevalence in and characteristics of 700 patients," *Eur J Heart Fail,* vol. 9, pp. 251-7, Mar 2007.

[261] V. Baslas, S. Kaur, P. Kumar, P. Chand, and H. Aggarwal, "Oral appliances: A successful treatment modality for obstructive sleep apnea category," *Indian J Endocrinol Metab,* vol. 18, p. 873, Nov 2014.

[262] T. E. Weaver, G. Maislin, D. F. Dinges, T. Bloxham, C. F. George, H. Greenberg*, et al.*, "Relationship between hours of CPAP use and achieving normal levels of sleepiness and daily functioning," *Sleep,* vol. 30, pp. 711-9, Jun 2007.

[263] T. D. Bradley, A. G. Logan, R. J. Kimoff, F. Series, D. Morrison, K. Ferguson*, et al.*, "Continuous positive airway pressure for central sleep apnea and heart failure," *N Engl J Med,* vol. 353, pp. 2025-33, Nov 10 2005.

[264] A. J. Impens, S. Wangkaew, and J. R. Seibold, "The 6-minute walk test in scleroderma--how measuring everything measures nothing," *Rheumatology (Oxford),* vol. 47 Suppl 5, pp. v68-9, Oct 2008.

[265] A. T. S. C. o. P. S. f. C. P. F. Laboratories, "ATS statement: guidelines for the six-minute walk test," *Am J Respir Crit Care Med,* vol. 166, pp. 111-7, Jul 1 2002.

[266] T. D. Bradley, R. M. Holloway, P. R. McLaughlin, B. L. Ross, J. Walters, and P. P. Liu, "Cardiac output response to continuous positive airway pressure in congestive heart failure," *Am Rev Respir Dis,* vol. 145, pp. 377-82, Feb 1992.

[267] A. Hetzenecker, T. Roth, C. Birner, L. S. Maier, M. Pfeifer, and M. Arzt, "Effects of adaptive servo-ventilation and continuous positive airway pressure in patients with chronic heart failure and central sleep apnea: a long-term observational study," in *A29. SEEING IS BELIEVING: CARDIOVASCULAR SYSTEM OUTCOMES OF SLEEP DISORDERED BREATHING*, ed: Am Thoracic Soc, 2015, pp. A1232-A1232.

[268] F. Y. Macedo, V. Pacheco, A. Ansari, J. Brown, J. Vieira, R. Bogaev*, et al.*, "IN PATIENTS WITH SEVERE ADVANCED HEART FAILURE THE USE OF ADAPTIVE SERVO-VENTILATION (ASV) DECREASES HEART FAILURE EVENTS: A POOLED META ANALYSIS OF 629 PATIENTS WITH CENTRAL SLEEP APNEA AND CHENEY STOKES RESPIRATION (CSA-CSR)," *Journal of the American College of Cardiology,* vol. 65, 2015.

[269] R. J. Farney, J. M. Walker, K. M. Boyle, T. V. Cloward, and K. C. Shilling, "Adaptive servoventilation (ASV) in patients with sleep disordered breathing associated with chronic opioid medications for non-malignant pain," *J Clin Sleep Med,* vol. 4, pp. 311-319, 2008.

[270] M. R. Cowie, H. Woehrle, K. Wegscheider, C. Angermann, M.-P. d'Ortho, E. Erdmann*, et al.*, "Adaptive servo-ventilation for central sleep apnea in systolic heart failure," *New England Journal of Medicine,* vol. 373, pp. 1095-1105, 2015.

[271] A. A. o. S. Medicine, "Special Safety Notice: ASV therapy for central sleep apnea patients with heart failure," ed, 2015.

[272] C. G. Douglas and J. Haldane, "The causes of periodic or Cheyne-Stokes breathing," *The Journal of physiology,* vol. 38, p. 401, 1909.

[273] E. Kirkman, "Respiration: control of ventilation," *Thoracic anaesthesia / physics,* vol. 15, pp. 540-543, 2014.

[274] J. A. Dempsey, S. C. Veasey, B. J. Morgan, and C. P. O'Donnell, "Pathophysiology of sleep apnea," *Physiological reviews,* vol. 90, pp. 47-112, 2010.

[275] J. A. Dempsey, A. Xie, D. S. Patz, and D. Wang, "Physiology in medicine: obstructive sleep apnea pathogenesis and treatment—considerations beyond airway anatomy," *Journal of Applied Physiology,* vol. 116, pp. 3-12, 2014.

[276] P. Solin, T. Roebuck, D. P. Johns, E. H. Walters, and M. T. Naughton, "Peripheral and central ventilatory responses in central sleep apnea with and without congestive heart failure," *Am J Respir Crit Care Med,* vol. 162, pp. 2194-200, Dec 2000.

[277] M. T. Naughton, D. C. Benard, P. P. Liu, R. Rutherford, F. Rankin, and T. D. Bradley, "Effects of nasal CPAP on sympathetic activity in patients with heart failure and central sleep apnea," *Am J Respir Crit Care Med,* vol. 152, pp. 473-9, Aug 1995.

[278] P. Solin, D. M. Kaye, and P. J. Little, "Impact of sleep apnea on sympathetic nervous system activity in heart failure," *Chest,* vol. 123, pp. 1119-1126, 2003.

[279] J. A. Dempsey, "Crossing the apnoeic threshold: causes and consequences," *Exp Physiol,* vol. 90, pp. 13-24, Jan 2005.

[280] M. C. K. Khoo, R. E. Kronauer, K. P. Strohl, and A. S. Slutsky, "Factors inducing periodic breathing in humans: a general model," *J. Appl. Physiol.,* vol. 53, pp. 644-659, 1982.
[281] S. Andreas, K. Weidel, G. Hagenah, and S. Heindl, "Treatment of Cheyne-Stokes respiration with nasal oxygen and carbon dioxide," *Eur Respir J,* vol. 12, pp. 414-9, Aug 1998.
[282] A. Xie, J. B. Skatrud, and J. A. Dempsey, "Effect of hypoxia on the hypopnoeic and apnoeic threshold for CO(2) in sleeping humans," *J Physiol,* vol. 535, pp. 269-78, Aug 15 2001.
[283] S. Al-Saif, R. Alvaro, J. Manfreda, K. Kwiatkowski, D. Cates, and H. Rigatto, "Inhalation of Low (0.5-1.5%) CO2 As a Potential Treatment for Apnea of Prematurity," *Pediatric Research,* vol. 45, pp. 293A-293A, 1999.
[284] S. Al-Saif, R. Alvaro, J. Manfreda, K. Kwiatkowski, D. Cates, M. Qurashi*, et al.*, "A randomized controlled trial of theophylline versus CO 2 inhalation for treating apnea of prematurity," *The Journal of pediatrics,* vol. 153, pp. 513-518, 2008.
[285] M. Shokoueinejad, A. Pazouki, J. Levin, F. Wang, C. Fernandez, S. Rusk*, et al.*, "A Modeling Study on Inspired CO2 Rebreathing Device for Sleep Apnea Treatment by Means of CFD Analysis and Experiment," *Journal of Medical and Biological Engineering,* vol. 37, pp. 288-297, 2017// 2017.
[286] B. Skadberg, Å. Oterhals, K. Finborud, and T. Markestad, "CO2 rebreathing: a possible contributory factor to some cases of sudden infant death?," *Acta paediatrica,* vol. 84, pp. 988-995, 1995.
[287] T. Stocker, *Introduction to climate modelling*: Springer Science & Business Media, 2011.
[288] T. R. Marrero and E. A. Mason, "Gaseous diffusion coefficients," *Journal of Physical and Chemical Reference Data,* vol. 1, pp. 3-118, 1972.
[289] Comsol, *COMSOL Multiphysics: Version 4.2*: Comsol, 2011.
[290] A. Nunn and I. Gregg, "New regression equations for predicting peak expiratory flow in adults," *BMj,* vol. 298, pp. 1068-1070, 1989.
[291] J. Webster, I. dos Santos, M. Shokoueinejad, J. Levin, J. Dempsey, F. Wang*, et al.*, "Sleep apnea therapy device that automaticlly adjusts the fraction of inspired carbon dioxide," 2016.
[292] A. Giannoni, R. Baruah, K. Willson, Y. Mebrate, J. Mayet, M. Emdin*, et al.*, "Real-time dynamic carbon dioxide administration: a novel treatment strategy for stabilization of periodic breathing with potential application to central sleep apnea," *Journal of the American College of Cardiology,* vol. 56, pp. 1832-1837, 2010.
[293] M. Shokoueinejad, R. Alkashgari, H. Mosli, N. Alothmany, and J. Webster, "Video voiding device for diagnosing lower urinary tract dysfunction in men," *Journal of Medical and Biological Engineering* 2016
[294] N. Alothmany, H. Mosli, J. G. Webster, M. Shokoueinejad, R. Alkashgari, M. Chiang*, et al.*, "Critical Review of Uroflowmetry Methods," *JMBE,* 2016.
[295] A. Wein and D. Barrett, "Practical urodynamics," *American Urology Association Update Series,* vol. 12, 1993.
[296] A. J. Wein, "Re: Committee Opinion No. 603: Evaluation of Uncomplicated Stress Urinary Incontinence in Women before Surgical Treatment," *The Journal of urology,* vol. 194, p. 1698, 2015.
[297] A. M and R. H. E, "Urodynamic Testing ", N. I. o. D. a. D. a. K. D. (NIDDK), Ed., ed. niddk.nih.gov, 2014.
[298] M. Drinnan and C. Griffiths, *The Physiological Measurement Handbook*. New York, NY: CRC press 2014.
[299] W. Schäfer, P. Abrams, L. Liao, A. Mattiasson, F. Pesce, A. Spangberg*, et al.*, "Good urodynamic practices: Uroflowmetry, filling cystometry, and pressure-flow studies," *Neurourology and urodynamics,* vol. 21, pp. 261-274, 2002.

[300] R. L. Ryall and V. R. Marshall, "Measurement of urinary flow rate," *Urology,* vol. 22, pp. 556-564, 1983.
[301] J. B. Jørgensen and K. M.-E. Jensen, "Uroflowmetry," *Urologic Clinics of North America,* vol. 23, pp. 237-242, 1996.
[302] W. Schäfer, H. Rübben, R. Noppeney, and F.-J. Deutz, "Obstructed and unobstructed prostatic obstruction," *World Journal of Urology,* vol. 6, pp. 198-203, 1989.
[303] J. B. Jørgensen, K. E. Jensen, P. Klarskov, I. Bernstein, I. Abel, and P. Mogensen, "Intra-and inter-observer variations in classification of urinary flow curve patterns," *Neurourology and Urodynamics,* vol. 9, pp. 535-539, 1990.
[304] K. Backman, B. Von Garrelts, and R. Sundblad, "Micturition in normal women. Studies of pressure and flow," *Acta chirurgica Scandinavica,* vol. 132, pp. 403-412, 1966.
[305] S. Altunay, Z. Telatar, O. Erogul, and E. Aydur, "Interpretation of Uroflow Graphs with Artificial Neural Networks," in *2006 IEEE 14th Signal Processing and Communications Applications*, 2006, pp. 1-4.
[306] B. Urbonavičius and P. Kaškonas, "Urodynamic measurement techniques: A review," *Measurement,* vol. 90, pp. 64-73, 2016.
[307] E. C.-L. Chou, P.-Y. Yang, W.-H. Hsueh, C.-H. Chang, and N.-H. Meng, "Urinating in the standing position: a feasible alternative for elderly women with knee osteoarthritis," *The Journal of urology,* vol. 186, pp. 949-953, 2011.
[308] M. Amjadi, S. Hajebrahimi, and F. Soleimanzadeh, "The Effect of Voiding Position on Uroflowmetric Parameters in Healthy Young Men," *UroToday International Journal,* vol. 4, 2011.
[309] M. Riehmann, W. H. Bayer, P. J. Drinka, S. Schultz, P. Krause, P. R. Rhodes*, et al.*, "Position-related changes in voiding dynamics in men," *Urology,* vol. 52, pp. 625-30, Oct 1998.
[310] J. Susset, P. Picker, M. Kretz, and R. Jorest, "Critical evaluation of uroflowmeters and analysis of normal curves," *The Journal of urology,* vol. 109, pp. 874-878, 1973.
[311] E. G. Ballenger and H. P. Mcdonald, "Voiding distance decrease an important early symptom of prostatic obstruction," *Southern Medical Journal,* vol. 25, pp. 863-864, 1932.
[312] C. F. Møller and T. Hald, "Clinical Urodynamics: Methods and Results," *Scandinavian Journal of Urology and Nephrology,* vol. 6, pp. 143-155, 1972/01/01 1972.
[313] A. Gammie, B. Clarkson, C. Constantinou, M. Damaser, M. Drinnan, G. Geleijnse*, et al.*, "International Continence Society guidelines on urodynamic equipment performance," *Neurourology and urodynamics,* vol. 33, pp. 370-379, 2014.
[314] D. Cardus, E. Quesada, and F. Scott, "Use of an electromagnetic flowmeter for urine flow measurements," *Journal of applied physiology,* vol. 18, pp. 845-847, 1963.
[315] T. Peters, J. Donovan, H. Kay, P. Abrams, J. De La Rosette, D. Porru*, et al.*, "The International Continence Society “benign prostatic hyperplasia” study: the bothersomeness of urinary symptoms," *The Journal of urology,* vol. 157, pp. 885-889, 1997.
[316] B. Von Garrelts, "Analysis of micturition; a new method of recording the voiding of the bladder," *Acta Chirurgica Scandinavica,* vol. 112, pp. 326-340, 1957.
[317] B. Von Garrelts, "Micturition in the normal male," *Acta Chirurgica Scandinavica,* vol. 114, p. 197, 1958.
[318] J. Gierup, "Micturition studies in infants and children: intravesical pressure, urinary flow and urethral resistance in boys without infravesical obstruction," *Scandinavian journal of urology and nephrology,* vol. 4, pp. 217-230, 1970.
[319] K. Kadow, S. Howell, P. Lewis, and D. Protheroe, "A FLOW-RATE NOMOGRAM FOR NORMAL MALES AGED 50-80 YEARS," in *JOURNAL OF UROLOGY*, 1986, pp. A263-A263.
[320] M. B. Siroky, C. A. Olsson, and R. J. Krane, "The flow rate nomogram: I. Development," *The Journal of urology,* vol. 122, pp. 665-668, 1979/11// 1979.

[321] P. Abrams, "Urodynamic equipment," *Urodynamics. Principles, practice and applications. Churchill Livingstone, Edinburgh London Melbourne New York,* 1984.
[322] A. Bray, C. Griffiths, M. Drinnan, and R. Pickard, "Methods and value of home uroflowmetry in the assessment of men with lower urinary tract symptoms: a literature review," *Neurourology and urodynamics,* vol. 31, pp. 7-12, 2012.
[323] N. Viarani, N. Massari, M. Gottardi, A. Simoni, B. Margesin, A. Faes*, et al.*, "A low-cost microsystem for noninvasive uroflowmetry," *IEEE transactions on instrumentation and measurement,* vol. 55, pp. 964-971, 2006.
[324] R. B. K. Dejhan and S. Yimman, "Uroflowmetry recording design," in *TENCON 2014-2014 IEEE Region 10 Conference*, 2014, pp. 1-5.
[325] A. Otero, T. Akinfiev, R. Fernandez, and F. Palacios, "A device for automatic measurement of the critical, care patient's urine output," in *Intelligent Signal Processing, 2009. WISP 2009. IEEE International Symposium on*, 2009, pp. 169-173.
[326] G. L. Carter and V. B. Weeks, "Toilet mounted urine flow meter," ed: Google Patents, 1985.
[327] A. Suryawanshi and A. Joshi, "A method to examine functioning and dysfunctioning of lower urinary tract," in *2012 IEEE 7th International Conference on Industrial and Information Systems (ICIIS)*, 2012, pp. 1-6.
[328] H. Wurster, "Apparatus for measuring rates of urine flow electrically," ed: Google Patents, 1977.
[329] G. Drach and W. Binard, "Disposable peak urinary flowmeter estimates lower urinary tract obstruction," *The Journal of urology,* vol. 115, pp. 175-179, 1976.
[330] J. Caffarel, W. Robson, R. Pickard, C. Griffiths, and M. Drinnan, "Flow measurements: can several "wrongs" make a "right"?," *Neurourol Urodyn,* vol. 26, pp. 474-80, 2007.
[331] R. J. Currie, "The Streamtest cup: a new uroflow device," *Urology,* vol. 52, pp. 1118-21, Dec 1998.
[332] J. De La Rosette, W. Witjes, F. Debruyne, P. Kersten, and H. Wijkstra, "Improved reliability of uroflowmetry investigations: results of a portable home-based uroflowmetry study," *British journal of urology,* vol. 78, pp. 385-390, 1996.
[333] R. P. Lyon and D. R. Smith, "Distal urethral stenosis," *The Journal of urology,* vol. 89, pp. 414-421, 1963.
[334] D. Hitt, K. Zvarova, and P. Zvara, "Urinary Flow Measurements Via Acoustic Signatures with Application to Telemedicine," *Institute of Aeronautics and Astronautics,* pp. 1-10, 2009.
[335] J. Krhut, M. Gärtner, R. Sýkora, P. Hurtík, M. Burda, K. Zvarová*, et al.*, "MP71-07 VALIDATION OF A NEW SOUND-BASED METHOD FOR RECORDING VOIDING PARAMETERS USING SIMULTANEOUS UROFLOWMETRY," *The Journal of Urology,* vol. 193, p. e914, 2015.
[336] A. Terai, N. Ueda, N. Utsunomiya, N. Kohei, T. Aoyama, and K. Inoue, "Automatic switching and guidance system to facilitate unassisted uroflowmetry using commercial electronic devices," *International journal of urology,* vol. 13, pp. 1154-1155, 2006.
[337] C. M. Gomes, S. Arap, and F. E. Trigo-Rocha, "Voiding dysfunction and urodynamic abnormalities in elderly patients," *Revista do Hospital das Clinicas,* vol. 59, pp. 206-215, 2004.
[338] P. Sand. Diagnostic procedures in the evaluation of female urinary incontinence and voiding dysfunction [Online]. Available: https://www.glowm.com/resources/glowm/cd/pages/v1/v1c079.html
[339] J. Jørgensen, H. Jacobsen, P. Bagi, H. Hvarnes, and H. Colstrup, "Home uroflowmetry by means of the Da CapoTM home uroflowmeter," *European urology,* vol. 33, pp. 64-68, 1998.
[340] Z. Guan, X. Deng, and Q. Zhang, "[Comparison of new portable home electronic uroflowmeter with Laborie uroflowmeter]," *Beijing da xue xue bao. Yi xue ban= Journal of Peking University. Health sciences,* vol. 43, pp. 616-619, 2011.

[341] C. K. Chan, S. K. H. Yip, I. P. Wu, M. L. Li, and N. H. Chan, "Evaluation of the clinical value of a simple flowmeter in the management of male lower urinary tract symptoms," *BJU international,* vol. 109, pp. 1690-1696, 2012.

[342] R. Boci, M. Fall, M. Waldén, T. Knutson, and C. Dahlstrand, "Home uroflowmetry: improved accuracy in outflow assessment," *Neurourology and urodynamics,* vol. 18, pp. 25-32, 1999.

[343] G. Mombelli, S. Picozzi, G. Messina, D. Truffelli, C. Marenghi, G. Maffi*, et al.*, "Free uroflowmetry versus "Do-It-Yourself" uroflowmetry in the assessment of patients with lower urinary tract symptoms," *International urology and nephrology,* vol. 46, pp. 1915-1919, 2014.

[344] J. M. Reynard, T. J. Peters, C. Lim, and P. Abrams, "The value of multiple free-flow studies in men with lower urinary tract symptoms," *Br J Urol,* vol. 77, pp. 813-8, Jun 1996.

[345] A. Ünsal and E. Çimentepe, "Voiding Position does not Affect Uroflowmetric Parameters and Post-void Residual Urine Volume in Healthy Volunteers," *Scandinavian journal of urology and nephrology,* vol. 38, pp. 469-471, 2004.

[346] K. Wiens, S. Green, and D. Grecov, "Novel optical uroflowmeter using image processing techniques," *Measurement,* vol. 47, pp. 314-320, 2014.

[347] C. L. van der Walt, C. F. Heyns, A. E. Groeneveld, R. S. Edlin, and S. P. van Vuuren, "Prospective comparison of a new visual prostate symptom score versus the international prostate symptom score in men with lower urinary tract symptoms," *Urology,* vol. 78, pp. 17-20, Jul 2011.

[348] A. J. Schaeffer, J. R. Landis, J. S. Knauss, K. J. Propert, R. B. Alexander, M. S. Litwin*, et al.*, "Demographic and clinical characteristics of men with chronic prostatitis: the national institutes of health chronic prostatitis cohort study," *J Urol,* vol. 168, pp. 593-8, Aug 2002.

[349] A. C. o. Obstetricians and Gynecologists, "Evaluation of uncomplicated stress urinary incontinence in women before surgical treatment. Committee Opinion No. 603," *Obstet Gynecol,* vol. 123, pp. 1403-7, 2014.

[350] J. J. Pel and R. van Mastrigt, "Development of a low-cost flow meter to grade the maximum flow rate," *Neurourol Urodyn,* vol. 21, pp. 48-54, 2002.

[351] H. Dietz, "Does bladder neck descent increase with age?," *International Urogynecology Journal,* vol. 18, pp. 665-669, 2007.

[352] S. Madersbacher, G. Alivizatos, J. Nordling, C. R. Sanz, M. Emberton, and J. J. de la Rosette, "EAU 2004 guidelines on assessment, therapy and follow-up of men with lower urinary tract symptoms suggestive of benign prostatic obstruction (BPH guidelines)," *Eur Urol,* vol. 46, pp. 547-54, Nov 2004.

[353] C. C. Yang, K. P. Weinfurt, R. M. Merion, Z. Kirkali, and L. S. Group, "The Symptoms of Lower Urinary Tract Dysfunction Research Network (LURN)," *The Journal of urology,* 2016.

[354] S. K. Addla, R. R. Marri, S. L. Daayana, and P. Irwin, "Avoid cruising on the uroflowmeter: evaluation of cruising artifact on spinning disc flowmeters in an experimental setup," *Neurourol Urodyn,* vol. 29, pp. 1301-5, Sep 2010.

[355] D. A. Bloom, W. D. Foster, D. G. McLeod, B. T. Mittemeyer, and R. E. Stutzman, "Cost-effective uroflowmetry in men," *J Urol,* vol. 133, pp. 421-4, Mar 1985.

[356] R. Boci, M. Fall, M. Walden, T. Knutson, and C. Dahlstrand, "Home uroflowmetry: improved accuracy in outflow assessment," *Neurourol Urodyn,* vol. 18, pp. 25-32, 1999.

[357] J. Caffarel, W. Robson, R. Pickard, D. Newton, C. Griffiths, and M. Drinnan, "Home uroflow device: Basic but more accurate than standard in-clinic uroflowmetry?," *Neurourology And Urodynamics,* vol. 25, pp. 632-633, 2006.

[358] J. Caffarel, W. Robson, R. Pickard, C. Griffiths, and M. Drinnan, "Flow measurements: Can several "wrongs" make a "right"?," *Neurourology and urodynamics,* vol. 26, pp. 474-480, 2007.

[359] R. M. Nesbit and W. C. Baum, "Diagnosis and surgical management of obstructive uropathy in childhood," *AMA Am J Dis Child,* vol. 88, pp. 239-50, Aug 1954.

[360] J. Bryndorf and E. Sandoe, "The hydrodynamics of micturition," *Dan Med Bull,* vol. 7, pp. 65-71, Jun 1960.
[361] N. R. Zinner, R. C. Ritter, A. M. Sterling, and D. C. Harding, "Drop spectrometer: a non-obstructive, non-interfering instrument for analyzing hydrodynamic properties of human urination," *J Urol,* vol. 101, pp. 914-8, Jun 1969.
[362] R. L. Ryall and V. R. Marshall, "Measurement of urinary flow rate," *Urology,* vol. 22, pp. 556-64, Nov 1983.
[363] H. A. Mosli, N. Alothmany, J. G. Webster, M. S. Maragheh, and R. Alkashgari, "Video Voiding Device For Diagnosing Lower Urinary Tract Dysfunction," U.S. Patent, 2014.
[364] J. M. Bland and D. Altman, "Statistical methods for assessing agreement between two methods of clinical measurement," *The lancet,* vol. 327, pp. 307-310, 1986.
[365] J. C. a. D. Winters, Roger R and Goldman, Howard B and Herndon, CD Anthony and Kobashi, Kathleen C and Kraus, Stephen R and Lemack, Gary E and Nitti, Victor W and Rovner, Eric S and Wein, Alan J, "Urodynamic studies in adults: AUA/SUFU guideline," *The Journal of urology,* vol. 188, pp. 2464--2472, 10/9/2012 2012.
[366] V. W. Nitti, "Pressure flow urodynamic studies: the gold standard for diagnosing bladder outlet obstruction," *Rev Urol,* vol. 7 Suppl 6, pp. S14-21, 2005.
[367] C. Aranda, J. Barragan, G. Graham, and H. e. a. Hufnagel. (2012, Medical Devices Unit, Local Production and Technology Transfer to Increase Access to Medical Devices. Available: http://www.who.int/medical_devices/1240EHT_final.pdf
[368] M. S. a. A.-F. Khorsheed, Mohammad A, "Fostering university--industry collaboration in Saudi Arabia through technology innovation centers," *Innovation,* vol. 16, pp. 224-237, 2014.